STUDY OF SOME INTEGRABLE COUPLED DYNAMICAL SYSTEMS RELATED TO OPTICAL SOLITONS AND THEIR APPLICATIONS

by

Abhijit Borah

DEPARTMENT OF PHYSICS

INDIAN INSTITUTE OF TECHNOLOGY, GUWAHATI

28th January 2005

STUDY OF SOME INTEGRABLE COUPLED DYNAMICAL SYSTEMS RELATED TO OPTICAL SOLITONS AND THEIR APPLICATIONS

A Thesis Submitted

in Partial Fulfilment of the Requirements

for the Award of the Degree of

Doctor of Philosophy

by

Abhijit Borah

to the

DEPARTMENT OF PHYSICS

INDIAN INSTITUTE OF TECHNOLOGY, GUWAHATI

28th January 2005

To my late supervisor, Sasanka Ghosh,
&
to my parents.

Certificate

It is certified that the work contained in the thesis entitled "STUDY OF SOME INTEGRABLE COUPLED DYNAMICAL SYSTEMS RELATED TO OPTICAL SOLITONS AND THEIR APPLICATIONS", by Abhijit Borah, a student in the department of Physics, Indian Institute of Technology, Guwahati for the award of the degree of Doctor of Philosophy has been carried out under my supervision and that this work has not been submitted elsewhere for a degree.

Dr. Sasanka Ghosh
Assoc. Professor
Physics Department
IIT Guwahati

Dr.C.Y.Kadolkar
(Caretaker Supervisor)
Assoc. Professor
Physics Department
IIT Guwahati

Acknowledgement

I am deeply indebted to my thesis supervisor, the late Dr.Sasanka Ghosh whose guidance, instruction and invaluable criticism were instrumental in the progress of my work. To me he was more than just my supervisor, he was a true teacher and guide. Whatever I learnt about integrable models, I owe it to him.

In wish to express my sincere gratitude to Dr.C.Y.Kadoulkar, Associate Professor, Physics Department, IIT, Guwahati, for coming forward as my caretaker supervisor during the untimely death of my late supervisor.

To the head of Physics Department, Dr.A.Srinivasan and other faculty and students of the physics department at IIT, Guwahati, my sincere gratitude for their continued encouragement during the course of my research. In particular, I wish to thank my friends and fellow researchers Dr.Sudipta Nandy and Dr.Debojit Sarma for all the help that they gave me.

To my friends at Kohima Science College, where I work, I sincerely acknowledge their support specially from Mr.Khrote Doulo and Mr.I.Sunep during the last three years.

To my parents, wife, sisters and brother-in-law, I owe a special debt of gratitude. As in all endeavours, their encouragement and selfless support gave me the strength to continue the work even in the most difficult circumstances.

Abhijit Borah

Guwahati, 28th January 2005.

Contents

List of Figures

Chapter 1

Introduction

NONLINEAR science is assumed to be the most important frontier for the fundamental understanding of nature today, and a major constituent of these nonlinear sciences are the integrable models. These integrable models are characterised by special localized solutions called solitons. After a formative period of a hundred and fifty years, the concept of solitons at present, is firmly established. As interesting as it is in the field mathematical physics, solitons have made their presence felt in some wide branches of physics such as condensed matter physics, plasma physics, hydrodynamics, low temperature physics, particle physics, nuclear physics, astrophysics, biophysics and of course nonlinear optics.

The first observation of solitons is recorded by John Scott Russell in 1834. He had watched a rounded smooth well defined heap of water proceed at a constant speed and without change of shape, over a two mile stretch along a narrow and shallow channel [1]. This was followed by extensive water tank and water channel experiments by H.Brazin [2], and associated theoretical developments by Joseph Boussinesq [3], Lord Rayleigh [4] etc. In 1876, Korteweg and de Vries developed a model equation which described the propagation of such unidirectional shallow water waves [5] and later, this equation became the famous Korteweg-de Vries (KdV) equation. At present, any study of solitons starts with the KdV equation. Korteweg and de Vries found that two types of solutions to their equation exist. The periodic solutions called as the cnoidal waves and a localized solution of a single positive

elevation which later came to be called as the soliton. The soliton can also be treated as a limit of the cnoidal wave under infinite wavelength. Later, in the study of the Fermi-Pasta-Ulam (FPU) heat transfer problem [6], N. Zabusky and M. Kruskal tried to model it on the KdV equation. As the KdV equation was nonlinear they resorted to numerical simulations and, in which they observed single pulse-like waves travelling through a one-dimensional crystal lattice [7]. These solitary waves collided with one another elastically and displayed quasi-particle like properties and consequently were named as *solitons*. The next important breakthrough followed when Gardner, Greene, Kruskal and Miura derived the localised wave solutions or the soliton solutions of the KdV equation analytically, using the so called inverse scattering transformations [8, 9]. The obtained soliton solutions displayed the elastic collision property that is today characteristic of solitons [10]. The inverse scattering method (ISM) of Gardner *et.al.*, triggered a study of nonlinear equations of KdV and the like, leading to a strong mathematical development of nonlinear equations. P.Lax reformulated the work of Gardner *et.al.*, and constructed a hierarchy of the KdV equation solvable by ISM [11]. It was shown by Zakharov [12] that the time evolution of the envelope of a weakly nonlinear deep-water wave train is described by the nonlinear Schrödinger equation (NLS). By applying the ISM technique, the exact analytical solution of the NLS equation was discovered by Zakharov and Shabat [13]. These water envelope soliton solutions of NLS were verified by Yuen and Lake [14]. The next step in the evolution of the ISM followed when the solution of the modified KdV equation (mKdV) was established by Wadati [15, 16] and by Ablowitz, Kaup, Newell and Segur (AKNS) who went on to show that a class of nonlinear equations solvable by ISM can also be solved in the same pattern [17]. This powerful technique is called as the AKNS scheme and can handle a wide variety of very general inital conditions.

In the course of time these nonlinear equations that could be solved exactly came to be known as Integrable Systems. The soliton solutions of these integrable models bore specific properties. The one soliton solution of an integrable model is a single peaked envelope which travels in a non dispersive manner. The two soliton solution of an integrable system describes two

independent peaks travelling with different velocities, and in some cases the taller peak moving faster. In a similar manner the N soliton solution is a system of N peaks each moving with its own velocity. Whenever two such peaks collided, as was observed in the numerical simulations of Zabusky and Kruskal [7], they moved on without any change of shape, indicating their robust nature. The only signature that an interaction has taken place is the jump in phase of the soliton after the interaction.

Side by side, other ingenious mathematical methods for dealing with these nonlinear equations were being developed. The Hirota method [18]–[27] is a very efficient and direct method of finding soliton solutions of low orders — like the one soliton solution or the two soliton solution explicitly. In the Hirota bilinear method one tranforms the nonlinear equation into a bilinear form by employing the gauge invarient Hirota derivative. This is the critical step as there happens to be no algorithmic procedure in the consideration of the correct transformation for obtaining the correct form of the equation which is amenable for bilinearization and relies solely on intution. The advantage of this technique is that once the nonlinear equation is bilinearized, one and two solition solutions are guaranteed. However, the three soliton solution is a requirement for establishing the integrability of a system. Another method of solving a certain class of nonlinear partial differential equations is associated with a transformation known as the Bäcklund transformation [28, 29], which either connects two distinct solutions of the same equation or else the solutions of two nonlinear equations. Thus one can proceed from a simple solution such as the one soliton solution and then by repeated application of the procedure arrive at the N soliton solution. In yet another technique, in order to check whether a nonlinear differential equation is solvable by ISM, one may utilize the Painlevé analysis. In this method, one tries to exactly reduce the nonlinear partial differential equation into some associated ordinary differential equations. If these ordinary differential equations do not posess movable critical points, they satisfy the Painlevé property and according to the Painlevé conjecture [30, 31, 32, 33], the mother nonlinear equation is solvable by ISM. Some of the other mathematical methods developed for the study of these integrable systems are bi-Hamiltonian theory

[34, 35], **r**-matrix structure [36], symmetry approach [37, 38], perturbation methods [39, 40], algebraic study based on Lie algebras [41, 42] and Jordan algebras [43, 44, 45, 46] and of course numerical analysis [47].

With these developments, some distinct features of the integrable models have been established. The localised and robust nature of the solitons represent the huge number of symmetries associated with the integrable models. This is manifested by the existence of an infinite number of conserved quantities which are also in involution with each other. This is known as the Liouville integrability [36]. Another important feature of integrable models is the existance of Lax-pairs. However it is seen that some integrable models (like those represented by the Sasa Satsuma equation [59]) do not have directly related Lax-pairs. In such cases, as in the Sasa Satsuma equation, the equation itself is shown to be related to another equation via some transformations and the Lax-pair for this transformed equation is shown to exist. The existence of bi-Hamiltonian structers and the r-matrix are other features of the integrable models. However, the existence of the exact solutions, viz, the solution solitons of the nonlinear dynamical equations representing the integrable models remain as their primary characteristic.

In nonlinear optics, there are many situations where the nonlinear effects cannot be treated as a weak perturbation and this has led to the successfull application of the soliton concepts. Indeed solitons are found to be the final stage in evolution of an inital electromagnetic wave field in a broad class of nonlinear optical media.

Studies in nonlinear optics began with the predictions that electromagnetic waves travelling through nonlinear dispersive medium were unstable [48, 49, 50]. Hasegawa and Tappert showed that the propagation of light waves through a dielectric optical fiber could be modelled upon the NLS equation [51]. The resulting solitons were envelopes of a light pulse having low intensity and were called as “dark” solitons. This was due to the fact that at that time the dispersive property of a dielectric fiber was not yet known and consequently the group velocity dispersion (GVD) was considered as positive. Subsequently it was also shown that with a negative GVD it is possible to obtain “bright” envelope optical soliton solutions [52]. These pre-

dictions was verified by Mollenauer *et.al.*, when he observed the propagation of bright solitons through optical fibers [53].

The study of nonlinear optical systems is important because soliton based communication through optical fibers have the capacity for sustaining the enormous traffic requirements demanded by modern technology. In this system each optical soliton carry one bit of information. The presence or absence of a soliton represents the arrival of a binary **1** or **0** digit of information. Due to robustness of the solitons to collisions with other solitons and due to their nondispersive nature, the distance of propagation before attenuation and absorbtion takes over is considerably larger as compared to gaussian or square wave pulses that are being currently used in communication systems. Besides, the solitons being pulses of picosecond to femtosecond widths, more pulses can be packed in an interval of time giving rise to increased bandwidth. All these features, promise of speedier and more reliable communications using optical solitons in fibers. It has been experimentally shown that transmissions with bandwidths of 40 Gigabit/sec over a distance of 10,000 kms by Morita *et.al.* [54] and 1.1 Terabits/sec over a distance of 3,000 kms by Fukuchi *et.al.* [55] is possible. Besides this, a study of optical solitons are important from the standpoint of it being an important member in the theory of integrable models.

Truly, a wide variety of solitons — dynamic and topological —are exhibited in nonlinear optics and they follow from the different properties of their propagating media. Such properties include nonlinearity of the material and geometric dispersion. In this context, solitons may be the dynamical solitons like the NLS bright solitons which are localised wave excitations, or the topological solitons like the sine-Gordon solitons when describing self induced transparency (SIT). The dynamical solitons may be spatial of temporal. Spatial optical solitons [56, 57] concern with the study of self-guided (or self-trapped) optical beams that propagate in slab waveguides or bulk nonlinear media without supporting waveguide structures. As it travels through the bulk media, the beam diffraction is counter balanced by its self focusing. This self focusing arises due to the change of the refractive index of the media around the beam and is caused by the beam itself through the nonlinear

effects. Temporal solitons are solitons where pulse broadening due to group velocity dispersion (GVD) is counter balanced by the nonlinear compression of the pulse through a process known as self phase modulation (SPM). Thus temporal solitons can travel great distances without distorsion as compared with ordinary pulses (square or gaussian) but require waveguides.

Self phase modulation occurs as a result of the intensity dependence of the refractive index that is exhibited by nonlinear media. It broadens the pulse spectrum by energy redistribution among the different harmonics resulting a compression of the pulse shape. The nonlinear media exhibiting SPM are also known as Kerr media. As shown by Hasegawa, the electromagnetic wave equations based on these low order effect of GVD together with SPM, and neglecting fiber losses takes the form of the NLS equation [104]. SPM appears due to the nonlinear part of the electric polarization (in the third order electric suseptibility tensor) and become appreciable with pulse widths of 10^{-12}sec and pulse intensities of 100 milliWatt. But with the zero-dispersion fibers available today, the higher order nonlinear effects can no longer be ignored. The higher order GVD is known as third order dispersion (TOD) and is very prevelant in pulses of femto-seconds width. For such ultra-short pulses the spectrum being wide, Raman gain transfers energy from the higher frequency components to the lower frequency components leading to an asymetrical broadening of the pulse. But the process of stimulated inelastic scattering may cause partial transfer of energy from the optical field to the media. If the energy transfer that takes place is high, optical phonons take part in the transfer and the process is called as stimulated Raman scattering (SRS). On the other hand for low energy transfers acoustic phonons participate, and the phenomena is known as stimulated Brillouin scattering (SBS). In optical solitons it is the SRS which plays a dominant role as compared to SBS. In both the cases a photon of the incident field get anhillated to create a photon of the downshifted Strokes frequency or upshifted anti-Strokes frequency. This processes a governed by the availability of quantum states and the energy-momentum conservations. The other higher order nonlinear effect is called as self steepening (SS) and causes an asymetrical compression of the pulse width. Under the right conditions it

is possible to cancel the effect of TOD with that of SRS and SS. The inclusion of these effect to the wave equation gives the higher order nonlinear Schrödinger equation (HNLS) as was shown by Hasegawa [58]. Under some specific conditions involving the coefficients of the various terms in the HNLS equation it is also integrable [59, 60, 61, 62, 20] and supports optical solitons.

The NLS and HNLS equations asociated with optical solitons have the electric field pointing in a particular direction, while travelling in a direction perpendicular to it. As commonly seen with electromagnetic waves it is possible to have two such mutually perpendicular planes of polarization of the electric field inside the fiber. This results in optical solitons with their envelope functions lying in two mutually perpendicular directions. The intensity dependent nonlinear refractive index causes the two mutually perpedicular solitons to interact with each other. Zakharov and Berkhoer [63] studied these interactions of perpendicularly polarised solitons in isotropic medium. IST was first applied by Manakov for such polarised optical solitons [64, 65] with nonlinearity in the propagating fiber. For this dependence of the index of refraction on the direction of polarization has to be considered. This nonlinear effect arises due to fiber birefringence and the phenomena is called as cross phase modulation (XPM). Inclusion of XPM in the NLS equation leads to a pair of coupled NLS equations (CNLS) where XPM occurs in the nonlinear term of both the equations. This model, also known as the Manakov model. Menyuk studied the propagation of optical solitons in two perpendicular polarizations and with different group velocities [66]. The energy exchanges between the two modes of polarizations was studied by Doran and Wood [67]. The same was also studied using numerical simulations too [68]. Later Christodoulides and Joseph [69, 70] extended the Manakov model to a new class of solitons which they called as vector solitons.

Inclusion of the higher order effects to the Manakov model has lead to the modelling of the coupled version of the HNLS equation (CHNLS) which is found to be integrable under specific conditions [71, 72, 73, 74].

One of the first investigations to the collisions of scalar solitons was done by Zakharov *et.al.* [75] where it was established theoretically that solitons collisions are elastic. Similar analysis were carried out by Gordon [76], Gorshkov

and Ostrovsky [77] and Karpman and Solov'ev [78]. The numerical studies of soliton collisions were carried out by Blow and Doran [79], and Hermansson and Yervick [80]. Experiments to study the interactions of solitons were carried out by Mitschke and Mollenauer [81]. In these experimental studies, it was found that short range soliton collisions were inelastic [82] and this was attributed to electrostrictional mechanism by Dianov *et.al.* [83]. However, the long range soliton collisions as observed by Smith and Mollenauer [84] were phase-independent.

For coupled NLS systems it was shown that soliton collisions were not elastic at component level [85, 86, 87]. That is, during a collision of solitons in a coupled system, and energy exchange may occur between the different polarization states. This study was also extended to the CHNLS system [88]. The collision of solitons in the Manakov model have also been studied by Tsuchida [89].

Prior to these discoveries, the robustness of solitons for logical computations had been attempted by using the (nonintegrable) saturable NLS equation [90]. But later the component switching during soliton collisions in coupled systems was utilized to develop optical logic gates in bulk media [91]. The energy exchange between colliding vector solitons were experimentally demonstarted by Anastassiou *et.al.* [92]. The capability for information transfer using cascaded collisions of vector solitons was experimentally observed too [93]. Steiglitz theoretically designed, an all optical NAND gate [94] and multistable states for optical logic storage [95].

Such developments promise of an all optical computer based on vector solitons collisions. Such a model offer the advantages of faster switching or speedier operation in comparision to conventional logic gates based on solid state electronics. Optical logic gates are also free from the usual noise that affect electronic devices. The current status for such developments, as has been mentioned in [96] requires further study of the properties involved in soliton collisions. The study of such aspects are some of the objectives of this thesis.

For developing the suitable logic-transformations required for the construction of more complicated logic gates all the characteristic features of

collisions among vector solitons are to be known in detail. In this regard, this thesis selects the CNLS and the CHNLS systems for the study of soliton collisions. The CNLS system has been considered as it is one of the simplest system governing the dynamics of optical solitons. On the other hand, altough the CHNLS system includes the higher order effects present in the transfer of electromagnetic pulses in fibers and may have extra terms to take care of, the CHNLS system supports ultrashort pulses leading to higher bandwidth and hence faster switching of logic gates.

The study of the soliton collisions is based fact that the collision of N solitons is given by the N soliton solution (NSS) [75]. This is extended to include the n-component NSS in this work. This extension to coupled systems is a requirement for observing optical logic operations. The n-component NSS is derived by exactly solving the integrable systems taken up for study. The technique used to obtain the NSS is the Inverse Scattering Method.

Next, starting with the study of the simple n-component one soliton solution, and developed further for the n-component two and three soliton solutions, the sailent features of these vector solitons are highlighted. Such a diagnosis is then generalised for the n-component NSS. Such a study paves the way for a detailed analysis of the collision of vector solitons.

Once the nature of the collisions among vector solitons have been understood, their feasibility in the construction of the simplest logic gates under various conditions is investigated. This study is important as it is would throw the candidature of optical solitons for building optical computers in the proper perspective.

The chapter wise breakup of the thesis is given below. In *Chapter 2*, a review of the Inverse Scattering Method, particularly in the context of earlier relevant work is given. After the basic ISM is explained, its extension to the AKNS scheme is shown. In *Chapter 3*, a few dynamical systems related to optical solitons — the coupled nonlinear Schrödinger equation, the coupled higher order nonlinear Schrödinger equation of the Hirota type are introduced. Using ISM their n-component NSS is obtained explicitly. The soliton solutions of another dynamical system related to optical solitons — the coupled higher order nonlinear Schrödinger equation of the Sasa-Satsuma

type (Sasa-Satsuma equation) is also obtained using ISM in the same chapter. In *Chapter 4*, the properties of the n-component NSS of the coupled nonlinear Schrödinger equation and the coupled higher order nonlinear Schrödinger equation of the Hirota type are studied in detail while in *Chapter 5* the solition collisions of these two dynamical systems are studied. The results of this chapter are applied in *Chapter 6* to develop optical logic gates. *Chapter 7* is the concluding one.

In brief, this thesis attempts a thorough investigation into the dynamics of collisions inbetween N soliton, each having n components, and to apply the results in the designing of soliton based optical logic gates.

Chapter 2

Review of Inverse Scattering Method

2.1 Introduction to the Lax Formalism

This chapter introduces the Inverse Scattering Method (ISM). It is used in the following chapters to obtain the N soliton solutions of some Integrable Models. The ISM is one of the most elegant tool for obtaining the complete N soliton solutions of an integrable nonlinear partial differential equation. As in any transform, in ISM too, one defines a transformation of the original problem into a space of functions where the time dependence is simple. Then after having determined the transformed data at a later time, the inverse transform is applied to find the solution. Following Lax [11], in ISM one starts by considering a general nonlinear partial differential equation

$$\phi(x,t)_t = \mathbf{K}\{\phi(x,t)\} \tag{2.1}$$

where $\mathbf{K}$ is a nonlinear operator and the subscripts denote partial differentiation. For the KdV[1] equation its explicit form is

$$\mathbf{K} = 6\phi(x,t)\frac{\partial}{\partial x} - \frac{\partial^3}{\partial x^3} \tag{2.2}$$

The crucial next step is to find two linear operators $L(\phi)$ and $B(\phi)$ associated with equation (2.1) such that they satisfy the following operator equation for

[1]The KdV equation has been selected as an example.

any arbitrary function.

$$\mathtt{i}L_t = [B, L] \tag{2.3}$$

where $[B, L] = BL - LB$ is the commutator. The integrability aspect of any dynamical system using ISM purely depends on the discovery of these operators for that dynamical system. The first operator is time dependent and the second operator has to be self-adjoint, *i.e.*,

$$L = L(t), \quad B^\dagger = B \tag{2.4}$$

For KdV, these operators[2] are,

$$L = -\frac{\partial^2}{\partial x^2} + \phi \tag{2.5}$$

$$B = -4\mathtt{i}\frac{\partial^3}{\partial x^3} + 3\mathtt{i}\left(\phi\frac{\partial}{\partial x} + \frac{\partial}{\partial x}\phi\right) \tag{2.6}$$

After the Lax operators has been established, ISM is applied in three steps

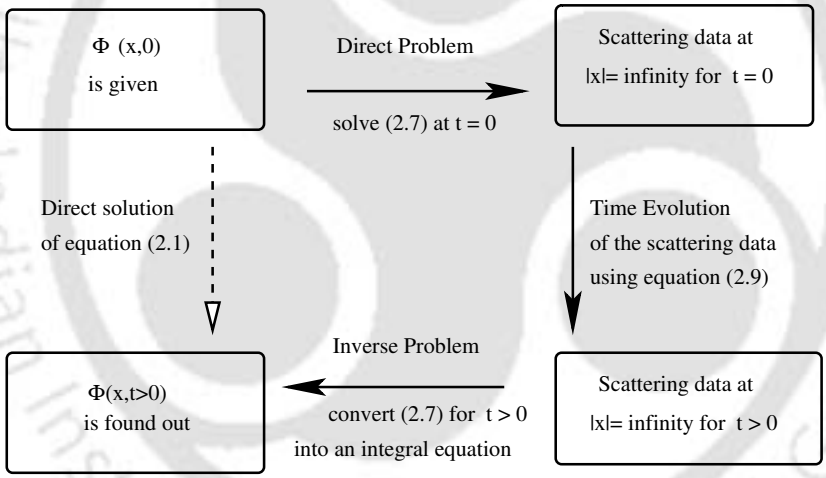

Figure 2.1: Inverse Scattering Method - Schematic Representation.

as shown in `Fig:`2.1. These are:

1. **The direct problem:** An eigenvalue equation (or a Sturm-Liouville equation) is formed with L.

$$L(t)\psi(x,t) = \lambda\psi(x,t) \tag{2.7}$$

[2]All verifications of this section are shown in Appendix A.1 & A.2

For a given ϕ, the above eigenvalue equation is solved at $t = 0$. This provides the scattering data — the reflection coefficient $R(t = 0)$, the transmission coefficient $T(t = 0)$, the normalization constant $c_n(t = 0)$ for ψ at $|x| = \infty$, and the number of bound states N. For KdV, (2.7) takes the form,

$$L(t = 0)\psi = -\psi_{xx} + \phi(x, 0)\psi = \lambda\psi \tag{2.8}$$

which is the Schrödinger wave equation with the solution of the KdV equation $\phi(x, t = 0)$ acting as the potential function and λ as the energy of the wave function $\psi(x, t)$. In the equations (2.7, 2.8) λ has to be independent of time. This should be so, despite the fact that the operator $L(t)$ through its dependence on $\phi(x, t)$, is time dependent. The time independent nature of λ can be established from the self adjoint nature of the operator B.

2. **The time-evolution of the scattering data:** Once the scattering data at the initial time has been found, the time evolution of the scattering data is calculated *i.e.*, $R(t > 0)$, $T(t > 0)$ and $c_n(t > 0)$ are determined. For this the asymptotic form of B at $|x| = \infty$ together with the time evolution of the wave function $\psi(x, t)$ is used. The time evolution of ψ is governed by B.

$$\mathtt{i}\psi(x, t)_t = B\psi(x, t) \tag{2.9}$$

3. **The inverse problem:** In the final step, an inverted or an integral form of (2.7) is used. In contrast to the first step in this procedure, here the scattering data is used to get back the scattering potential. As the scattering data used in this step is time evolved, the potential we get is the time evolved potential $\phi(x, t > 0)$. Thus the solution to the original nonlinear dynamical equation (2.1) is obtained.

2.2 Application of ISM: An example

In order to elucidate the *modus operandi* of ISM, its application to the KdV equation is considered in a brief manner in this section and next.

2.2.1 The direct problem

After having determined the Lax operators (2.5 & 2.6) for the KdV equation (*i.e.*, 2.1 with 2.2) the eigenvalue problem is formulated with the initial shape of (2.1) *i.e.*, $\phi(x, t = 0) = \phi_0(x)$ as its scattering potential.

$$\begin{aligned} & L(0)\psi(x,0) = \lambda\psi(x,0) \\ \Rightarrow \quad & \psi(x,0)_{xx} + [\lambda - \phi_0(x)]\psi(x,0) = 0 \end{aligned} \tag{2.10}$$

This is the Schrödinger wave equation with the initial energy of the wave function $\lambda > 0$ and $\lambda < 0$ depicting the scattering and bound state solutions respectively. This equation is solved to get the scattering parameters at the inital time.

$$\left.\begin{array}{rcc} R(k,0) & \rightarrow & \text{reflection coefficient for } \psi \\ & & \text{across the potential } \phi_0 \\ T(k,0) & \rightarrow & \text{transmission coefficient for } \psi \\ & & \text{across the potential } \phi_0 \\ c_n(0) & \rightarrow & \text{normalization factor for } \psi \\ \kappa_n = \sqrt{-\lambda_n} & \rightarrow & \text{allowed discrete energy levels for } \psi \\ N & \rightarrow & \text{no. of allowed discrete energy levels} \end{array}\right\} \tag{2.11}$$

The direct problem is complete once these scattering data at $t = 0$ has been evaluated at $|x| \rightarrow \infty$.

2.2.2 Time evolution of the scattering data

The scattering data extracted from the direct problem contains the eigen values $\kappa_n = \sqrt{-\lambda_n}$. As these eigen values are time independent, so also does the number of bound states N, remain time invariant. Thus, what is required is the time evolution of the remaining scattering data *i.e.*, $R(k, 0)$, $T(k, 0)$ and $c_n(0)$. For this the explicit form of B operator at $|x| \rightarrow \infty$ is considered.

$$B_\infty = -4\mathtt{i}\frac{\partial^3}{\partial x^3} \tag{2.12}$$

At $x \rightarrow -\infty$, with $\phi, \phi_x \rightarrow 0$, the bound states of (2.10) are,

$$\psi_n(x,t) = c_n(t)e^{\kappa_n x} \tag{2.13}$$

Thus, considering (2.9) and (2.12) with the fact that the eigenvalues are time invariant gives,

$$\begin{aligned} \mathtt{i}\frac{\partial \psi_n(x,t)}{\partial t} &= B_\infty \psi_n(x,t) \\ \Rightarrow \qquad c_n(t) &= c_n(0)e^{-4\kappa_n^3 t} \end{aligned} \tag{2.14}$$

Again, at $x \to \infty$, for the scattering states

$$\psi(x,t) = a(t)e^{-\mathtt{i}kx} + b(t)e^{\mathtt{i}kx} \tag{2.15}$$

and in a similar manner with B_∞

$$\frac{\partial}{\partial t}a(t)e^{-\mathtt{i}kx} + \frac{\partial}{\partial t}b(t)e^{\mathtt{i}kx} = -4(-\mathtt{i}k)^3 a(t)e^{-\mathtt{i}kx} - 4(\mathtt{i}k)^3 b(t)e^{\mathtt{i}kx}$$

Equating the linearly independent exponentials in the above equation and integrating gives,

$$a(t) = a(0)e^{-4\mathtt{i}k^3 t} \tag{2.16}$$

$$b(t) = b(0)e^{4\mathtt{i}k^3 t} \tag{2.17}$$

Consequently the reflection & transmission coefficients of (2.10) are

$$R(k,t) = \frac{b(t)}{a(t)} = \frac{b(0)}{a(0)}e^{8\mathtt{i}k^3 t} = R(k,0)e^{8\mathtt{i}k^3 t} \tag{2.18}$$

$$T(k,t) = \frac{1}{a(t)} = T(k,0)e^{4\mathtt{i}k^3 t} \tag{2.19}$$

2.2.3 The inverse problem

From the time evolved scattering data, the time evolved potential is calculated. For this inverse problem, the linear integral equation known as Gel'fand-Levitan-Marchenko (GLME) equation is used.

$$K(x,y;t) + F(x+y;t) + \int_x^\infty K(x,z;t)F(y+z;t)dz = 0 \quad \text{with} \quad y \geq x \tag{2.20}$$

This equation is deduced from the eigenvalue equation (2.7) considered at $t > 0$. It is a variant of the linear Fredholm integral equation, and can be

solved in closed form for a suitable F, and for which, existence and uniqueness of the kernel K can be confirmed by Neumann expansion solution.

In (2.20), the function F depends on the time evolved scattering data.

$$F(x+y;t) = \frac{1}{2\pi}\int_{-\infty}^{+\infty} R(k,t)e^{\mathtt{i}k(x+y)} + \sum_{n=1}^{N} c_n^2(t)e^{-\kappa_n(x+y)} \tag{2.21}$$

The first term on the *rhs* in the above equation is the fourier transform of the reflection coefficient. The transmission coefficient $T(k)$ doesnot appear in the GLME as it is eliminated in its derivation. The bound state eigenvalues κ_n show up as simple poles of $T(k)$ on the positive imaginary k-axis.

$$T(k) \sim \frac{1}{k - \mathtt{i}\kappa_n} \tag{2.22}$$

Thus the bound state eigenvalues can be noted from the denominator of the transmission coefficient.

Once the GLME (2.20) is solved for $K(x,y;t)$, $\phi(x,t)$ is calculated from it.

$$\phi(x,t) = -2\frac{d}{dx}K(x,x;t) \tag{2.23}$$

2.3 Soliton Solutions

Altough a nonlinear PDE may offer general solutions, here soliton solutions are of interest. Such solitons progresses without any change of its shape even when it passes through another soliton. This implies that a soliton acts as a reflectionless potential. Such potentials are also called as Poschel-Teller potentials and they usually have $sech^2$ forms. Thus we look for solution with $R(k) = 0 = b(k) \ \ \forall\ k$, and consequently there is no continuous spectrum. For the N soliton solution let the inital profile be

$$\phi(x,0) = -N(N+1)\mathrm{sech}^2 x \tag{2.24}$$

where N is the number of discrete states. Then

$$F(x+y;t) = \sum_{n=1}^{N} c_n^2(0)e^{8\kappa_n^3 t - \kappa_n(x+y)} \tag{2.25}$$

and (2.20) is

$$K(x,y;t)+\sum_{n=1}^{N} c_n^2(0)e^{8\kappa_n^3 t-\kappa_n(x+y)}+\int_x^{\infty} K(x,z;t)\sum_{n=1}^{N} c_n^2(0)e^{8\kappa_n^3 t-\kappa_n(x+z)}dz=0 \tag{2.26}$$

Looking for solution of the kernel in the form

$$K(x,y;t)=\sum_{n=1}^{N} L_n(x,t)e^{-\kappa_n y} \tag{2.27}$$

the GLME is replaced by a linear system

$$XY+Z=0 \tag{2.28}$$

where Y and Z are column vectors with elements Y_m and $Z_n = c_n^2(0)e^{8\kappa_n^3 t-\kappa_n(x+y)}$ respectively. The $N \times N$ matrix X has elements

$$X_{nm}=\frac{c_n^2(0)e^{8\kappa_n^3 t-\kappa_n(m+n)x}}{m+n} \tag{2.29}$$

Thus,

$$K(x,y;t)=X_{nm}^{-1}\frac{d}{dx}X_{nm} \tag{2.30}$$

and using (2.23) we get the time evolved potential $\phi(x,t)$.

$$\phi(x,t)=-\frac{\partial^2}{\partial x^2}\log|X| \tag{2.31}$$

with $|X|$ denoting the determinant of X. The solitary wave solutions or the one soliton solution for the KdV equation at different times is graphically depicted in `Fig:`2.2. The two soliton solution of the KdV equation depicts a two peaked pulse of `Fig:`2.3. At $t<0$, the taller peak is lagging behind the shorter peak. The taller pulse moves faster and coalesces to form a single peaked pulse at $t=0$. This is the initial profile $\phi(x,0)=-6\ \mathrm{sech}^2 x$ which is used to get the two soliton solution for the KdV equation using $N=2$. In a similar manner the N soliton solutions portray N pulses with the taller ones moving faster than the shorter ones.

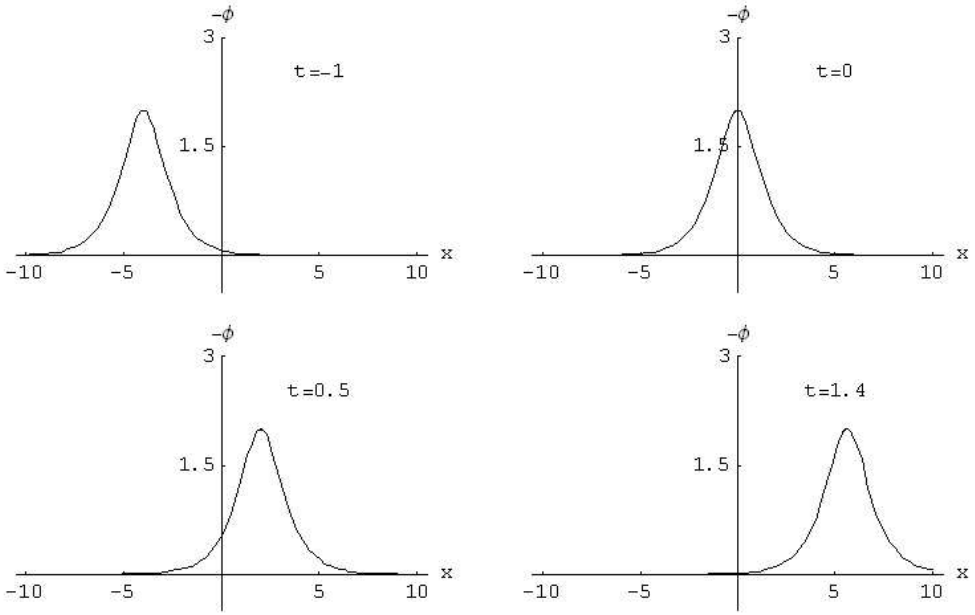

Figure 2.2: KdV solitary waves at $t = -1, 0, 0.5, 1.4$ respectively.

2.4 AKNS Scheme

2.4.1 AKNS formalism

In the AKNS formalism, the inverse scattering is applied in a slightly different manner to that outlined in the previous section. But the time independence of the eigenvalues λ for the time evolving Lax operator remains as the foundation. The nonlinear equation (2.1) is cast in terms of two linear equation,

$$\Psi_x = L\ \Psi \tag{2.32}$$

$$\Psi_t = M\ \Psi. \tag{2.33}$$

Here, $\Psi(x,t)$ is an n-component vector and L, M are $n \times n$ matrix operators which also contain the spectral parameter λ. The Lax pair L & M also contain $\phi(x,t)$, from the original nonlinear equation. The choice of a particular form of the Lax operators for a nonlinear equation has to satisfy the operator equation (also known as the zero-curvature condition).

$$L_t - M_x + [L, M] = 0 \tag{2.34}$$

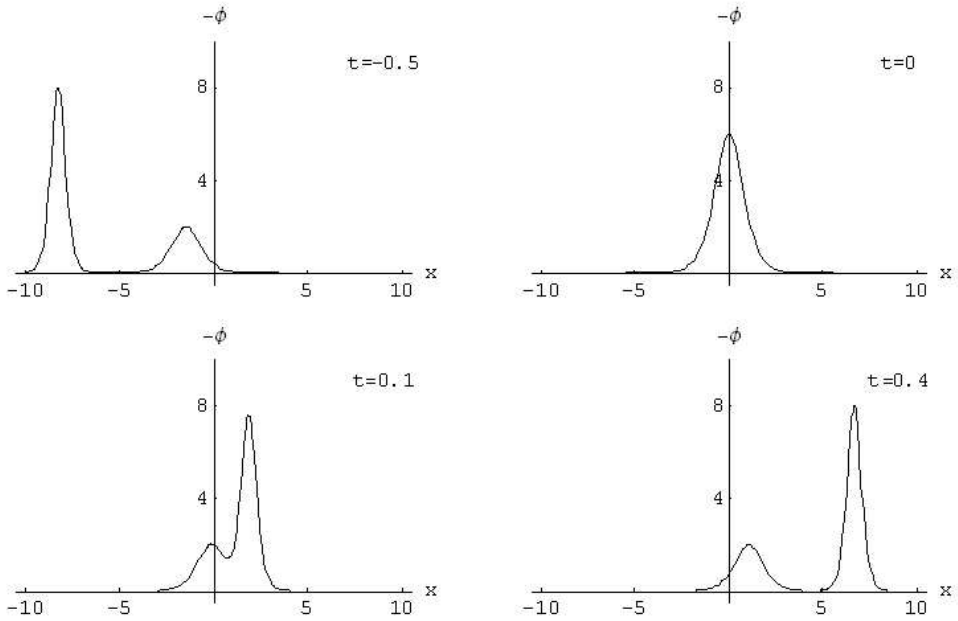

Figure 2.3: KdV two soliton solutions at $t = -0.5, 0, 0.1, 0.4$ respectively.

This is arrived at by applying the compatibility condition $\Psi_{xt} = \Psi_{tx}$ to the Lax equations (2.32, 2.33).

Following AKNS [17], L is considered to be a 2×2 matrix of the form

$$L = \begin{pmatrix} -\mathtt{i}\lambda & q \\ r & \mathtt{i}\lambda \end{pmatrix} \tag{2.35}$$

with $q = q(x,t)$ and $r = r(x,t)$ as functions of x and t. Using this form of L, it is possible to generate a class of integrable models. For example, with

$$M = \mathtt{i}\lambda^2 \begin{pmatrix} -2 & 0 \\ 0 & 2 \end{pmatrix} + \lambda \begin{pmatrix} 0 & 2q \\ 2r & 0 \end{pmatrix} + \mathtt{i} \begin{pmatrix} -qr & q_x \\ -r_x & qr \end{pmatrix} \tag{2.36}$$

and applying (2.34), with $r = -q^\star$ – the conjugate field of q, one arrives at the nonlinear Schrödinger equation (NLS).

$$\begin{aligned} \mathtt{i}q_t + q_{xx} + 2|q|^2 q &= 0 \\ -\mathtt{i}q_t^\star + q_{xx}^\star + 2|q|^2 q^\star &= 0 \end{aligned} \tag{2.37}$$

with $|q| = \sqrt{q^\star q}$. With another choice of M, *i.e.*,

$$M = \mathtt{i}\lambda^3 \begin{pmatrix} -4 & 0 \\ 0 & 4 \end{pmatrix} + \lambda^2 \begin{pmatrix} 0 & 4q \\ 4r & 0 \end{pmatrix} + \mathtt{i}\lambda \begin{pmatrix} -2qr & 2q_x \\ -2r_x & 2qr \end{pmatrix} + \begin{pmatrix} q_x r - q r_x & -q_{xx} + 2q^2 r \\ -r_{xx} + 2r^2 q & -q_x r + q r_x \end{pmatrix} \tag{2.38}$$

and with $r = \pm q$, one gets the modified KdV (mKdV) equation.

$$q_t + q_{xxx} \pm 6 q_x q^2 = 0 \tag{2.39}$$

On the other hand $r = \pm q^\star$, it is the complex mKdV equation.

$$q_t + q_{xxx} \pm 6 q_x |q|^2 = 0 \tag{2.40}$$

Finally, $r = -1$ gives the KdV equation

$$q_t + q_{xxx} + 6 q q_x = 0 \tag{2.41}$$

Again with,

$$M = \frac{\mathtt{i}}{\lambda} \begin{pmatrix} u & -\frac{1}{2} q_t \\ \frac{1}{2} r_t & -u \end{pmatrix} \tag{2.42}$$

one gets a set of dynamical equations

$$\begin{aligned} u_x &= \frac{1}{2}(qr)_t \\ q_{tx} &= 4uq \\ r_{tx} &= 4ur \end{aligned} \tag{2.43}$$

Choosing

$$u = \frac{1}{4}\cos v, \qquad q = -r = -\frac{1}{2} v_x \tag{2.44}$$

gives the sine-Gordon equation

$$v_{xt} = \sin v \tag{2.45}$$

and choosing

$$v = \frac{1}{4}\cosh u, \qquad q = r = \frac{1}{2} v_x \tag{2.46}$$

gives the sinh-Gordon equation

$$v_{xt} = \sinh v \tag{2.47}$$

Thus a number of dynamical equations can be formulated with the same time-evolving Lax operator L. All these dynamical equations comply to the same eigenvalue equation (2.32). As a result the scattering data at the inital time are identical. This leads to many common properties among these set of evolution equations, like having the same set of conserved quantities. By proper expansion of M in powers of the spectral parameter λ it is possible to generate an infinite number of integrable nonlinear equations. Such a set of evolution equations are said to belong to the same heirarchy, in this case, the ANKS heirarchy.

The time evolution of the scattering data differentiates these dynamical systems from each other. But as far as soliton solutions are concerned, only the normalization constants – $c_n(t)$'s are used. This is due to the fact that solitons solutions are associated with reflectionless coefficients and the transmission coefficients do not figure in the inverse scattering *i.e.*, in the GLME. Thus ISM can be applied to all the members of the heirarchy in a more or less comprehensive manner.

2.4.2 Inverse Scattering in the AKNS Scheme

In this sub-section the application of ISM to the AKNS heirarcy is briefly shown. The AKNS scheme is an improvization of ISM to solve integrable systems in the AKNS heirarchy in a more algorithimic manner. An application of this scheme to a simple 2×2 eigenvalue problem for the scalar NLS equation is considered first. The exact application of the AKNS scheme to multicomponent system of dynamical equations will be taken up in the next chapter.

The NLSE is given as

$$\mathtt{i}q(x,t)_t + q(x,t)_{xx} + |q(x,t)|^2 q(x,t) = 0, \tag{2.48}$$

where $q(x,t)$ represents a one dimensional dynamical field and vanish appropriately at the asymptotes.

$$\lim_{x\to\pm\infty} q(x,t) = 0 \tag{2.49}$$

In the AKNS scheme the asociated 2×2 eigenvalue problem *i.e.*, equations (2.32, 2.33) are

$$\Psi(x,t;\lambda)_x = \mathbf{L}(\lambda, q(x,t))\ \Psi(x,t;\lambda) \tag{2.50}$$

$$\Psi(x,t;\lambda)_t = \mathbf{M}(\lambda, q(x,t))\ \Psi(x,t;\lambda). \tag{2.51}$$

Here, $\Psi(x,t;\lambda)$ represents well behaved wave functions describing the scattering process and $\mathbf{L}$ & $\mathbf{M}$ are the Lax operators. In accordance to the zero curvature condition their explicit forms for the NLS equation are

$$\mathbf{L} = \begin{pmatrix} -\mathtt{i}\lambda & q \\ -q^\star & \mathtt{i}\lambda \end{pmatrix}; \qquad \mathbf{M} = \begin{pmatrix} -2\mathtt{i}\lambda^2 + \mathtt{i}|q|^2 & 2\lambda q + \mathtt{i}q_x \\ -2\lambda q^\star + \mathtt{i}q_x^\star & 2\mathtt{i}\lambda^2 - \mathtt{i}|q|^2 \end{pmatrix}; \tag{2.52}$$

By considering the scattering equation (2.50) at the asymptotes, we get its four possible solutions.

$$\Psi^{(1+)} \sim \begin{pmatrix} 1 \\ 0 \end{pmatrix} e^{-\mathtt{i}\lambda x}; \qquad \Psi^{(2+)} \sim \begin{pmatrix} 0 \\ 1 \end{pmatrix} e^{\mathtt{i}\lambda x}, \qquad x \to +\infty \tag{2.53}$$

and,

$$\Psi^{(1-)} \sim \begin{pmatrix} 1 \\ 0 \end{pmatrix} e^{-\mathtt{i}\lambda x}; \qquad \Psi^{(2-)} \sim \begin{pmatrix} 0 \\ 1 \end{pmatrix} e^{\mathtt{i}\lambda x}, \qquad x \to -\infty \tag{2.54}$$

As these Jost functions $\Psi^{(+)} = \{\Psi^{(1+)}, \Psi^{(2+)}\}$ and $\Psi^{(-)} = \{\Psi^{(1-)}, \Psi^{(2-)}\}$ are a linearly independent and complete set, they are connected via the scattering matrix $\{\alpha_{ij}\}$.

$$\Psi^{(i+)} = \{\alpha_{ij}\}\ \Psi^{(j-)} \tag{2.55}$$

Using the orthonormality of these vectors, the scattering matrix elements or the scattering data are

$$\Psi^{(j-)\dagger}\ \Psi^{(i+)} = \alpha_{ij}(\lambda). \tag{2.56}$$

From scattering theory, $\alpha_{1,1}^{-1}$ and $\alpha_{1,2}\alpha_{1,1}^{-1}$ are respectively identified as the reflection and transmission coefficients of the scattering potential $q(x,t)$. For solutions to the (2.50) an integral representation of the auxillary waves is considered.

$$\Psi^{(1-)} = \begin{pmatrix} 1 \\ 0 \end{pmatrix} e^{-\mathtt{i}\lambda x} + \int_x^\infty ds \mathbf{K}^{(1)}(x,s) e^{-\mathtt{i}\lambda s}, \tag{2.57}$$

$$\Psi^{(2-)} = \begin{pmatrix} 0 \\ 1 \end{pmatrix} e^{\mathtt{i}\lambda x} + \int_x^\infty ds \mathbf{K}^{(2)}(x,s) e^{\mathtt{i}\lambda s} \tag{2.58}$$

This representation is in accordance with the Jost functions (2.53, 2.54) and the kernels $\mathbf{K}^{(i)}(x,s) = (K_1^{(i)}(x,s), K_2^{(i)}(x,s))^T$, are well behaved functions of x & t. Besides,

$$\mathbf{K}^{(i)}(x,s) = \mathbf{0} \qquad \forall \qquad s < x.$$

Using (2.57, 2.58) in (2.50) gives an expression for the dynamical fields in terms of the Kernels.

$$q(x,t) = -2\ \mathbf{K}_1^{(2)}(x,x) \tag{2.59}$$

By considering the time evolution of $\Psi(x,t;\lambda)$ in terms of the second Lax equation (2.51) the time evolved scattering equation (2.50) can similarly be calculated and inverted to get a pair of coupled GLMEs.

$$\mathbf{K}^{(1)}(x,y) - \begin{pmatrix} 0 \\ 1 \end{pmatrix} F_1^\star(x+y) - \int_x^\infty ds \mathbf{K}^{(2)}(x,s) F_1^\star(s+y) \;=\; 0, \tag{2.60}$$

$$\mathbf{K}^{(2)}(x,y) - \begin{pmatrix} 1 \\ 0 \end{pmatrix} F_1(x+y) + \int_x^\infty ds \mathbf{K}^{(1)}(x,s) F_1(s+y) \;=\; 0 \tag{2.61}$$

These equations (2.60, 2.61) connect the time evolved scattering data with the Kernels as

$$F_1(x) = \sum_{j=1}^{N} \mathtt{i} \mathcal{C}_{2,1}^{(j)}(t) e^{-\mathtt{i}\lambda_j^\star x} + \int_{-\infty}^{+\infty} \frac{d\lambda}{2\pi} \frac{\alpha_{2,1}(\lambda)}{\alpha_{2,2}(\lambda)} e^{-\mathtt{i}\lambda x}. \tag{2.62}$$

In the above expression

$$\mathcal{C}_{2,1}^{(j)} = \frac{\alpha_{2,1}(\lambda_j,t)}{\alpha'_{2,2}(\lambda_j^\star,t)}, \tag{2.63}$$

where the time evolved scattering data are evaluated at the poles of $\alpha_{22}(\lambda)^{-1}$. These $j = 1,2,\ldots,N$ simple poles arise due to the fact that $\alpha_{22}(\lambda)^{-1}$ is analytic in the lower half of the λ-plane except at these N points.

In order to calculate the time evolution of the scattering data, the second Lax equation (2.51) is evaluated at the asymptotes where it takes the form

$$\Psi_t(x,t;\lambda) = -2\mathtt{i}\lambda^2 \Sigma\ \Psi(x,t;\lambda), \tag{2.64}$$

and then equation (2.56) is used. This gives

$$\begin{aligned} \alpha_{2,1}(\lambda,t) &= \alpha_{2,1}(\lambda,0)\ e^{-2\mathtt{i}\lambda^2 t}, \\ \alpha_{2,2}(\lambda,t) &= \alpha_{2,2}(\lambda,0). \end{aligned}$$

On the other hand the sets of GLMEs (2.60, 2.61) can be decoupled and the first component of the GLME for the kernel $\mathbf{K}^{(2)}$ is

$$\mathbf{K}_1^{(2)}(x,y)+F_1(x+y)+\int_x^\infty ds\int_x^\infty dz\mathbf{K}_1^{(2)}(x,z)F_1^\star(z+s)F_1(s+y)=0. \quad (2.65)$$

As the soliton solutions are associated with reflectionless potentials the second term in the r.h.s of (2.62) is absent. This makes it possible to attain solutions to the above equation in closed form. For this a trial solution in the form

$$\mathbf{K}_1^{(2)}(x,y)=\sum_{j=1}^{N}\omega_j(x,t)\ e^{-\mathtt{i}\lambda\star_j y} \quad (2.66)$$

is used in (2.65) and from (2.59) the N soliton solutions is obtained.

$$q(x,t)=-2\sum_{j=1}^{N}(\mathbf{B}\cdot\mathbf{C}^{-1})_j\ e^{-\mathtt{i}\lambda_j^\star x} \quad (2.67)$$

where,

$$\mathbf{B}_k = (B_1,B_2,\dots B_N)=\mathcal{C}_{2,1}^{(k)}(0)e^{-\mathtt{i}\lambda_k^\star x-4\mathtt{i}\lambda_k^{\star 2}t}, \quad (2.68)$$

$$\mathbf{C}_{k,j} = \sum_{l=1}^{N}\mathcal{C}_{2,1}^{(l)\star}\mathcal{C}_{2,1}^{(k)}\frac{e^{\mathtt{i}(2\lambda_l-\lambda_k^\star-\lambda_j^\star)x+4\mathtt{i}(\lambda_l^2-\lambda_k^{\star 2})t}}{(\lambda_l-\lambda_k^\star)(\lambda_l-\lambda_j^\star)}-\delta_{k,j} \quad (2.69)$$

are $1\times N$ and $N\times N$ matrices respectively.

2.5 Summary

In this chapter the technique of Inverse Scattering was reviewed form its simplest version to the more structured AKNS scheme. It should be mentioned that after the success of the AKNS scheme, variation appeared giving rise to other heirarchies of integrable models. Some of them are

1. Ablowitz and Ladik formalism — for discrete NLS,
2. Kaup and Newell formalism — for derivative NLS,
3. Takhtajan formalism — Heisenberg ferromagnet equation, and

4. Wadati, Konno and Ichikawa formalism — WKI integrable systems.

The AKNS scheme can be extended to support any $n \times n$ Lax operator based eigen value problem even if $n > 2$. This multi component version of the AKNS scheme is introduced and used in the next chapter to obtain the N soliton solutions for some coupled integrable models related to optical solitons.

Chapter 3

The Dynamical Systems and their Soliton Solutions

3.1 Introduction

The rate of transfer of information by means of optical fibers using pulse-code modulation is limited by the dispersive effect of group velocities. Ideally, this effect can be completely eliminated by using pulses of pico-seconds width and of moderately high intensities of a few hundred milli-Watts. This is possible because the nonlinear effects of SPM nullify GVD [51, 52] and such suggestions were experimentally demonstrated too [53, 97, 98]. Such pico-second pulses under certain conditions get transformed into optical solitons. The dynamics of such optical solitons in optical fibers is governed by the NLS equation.

$$\mathtt{i}q_{\zeta} + \alpha_1 q_{\tau\tau} + \alpha_2 |q|^2 q = 0 \tag{3.1}$$

This equation has been well investigated by many [13, 99, 100, 101, 102, 103]. In the above equation $q = q(z,t)$ denote the normalised slowly varying complex envelope of the optical pulse

$$E(z,t) \sim q(z,t)\mathtt{e}^{\mathtt{i}(\beta_0 z - \omega_0 t)} \tag{3.2}$$

travelling in z direction and with its electric field pointing in the direction perpendicular to the propagation direction and the subscripts with q denote partial derivatives. In (3.1), $\zeta = z/L_D$ and $\tau = (t - z/v_g)\Gamma_0^{-1}$ are the normalised position and time coordinates. Γ_0 is the pulse width at

$t = 0$ and v_g is the group velocity. The second term in the equation denote the pulse broadening due to GVD and $\alpha_1 = \pm 1$ denote the conditions of anomalous and normal dispersion respectively. The dispersion length is $L_D = 4\beta_0\Gamma_0^2(\partial^2\beta(\omega)/\partial\omega^2)^{-1}$. The effective refractive index in terms of the dispersion is $n_{\mathtt{eff}} = \beta(\omega)c/\omega$. $\alpha_2 = L_D/L_K$, where $L_K = c^2\beta_0(2\pi\omega_0^2|\chi_{K,\mathtt{eff}}|)^{-1}$ – is the Kerr length. $\chi_{K,\mathtt{eff}}$ – is the effective nonlinear susceptibility responsible for the Kerr effect. In practice, the NLS optical solitons do not exist in real communication systems in their ideal form, *i.e.*, as dispersionless optical pulses travelling forever. This is because of the higher order effects of susceptibility and absorption of energy via Rayleigh scattering by the fiber molecules in (3.1) which finally distort and absorb the NLS solitons. However, the distance of propagation by an optical soliton exceeds that of an ordinary weak pulse by a large margin.

For increasing the bandwidth of transmision, the propagation of pulses with ultrashort widths have to be considered. But such femto-second pulses acutely require the consideration of the higher order effects and the NLS equation has to be extended to include the higher order effects. Such an equation is the HNLS equation have the form

$$\mathtt{i}q_\zeta + \alpha_1 q_{\tau\tau} + \alpha_2|q|^2q + \mathtt{i}\{\beta_1 q_{\tau\tau\tau} + \beta_2|q|^2q_\tau + \beta_3 q(|q|^2)_\tau\} = 0 \qquad (3.3)$$

Here, β_1 represents the third order group velocity dispersion (TOD), and β_2,β_3 represent the two inertial contributions to the nonlinear polarization, *i.e.*, stimulated Raman scattering (SRS) and self-steeping (SS) [39, 82, 104, 105].

The exact solution of the general HNLS equation (3.3) has not been discovered as yet, but its complete integrability under specific conditions have been shown. They are the Derivative NLS equation (DNLS) of type I, where $\alpha_1 = 1, \alpha_2 = 0$ and $\beta_1 : \beta_2 : \beta_3 = 0 : 1 : 1$; DNLS equation of type II, where $\beta_2 : \beta_1 : \beta_3 = 0 : 1 : 0$ [106]; Hirota Equation, where $\beta_1 : \beta_2 : \beta_3 = 1 : \pm 6 : 0$ [20] and the Sasa-Satsuma Equation $\beta_1 : \beta_2 : \beta_3 = 1 : 6 : 3$ and $\alpha_1 : \alpha_2 = 1 : 2$ [59, 62, 107].

The coupled versions of these equations have the dynamical field q re-

placed by an one-dimensional array of dynamical fields, *i.e.*,

$$q \rightarrow \vec{q} = (q_1, q_2, \ldots, q_n)^T \tag{3.4}$$

In the above expression the dynamical fields $q_i, i = 1, 2, \ldots, n$ are mutually orthogonal. The coupled system with 2 components represent the two mutually perpendicular polarizations of the electric fields of the two co-propagating solitons. Such a 2-coupled NLS (2-CNLS) system for optical solitons was presented by Manakov [64] and also studied by others [108, 109, 110, 111]. The coupled HNLS equation (CHNLS) of the Hirota type was developed in [72, 112]. The multi component generalization of the Sasa-Satsuma Equation was studied in [71, 113, 114]. The generalised n-CNLS, n-CHNLS of the Hirota type and n-CHNLS of the Sasa-Satsuma type (n-CSS) are respectively

$$\mathtt{i}q_{i_t} + q_{i_{xx}} + 2q_j^\star q_j q_i = 0, \tag{3.5a}$$

$$\mathtt{i}q_{i_t} + q_{i_{xx}} + 2q_j^\star q_j q_i + \mathtt{i}\varepsilon(q_{i_{xxx}} + 3q_j^\star q_j q_{i_x} + 3q_j^\star q_{j_x} q_i) = 0, \tag{3.5b}$$

$$\mathtt{i}q_{i_t} + q_{i_{xx}} + 2q_j^\star q_j q_i + \mathtt{i}\varepsilon\{q_{i_{xxx}} + 6q_j^\star q_j q_{i_x} + 3(q_j^\star q_j)_x q_i\} = 0. \tag{3.5c}$$

In the above equations the subscripts $i, j = 1, 2, \ldots, n$, describe the component fields and Einstein's convention has been used for summations. The subscripts x, t are scaled coordinates of length and time and their appearance as subscripts represent partial derivatives of the fields with respect to them. It is important to note that the position and time coordinates x, t has interchanged places in relation to (3.1) or (3.3), as is commonly followed in the mathematical approach of integrable models. Such an interchange do not effect conclusions drawn from any analysis in this thesis.

The dynamical fields $q(x, t)$ represent the envelope function of the actual pulses of the electrical field. The small dimensionless parameter ε represents the ratio of the spectral width to the carrier frequency [104].

$$0 < \varepsilon = \frac{\Delta\omega}{\omega_0} < 1 \tag{3.6}$$

The above three dynamical systems are specific conditions of the generalised CHNLS equation

$$\mathtt{i}q_{i_t} + \alpha_1 q_{i_{xx}} + \alpha_2 q_j^\star q_j q_i + \mathtt{i}\varepsilon\{\beta_1 q_{i_{xxx}} + \beta_2 q_j^\star q_j q_{i_x} + \beta_3 (q_j^\star q_j)_x q_i\} = 0 \tag{3.7}$$

and, for $n = 1$ they reduce to their respective scalar forms. All these dynamical systems are related to optical solitons and belong to the AKNS heirarchy. In this chapter the n-component, N Soliton Solutions (NSS) of these coupled dynamical systems are derived.

3.2 Lax Operators

At first, a c-number diagonal matrix

$$\mathbf{\Sigma} = \sum_{i=1}^{n} e_{i,i} - e_{n+1,n+1} \tag{3.8}$$

and a matrix of the dynamical fields $\mathbf{A}(x,t)$ as

$$\mathbf{A}(x,t) = \sum_{i=1}^{n} q_i(x,t) e_{i,n+1} - \sum_{i=1}^{n} q_i^{\star}(x,t) e_{n+1,i} \tag{3.9}$$

is defined. In (3.8, 3.9), $e_{i,j}$'s are $n+1 \times n+1$ matrices with the i,j-th element as unity and all others elements are zeros. The stars ($\star$) denote the complex conjugates of the fields. Effectively, $\mathbf{A}$ and $\mathbf{\Sigma}$ are also $n+1 \times n+1$ matrices and from (3.8) and (3.9) it is easy to see that

$$\mathbf{\Sigma}^2 = \mathbf{I} \qquad (Identity\ matrix) \tag{3.10a}$$

$$\mathbf{\Sigma A} + \mathbf{A\Sigma} = 0 \qquad (Anti - commutation) \tag{3.10b}$$

Using the above, the Lax operators for the CNLS equation are,

$$\mathbf{L}(x,t;\lambda) = -\,\mathtt{i}\lambda\mathbf{\Sigma} + \mathbf{A} \tag{3.11a}$$

$$\mathbf{M}(x,t;\lambda) = -\,2\mathtt{i}\lambda^2\mathbf{\Sigma} + 2\lambda\mathbf{A} + \mathtt{i}\mathbf{\Sigma}(\mathbf{A}_x - \mathbf{A}^2) \tag{3.11b}$$

This is verified by the fact that on using the above Lax pairs in the zero curvature condition (2.34) we get

$$\mathbf{A}_t - \mathtt{i}\mathbf{\Sigma}\mathbf{A}_{xx} + 2\mathtt{i}\mathbf{\Sigma}\mathbf{A}^3 = \mathbf{0}$$

In driving the above equation, the set of properties (3.10) were utilised. Next, on expressing the above equation in terms of the basis using (3.9) and (3.8)

we get

$$\sum_{i=1}^{n} q_{i_t}\ e_{i,n+1} - \sum_{i=1}^{n} q^{\star}_{i_t}\ e_{n+1,i} - \mathtt{i}\sum_{i=1}^{n} q_{i_{xx}}\ e_{i,n+1} - \mathtt{i}\sum_{i=1}^{n} q^{\star}_{i_{xx}}\ e_{n+1,i}$$
$$-2\mathtt{i}\sum_{i,j=1}^{n} q^{\star}_j q_j q_i\ e_{i,n+1} - 2\mathtt{i}\sum_{i,j=1}^{n} q^{\star}_j q_j q^{\star}_i\ e_{n+1,i} = 0$$

By equating the coefficients of the same basis, we get n coupled equations — one for each component and their n complex conjugate equations, all of which are infact described by the equation (3.5a). This associates the Lax pair given in (3.11) with the CNLS equation.

In a similar manner, the Lax operators associated with the coupled Hirota Equation are,

$$\mathbf{L}(x,t;\lambda) = -\mathtt{i}\lambda\mathbf{\Sigma} + \mathbf{A} \tag{3.12a}$$
$$\begin{aligned}\mathbf{M}(x,t;\lambda) = &-2\mathtt{i}\lambda^2\mathbf{\Sigma} + 2\lambda\mathbf{A} + \mathtt{i}\mathbf{\Sigma}(\mathbf{A}_x - \mathbf{A}^2)\\ &-\varepsilon\mathbf{A}_{xx} + 2\varepsilon\mathbf{A}^3 + 4\varepsilon\lambda^2\mathbf{A} + \varepsilon(\mathbf{A}_x\mathbf{A} - \mathbf{A}\mathbf{A}_x)\\ &-2\mathtt{i}\varepsilon\lambda\mathbf{\Sigma}(\mathbf{A}_x - \mathbf{A}^2) - 4\mathtt{i}\varepsilon\lambda^3\mathbf{\Sigma}\end{aligned} \tag{3.12b}$$

and implimenting the zero curvature condition (2.34) with these Lax pairs give

$$\mathbf{A}_t - \mathtt{i}\mathbf{\Sigma}\mathbf{A}_{xx} + 2\mathtt{i}\mathbf{\Sigma}\mathbf{A}^3 + \varepsilon[\mathbf{A}_{xxx} - 3\mathbf{A}_x\mathbf{A}^2 - 3\mathbf{A}^2\mathbf{A}_x] = 0$$

Using (3.9) and (3.8) in the above equation yields the n-coupled Hirota equations and their complex conjugates.

The parameter λ which appears is the Lax pairs is called as the spectral parameter. As the CHNLS equation have the higher order effects added to the CNLS equation, these effect are ignored for the wider picosecond pulses of the CNLS. Accordingly, in the limit $\varepsilon \to 0$, (3.12) reduces to (3.11) just as (3.5b) and (3.5c) reduces to (3.5a) in the same limit.

On the other hand, a direct set of Lax pairs for the CSS equation (3.5c) have not been discovered as yet. Instead, using the following set of transfor-

mations,

$$u_i(\bar{x},\bar{t}) = q_i(z,t)\mathrm{e}^{\mathrm{i}(-\frac{x}{3\varepsilon}+\frac{2t}{27\varepsilon^2})} \tag{3.13a}$$

$$\bar{t} = t \tag{3.13b}$$

$$\bar{x} = x - \frac{t}{3\varepsilon} \tag{3.13c}$$

the equation (3.5c) is first reduced to the coupled complex modified KdV equation (CCmKdV).

$$u_{i_{\bar{t}}} + \varepsilon\{u_{i_{\bar{x},\bar{x},\bar{x}}} + 6u_j^\star u_j u_{i_{\bar{x}}} + 3(u_j^\star u_j)_{\bar{x}} u_i\} = 0 \tag{3.14}$$

Obtaining the NSS of this equation would also give the NSS of CSS equation after utilization of the transformations (3.13). The Lax pair for the CCmKdV equation (3.14) is

$$\mathbf{L}(\bar{x},\bar{t};\lambda) = -\mathrm{i}\lambda\bar{\mathbf{\Sigma}} + \bar{\mathbf{A}} \tag{3.15a}$$

$$\begin{aligned}\mathbf{M}(\bar{x},\bar{t};\lambda) =& -4\mathrm{i}\varepsilon\lambda^3\bar{\mathbf{\Sigma}} + 4\varepsilon\lambda^2\bar{\mathbf{A}} + 2\mathrm{i}\varepsilon\lambda\bar{\mathbf{\Sigma}}(\bar{\mathbf{A}}_{\bar{x}} - \bar{\mathbf{A}}^2) \\ &+ 2\varepsilon\bar{\mathbf{A}}^3 - \varepsilon\bar{\mathbf{A}}_{\bar{x}\bar{x}} + \varepsilon\bar{\mathbf{\Sigma}}(\bar{\mathbf{A}}_{\bar{x}}\bar{\mathbf{A}} - \bar{\mathbf{A}}\bar{\mathbf{A}}_{\bar{x}})\end{aligned} \tag{3.15b}$$

where,

$$\bar{\mathbf{\Sigma}} = \sum_{i=1}^{2n} e_{i,i} - e_{2n+1,2n+1} \tag{3.16a}$$

$$\begin{aligned}\bar{\mathbf{A}} =& \sum_{i=1}^{n} u_i(\bar{x},\bar{t})e_{2i-1,2n+1} + \sum_{i=1}^{n} u_i^\star(\bar{x},\bar{t})e_{2i,2n+1} \\ &- \sum_{i=1}^{n} u_i(\bar{x},\bar{t})e_{2n+1,2i-1} - \sum_{i=1}^{n} u_i^\star(\bar{x},\bar{t})e_{2n+1,2i}\end{aligned} \tag{3.16b}$$

Using the zerocurvature condition (2.34) with the above Lax pairs (3.15) yield the auxillary equation

$$\bar{\mathbf{A}}_t + \varepsilon[\bar{\mathbf{A}}_{xxx} - 3\bar{\mathbf{A}}_x\bar{\mathbf{A}}^2 - 3\bar{\mathbf{A}}^2\bar{\mathbf{A}}_x] = 0$$

As, $\bar{\mathbf{\Sigma}}$ and $\bar{\mathbf{A}}$ are $(2n+1)\times(2n+1)$ square matrices, so are the Lax pairs (3.15a) and (3.15b). Thus, using we get the explicit forms of $\bar{\mathbf{\Sigma}}$ and $\bar{\mathbf{A}}$ from (3.16) yield n equations and their complex conjugates of the n-CCmKdV and each equation appears twice in the martix implimentation of the zero curvature condition. Thus, the equations (3.14) and (3.5c) remain unchanged and the dynamical fields u_i of the CCmKdV have n components as before.

3.3 Direct Problem

3.3.1 Scattering data for CNLS and Coupled Hirota Equations

For solving the coupled dynamical equations (3.5a) and (3.5b) the 2×2 scattering problem outlined in secion (2.4.2) is extended to $(n+1) \times (n+1)$ dimensions [74]. The Lax equations are now

$$\Psi(x,t;\lambda)_x = \mathbf{L}(\lambda, q(x,t))\ \Psi(x,t;\lambda) \tag{3.17a}$$

$$\Psi(x,t;\lambda)_t = \mathbf{M}(\lambda, q(x,t))\ \Psi(x,t;\lambda) \tag{3.17b}$$

Here $\Psi(x,t;\lambda)$ is a $n+1$ dimensional vector

$$\Psi(x,t;\lambda) = \big(\psi_1(x,t;\lambda), \psi_2(x,t;\lambda), \ldots, \psi_{n+1}(x,t;\lambda)\big)^T \tag{3.18}$$

and $\mathbf{L}$ & $\mathbf{M}$ are $(n+1) \times (n+1)$ square matrices. At the two asymptotes, $x \to \pm\infty$, $q_i(x,t) \to 0$, *i.e.*, the dynamical fields are zero, and the scattering equation (3.17a) takes the form

$$\Psi(x,t;\lambda)_x = -\mathtt{i}\lambda\mathbf{\Sigma}\ \Psi(x,t;\lambda) \tag{3.19}$$

Thus solutions of (3.17a) at the two asymptotes are given as follows

$$\left.\begin{array}{rcl} \phi^{(i)} & = & e_i \mathtt{e}^{-\mathtt{i}\lambda x} \\ \phi^{(n+1)} & = & e_{n+1}\mathtt{e}^{\mathtt{i}\lambda x} \end{array}\right\} \quad \text{at} \quad x \to \infty \tag{3.20}$$

$$\left.\begin{array}{rcl} \psi^{(i)} & = & e_i \mathtt{e}^{-\mathtt{i}\lambda x} \\ \psi^{(n+1)} & = & e_{n+1}\mathtt{e}^{\mathtt{i}\lambda x} \end{array}\right\} \quad \text{at} \quad x \to -\infty \tag{3.21}$$

where, $i = 1, 2, \ldots, n$. e_i's are one dimensional basis vectors with their i-th element as one and rest of the elements are zeros. These Jost functions also form a linearly independent set and their orthonormality is expressed as

$$\phi^{(i)\dagger}\phi^{(j)} = \psi^{(i)\dagger}\psi^{(j)} = \delta_{i,j}, \qquad i,j = 1,2,\ldots,(n+1) \tag{3.22}$$

Thus it is possible to connect these set of solutions at the two asymptotes by a scattering matrix – $\{\alpha_{i,j}\}$.

$$\phi^{(i)}(x;\lambda) = \sum_{j=1}^{n+1} \alpha_{i,j}(\lambda)\psi^{(j)}(x;\lambda), \qquad j = 1,2,\ldots,(n+1) \tag{3.23}$$

Using (3.22), the elements of the scattering matrix can be expresed in terms of the Jost functions.

$$\alpha_{i,j}(\lambda) = \psi^{(j)\dagger}(x;\lambda)\phi^{(i)}(x;\lambda) \tag{3.24}$$

Finding the values of the scattering data at the initial time is the goal during the first step of the ISM (Fig:2.1).

3.3.2 Scattering data for Sasa-Satsuma Equation

For the CCmKdV equation (3.14), the form of the Lax Equations (3.17a, 3.17b) remain the same, but as demanded by the dimensions of the Lax operators (3.15), the scattering problem is now $(2n+1)\times(2n+1)$ dimensional. Consequently, $\Psi(\bar{x},\bar{t};\lambda)$ is a $(2n+1)$ dimensional vector.

$$\Psi(\bar{x},\bar{t};\lambda) = \big(\psi_1(\bar{x},\bar{t};\lambda), \psi_2(\bar{x},\bar{t};\lambda), \ldots, \psi_{2n+1}(\bar{x},\bar{t};\lambda)\big)^T \tag{3.25}$$

The Jost functions are now

$$\left.\begin{array}{rcl} \phi^{(i)} & = & e_i \mathsf{e}^{-\mathsf{i}\lambda\bar{x}} \\ \phi^{(2n+1)} & = & e_{2n+1}\mathsf{e}^{\mathsf{i}\lambda\bar{x}} \end{array}\right\} \quad \text{at} \quad \bar{x}\to\infty \tag{3.26}$$

$$\left.\begin{array}{rcl} \psi^{(i)} & = & e_i \mathsf{e}^{-\mathsf{i}\lambda\bar{x}} \\ \psi^{(2n+1)} & = & e_{2n+1}\mathsf{e}^{\mathsf{i}\lambda\bar{x}} \end{array}\right\} \quad \text{at} \quad \bar{x}\to-\infty \tag{3.27}$$

with $i = 1, 2, \ldots, 2n$, and e's are $(2n+1)$ dimensional basis vectors.

The orthonormality of the Jost functions (3.22), the scattering equation (3.23) and the scattering data (3.24) remain the same for the CCmKdV except for the fact that in these equations the indices $i, j = 1, 2, \ldots, (2n+1)$.

3.4 Gel'fand Levitan Marchenko Equation

To extend the GLME to the n-coupled and $2n$-coupled dynamical systems, some properties of the scattering matrix are considered first.

Using (3.20), (3.21) in the (3.24) gives the orthogonality of the scattering matrix elements.

$$\sum_{k=1}^{n+1} \alpha_{i,k}(\lambda)\alpha_{j,k}(\lambda) = \delta_{i,j} \tag{3.28}$$

Thus, (3.23) yields

$$\psi^{(i)}(x;\lambda) = \sum_{j=1}^{n+1} \alpha^{\star}_{j,i}(\lambda)\phi^{(j)}(x;\lambda) \tag{3.29}$$

Equation (3.28) implies the fact that the scattering matrix is unitary and gives the following relation for any of its elements.

$$\alpha^{\star}_{i,j}(\lambda) = \text{Cofactor of } \alpha_{i,j}(\lambda) \tag{3.30}$$

Using the above in conjunction with (3.23) yields

$$\frac{1}{\alpha^{\star}_{m,m}} \sum_{j=1}^{l} (Adj[\alpha_{m,m}])_{i,j}\phi^{(j)}\mathsf{e}^{\mathsf{i}\lambda x} = \psi^{(i)}\mathsf{e}^{\mathsf{i}\lambda x} - \frac{\alpha^{\star}_{m,i}}{\alpha^{\star}_{m,m}}\psi^{(m)}\mathsf{e}^{\mathsf{i}\lambda x} \tag{3.31a}$$

$$\frac{1}{\alpha_{m,m}}\phi^{(m)}\mathsf{e}^{-\mathsf{i}\lambda x} = \psi^{(m)}\mathsf{e}^{-\mathsf{i}\lambda x} - \frac{1}{\alpha_{m,m}} \sum_{j=1}^{l} \alpha_{m,j}\psi^{(j)}\mathsf{e}^{-\mathsf{i}\lambda x} \tag{3.31b}$$

In the above expressions the following convention has been followed. Unless explicitly mentioned, the same convention will also be followed in the rest of this section.

(♠) For the CNLS and the coupled Hirota equations, $l = n$, $m = n+1$ and $i, j = 1, 2, \ldots, n$; while for the CCmKdV equation $l = 2n$, $m = 2n+1$, $i, j = 1, 2, \ldots, 2n$ and x is replaced by $\bar{x}$.

Next, an integral representation of the Jost functions at finite values of x is considered.

$$\psi^{(i)}(x;\lambda) = e_i\mathsf{e}^{-\mathsf{i}\lambda x} + \int_x^{\infty} ds\mathbf{K}^{(i)}(x,s)\mathsf{e}^{-\mathsf{i}\lambda s} \tag{3.32a}$$

$$\psi^{(m)}(x;\lambda) = e_m\mathsf{e}^{\mathsf{i}\lambda x} + \int_x^{\infty} ds\mathbf{K}^{(m)}(x,s)\mathsf{e}^{\mathsf{i}\lambda s} \tag{3.32b}$$

where the kernel – $\mathbf{K}$'s can be written in component form as

$$\mathbf{K}^{(i)}(x,s) = \sum_{j=1}^{l} K^{(i)}_j(x,s)\ e_j \tag{3.33a}$$

$$\mathbf{K}^{(m)}(x,s) = \sum_{j=1}^{l} K^{(m)}_j(x,s)\ e_j \tag{3.33b}$$

Using (3.32) with (3.31b) gives

$$\frac{1}{\alpha_{m,m}}\phi^{(m)} = e_m \mathsf{e}^{\mathtt{i}\lambda x} + \int_x^\infty ds \mathbf{K}^{(m)}(x,s)\mathsf{e}^{\mathtt{i}\lambda s} + \sum_{i=1}^{l}\frac{\alpha_{m,i}}{\alpha_{m,m}} e_i \mathsf{e}^{-\mathtt{i}\lambda x} + \sum_{i=1}^{l}\frac{\alpha_{m,i}}{\alpha_{m,m}}\int_x^\infty ds \mathbf{K}^{(i)}(x,s)\mathsf{e}^{-\mathtt{i}\lambda s} \quad (3.34)$$

Multiplying both sides of the above by $\mathsf{e}^{-\mathtt{i}\lambda w}/(2\pi)$ where $w > z$ and integrating both sides from $-\infty$ to $+\infty$ with respect to λ gives:

$$\int_{-\infty}^{+\infty}\frac{d\lambda}{2\pi}\frac{\phi^{(m)}\mathsf{e}^{-\mathtt{i}\lambda w}}{\alpha_{m,m}(\lambda)} = \mathbf{K}^{(m)}(x,w) + \int_{-\infty}^{+\infty}\frac{d\lambda}{2\pi}\sum_{i=1}^{l}\frac{\alpha_{m,i}(\lambda)}{\alpha_{m,m}(\lambda)} e_i \mathsf{e}^{-\mathtt{i}\lambda(x+w)} + \int_{-\infty}^{+\infty}\frac{d\lambda}{2\pi}\int_x^\infty ds \sum_{i=1}^{l}\frac{\alpha_{m,i}(\lambda)}{\alpha_{m,m}(\lambda)}\mathbf{K}^{(i)}(x,s)\mathsf{e}^{-\mathtt{i}\lambda(s+w)} \quad (3.35)$$

As $1/\alpha_{m,m}(\lambda)$ is analytic in the lower half of the complex λ plane with N simple poles – $\lambda_k^\star,\ k = 1, 2, \ldots, N$, this allows the scattering equation (3.23) to be written as

$$\phi^{(m)}(x;\lambda_k^\star) = \sum_{p=1}^{l}\alpha_{m,p}(\lambda_k^\star)\psi^{(p)}(x;\lambda_k^\star). \quad (3.36)$$

Thus, using the above in the left hand side of (3.35) together with (3.32a) gives

$$\begin{aligned}\int_{-\infty}^{+\infty}\frac{d\lambda}{2\pi}\frac{\phi^{(m)}\mathsf{e}^{-\mathtt{i}\lambda w}}{\alpha_{m,m}(\lambda)} &= -\mathtt{i}\sum_{k=1}^{N}\frac{\mathsf{e}^{-\mathtt{i}\lambda_k^\star x}}{\alpha'_{m,m}(\lambda_k^\star)}\sum_{p=1}^{l}\alpha_{m,p}(\lambda_k^\star)\psi^{(p)}(x;\lambda_k^\star) \\ &= -\mathtt{i}\sum_{k=1}^{N}\frac{\mathsf{e}^{-\mathtt{i}\lambda_k^\star x}}{\alpha'_{m,m}(\lambda_k^\star)}\sum_{p=1}^{l}\alpha_{m,p}(\lambda_k^\star)\Big(e_p\mathsf{e}^{-\mathtt{i}\lambda_k^\star x} + \int_x^\infty ds\mathbf{K}^{(p)}(x,s)\mathsf{e}^{-\mathtt{i}\lambda_k^\star s}\Big).\end{aligned} \quad (3.37)$$

Using the above in (3.35) gives the GLME for the m-th kernel $\mathbf{K}^{(m)}$:

$$\mathbf{K}^{(m)}(x,w) + \sum_{p=1}^{l}e_p F_p(x+w) + \sum_{p=1}^{l}\int_x^\infty ds\mathbf{K}^{(p)}(x,s)F_p(w+s) = 0 \quad (3.38)$$

where,

$$F_p(x+s) = \mathtt{i}\sum_{k=1}^{N} \mathcal{C}_{m,p}^{(k)} \mathtt{e}^{-\mathtt{i}\lambda_k^\star(x+s)} + \int_{-\infty}^{+\infty} \frac{d\lambda}{2\pi} \frac{\alpha_{m,p}(\lambda)}{\alpha_{m,m}(\lambda)} \mathtt{e}^{-\mathtt{i}\lambda(x+s)} \tag{3.39}$$

with

$$\mathcal{C}_{m,p}^{(k)} = \frac{\alpha_{m,p}(\lambda_k^\star)|_{|x|\to\infty}}{\alpha'_{m,m}(\lambda_k^\star)} \tag{3.40}$$

In a similar manner, the integral GLME equations for the other kernels $\mathbf{K}^{(p)}, p = 1, 2, \ldots, l$, derived from (3.31a) and (3.32) is

$$\mathbf{K}^{(p)}(x,w) - e_m F_p^\star(x+w) - \int_x^\infty ds \mathbf{K}^{(m)}(x,s) F_p^\star(w+s) = 0 \tag{3.41}$$

Equations (3.38) and (3.41) are the set of generalised Gel'fand-Levitan-Marchenko equations. Using (3.33) in these equations the GLME equation for the p-th component of $\mathbf{K}^{(m)}$ can be derived.

$$K_p^{(m)}(x,w) + F_p(x+w) + \sum_{j=1}^{l} \int_x^\infty dv K_p^{(m)}(x,v) \int_x^\infty ds F_j(s+w) F_j^\star(s+v) = 0 \tag{3.42}$$

Using the GLME, the dynamical fields can be built back from the scattering data. In order to calculate the fields at a later time ($t > 0$), the time evolved scattering data is used.

3.5 Time Evolution of the Scattering Data

3.5.1 CNLS Case:

For calculating the time evolution of the scattering data (3.24) of the CNLS equation, the second Lax equation (3.17b) at $x \to \pm\infty$ is considered.

$$\Psi(x,t;\lambda)_t = -2\mathtt{i}\lambda^2 \mathbf{\Sigma} \tag{3.43}$$

Using the asymptotic solutions with (3.24) yield the time evolution of the scattering data.

$$\alpha_{i,i}(\lambda;t) = \alpha_{i,i}(\lambda;0) \qquad i = 1, 2, \ldots, (n+1) \tag{3.44a}$$

$$\alpha_{p,n+1}^\star(\lambda;t) = \alpha_{n+1,p}(\lambda;t) = \alpha_{n+1,p}(\lambda;0)\mathtt{e}^{4\mathtt{i}\lambda^2 t} \tag{3.44b}$$

$$\mathcal{C}_{n+1,p}^{(k)}(\lambda_k^\star;t) = \mathcal{C}_{n+1,p}^{(k)}(\lambda_k^\star;0)\mathtt{e}^{4\mathtt{i}\lambda_k^{\star 2} t} \tag{3.44c}$$

where $p = 1, 2, \ldots, n$.

3.5.2 Coupled Hirota Case:

Similarly for the coupled Hirota equation, the second Lax equation (3.17b) at $x \to \pm\infty$ yields

$$\Psi(x,t;\lambda)_t = -\mathtt{i}(2\lambda^2 + 4\varepsilon\lambda^3)\mathbf{\Sigma} \tag{3.45}$$

And using (3.24) the time evolution of the scattering data can be calculated

$$\alpha_{i,i}(\lambda;t) = \alpha_{i,i}(\lambda;0) \qquad i = 1, 2, \ldots, (n+1) \tag{3.46a}$$

$$\alpha^{\star}_{p,n+1}(\lambda;t) = \alpha_{n+1,p}(\lambda;t) = \alpha_{n+1,p}(\lambda;0)\mathtt{e}^{\mathtt{i}(4\lambda^2+8\varepsilon\lambda^3)t} \tag{3.46b}$$

$$\mathcal{C}^{(k)}_{n+1,p}(\lambda^{\star}_k;t) = \mathcal{C}^{(k)}_{n+1,p}(\lambda^{\star}_k;0)\mathtt{e}^{\mathtt{i}(4\lambda^{\star 2}_k+8\varepsilon\lambda^{\star 3}_k)t} \tag{3.46c}$$

with $p = 1, 2, \ldots, n$.

3.5.3 CCmKdV Case:

For the CCmKdV equation, the second Lax equation at $|\bar{x}| \to \infty$ gives

$$\Psi(\bar{x},\bar{t};\lambda)_{\bar{t}} = -4\mathtt{i}\varepsilon\lambda^3\bar{\mathbf{\Sigma}} \tag{3.47}$$

and the time evolution of the scattering data are

$$\alpha_{i,i}(\lambda;\bar{t}) = \alpha_{i,i}(\lambda;0) \qquad i = 1, 2, \ldots, (2n+1) \tag{3.48a}$$

$$\alpha^{\star}_{p,2n+1}(\lambda;\bar{t}) = \alpha_{2n+1,p}(\lambda;\bar{t}) = \alpha_{2n+1,p}(\lambda;0)\mathtt{e}^{8\mathtt{i}\varepsilon\lambda^3\bar{t}} \tag{3.48b}$$

$$\mathcal{C}^{(k)}_{2n+1,p}(\lambda^{\star}_k;t) = C^{(k)}_{2n+1,p}(\lambda^{\star}_k;0)\mathtt{e}^{8\mathtt{i}\varepsilon\lambda^{\star 3}_k\bar{t}} \tag{3.48c}$$

with $p = 1, 2, \ldots, 2n$.

3.6 N Soliton Solutions

By using (3.32b) in (3.17b) a relation between the dynamical fields and the kernels can be found out. This is given as

$$q_i(x,t) = -2\ K^{(m)}_i(x,x), \qquad i = 1, 2, \ldots, l. \tag{3.49}$$

Thus solving the GLME (3.42) for the kernel $K_i^{(m)}$ using time evolved scattering data and using (3.49), the time evolution of the dynamical fields can be found out. In equation (3.49), besides using the convention mentioned in (♠), $u_i(\bar{x},\bar{t})$ in the CCmKdV case has been replaced by $q_i(x,t)$.

As in the case of solitons, if the dynamical fields act as the scattering potential in the scattering equation (3.17a), then these potential have the characteristics of being reflectionless and $\alpha_{m,i}$'s of the scattering data are zeros. Consequently, for solitons

$$F_p(x+s) = \mathtt{i}\sum_{k=1}^{N} \mathcal{C}_{m,p}^{(k)} \mathtt{e}^{-\mathtt{i}\lambda_k^\star(x+s)} \tag{3.50}$$

3.6.1 CNLS Case:

Imposing the time dependance for the CNLS equation (3.44c) in above gives

$$F_p(x+s) = \mathtt{i}\sum_{k=1}^{N} \mathcal{C}_{n+1,p}^{(k)}(\lambda_k^\star;0)\mathtt{e}^{-\mathtt{i}\lambda_k^\star(x+s)+4\mathtt{i}\lambda_k^{\star 2}t} \tag{3.51}$$

To solve the GLME (3.42) for the p-th component of the kernel $K_p^{(m)}$, the following trial solution is considered

$$K_p^{(n+1)}(x,s) = \sum_{k=1}^{N} \mathcal{L}_{p,k}(x,t)\mathtt{e}^{-\mathtt{i}\lambda_k^\star s} \tag{3.52}$$

Using the above trial solution with (3.51) in (3.42) together with the condition $s=x$ imposed from the point of (3.49) gives n algebraic equations.

$$\sum_{k=1}^{N} \mathcal{L}_{p,k}(x,t)\mathtt{e}^{-\mathtt{i}\lambda_k^\star x} + \mathtt{i}\sum_{k=1}^{N} \mathcal{C}_{n+1,p}^{(k)}(0)\mathtt{e}^{-2\mathtt{i}\lambda_k^\star x+4\mathtt{i}\lambda_k^{\star 2}t} - \sum_{i,j,k=1}^{N}\sum_{l=1}^{n} \frac{\mathcal{L}_{p,j}\mathtt{e}^{-\mathtt{i}\lambda_k^\star x}}{(\lambda_j-\lambda_k^\star)(\lambda_j-\lambda_i^\star)} \mathcal{C}_{n+1,l}^{(k)}(0)\mathcal{C}_{n+1,l}^{(j)\star}(0) \times \mathtt{e}^{\mathtt{i}(2\lambda_j-\lambda_i^\star-\lambda_k^\star)x}\mathtt{e}^{4\mathtt{i}(\lambda_k^{\star 2}-\lambda_j^2)t} = 0 \tag{3.53}$$

Finally, the NSS for each component of the dynamical field can be expressed as

$$q_i(x,t) = 2\sum_{j=1}^{N} (\mathbf{B}\mathbf{C}^{-1})_{ij}\mathtt{e}^{-\mathtt{i}\lambda_j^\star x} \tag{3.54}$$

Here, $\mathbf{B}$ and $\mathbf{C}$ are $n \times N$ and $N \times N$ matrices respectively. Their elements are

$$(\mathbf{B})_{ij} = \mathtt{i}\mathcal{C}^{(j)}_{n+1,i}(0)\mathtt{e}^{-\mathtt{i}\lambda^{\star}_j x + 4\mathtt{i}\lambda^{\star 2}_j t} \tag{3.55}$$

and

$$(\mathbf{C})_{ij} = \sum_{k=1}^{N} \frac{\kappa_{k,j}}{\Lambda_{k,i}\Lambda_{k,j}} \mathtt{e}^{-\mathtt{i}(\lambda^{\star}_i + \lambda^{\star}_j - 2\lambda_k)x - 4\mathtt{i}(\lambda^2_k - \lambda^{\star 2}_j)t} + \delta_{ij} \tag{3.56}$$

In the above expresions we have used,

$$\kappa_{k,j} = \sum_{l=1}^{n} \mathcal{C}^{(k)\star}_{n+1,l}(0)\mathcal{C}^{(j)}_{n+1,l}(0), \tag{3.57}$$

$$\Lambda_{k,j} = \mathtt{i}(\lambda_k - \lambda^{\star}_j) \tag{3.58}$$

3.6.2 Coupled Hirota Case:

For the Coupled Hirota equation (3.5b), the time dependance (3.46c) reduces (3.50) to the form

$$F_i(x+s) = \mathtt{i}\sum_{k=1}^{N} \mathcal{C}^{(k)}_{n+1,i}(\lambda^{\star}_k; 0)\mathtt{e}^{-\mathtt{i}\lambda^{\star}_k(x+s) + \mathtt{i}(4\lambda^2_k + 8\varepsilon\lambda^3_k)t} \tag{3.59}$$

Following in an identical manner we arrive at the NSS for the coupled Hirota equation expressed by (3.54), but the $n \times N$ matrix $\mathbf{B}$, has elements

$$(\mathbf{B})_{ij} = \mathtt{i}\mathcal{C}^{(j)}_{n+1,i}(0)\mathtt{e}^{-\mathtt{i}\lambda^{\star}_j x + 4\mathtt{i}\lambda^{\star 2}_j t + 8\mathtt{i}\varepsilon\lambda^{\star 3}_j t} \tag{3.60}$$

and the $N \times N$ matrix $\mathbf{C}$, has elements

$$(\mathbf{C})_{ij} = \sum_{k=1}^{N} \frac{\kappa_{k,j}}{\Lambda_{k,i}\Lambda_{k,j}} \mathtt{e}^{-\mathtt{i}(\lambda^{\star}_i + \lambda^{\star}_j - 2\lambda_k)x - 4\mathtt{i}(\lambda^2_k - \lambda^{\star 2}_j + 2\varepsilon\lambda^3_k - 2\varepsilon\lambda^{\star 3}_j)t} + \delta_{ij} \tag{3.61}$$

3.6.3 CCmKdV Case:

For the CCmKdV equation (3.14), the time dependance (3.48c) reduces (3.50) to the form

$$F_i(\bar{x}+s) = \mathtt{i}\sum_{k=1}^{N} \mathcal{C}^{(k)}_{n+1,i}(\lambda; 0)\mathtt{e}^{-\mathtt{i}\lambda^{\star}_k(\bar{x}+s) + 8\mathtt{i}\varepsilon\lambda^3_k \bar{t}} \tag{3.62}$$

The p-th component of the GLME equation for the $(2n+1)$-th kernel $\mathbf{K}^{(2n+1)}$ (3.42) is

$$K_p^{(2n+1)}(\bar{x},w)+F_p(\bar{x}+w)+\sum_{j=1}^{2n}\int_{\bar{x}}^{\infty}dvK_p^{(2n+1)}(\bar{x},v)\int_{\bar{x}}^{\infty}dsF_j(s+w)F_j^{\star}(s+v)=0 \tag{3.63}$$

The Lax pair for the CCmKdV equation (3.15) controls the structure of its scattering data (3.24) and this in turn controls the values of $\mathcal{C}_{n+1,i}^{(k)}(\lambda,0)$'s and $\alpha'_{n+1,n+1}(\lambda_k^{\star})$'s. Thus structure of the Lax pairs for the CCmKdV allows the following simplification in (3.62).

$$\text{For } j=1,2,\ldots,n \Rightarrow F_j(s+w)F_j^{\star}(s+v)=F_j(s+w)F_j^{\star}(s+v) \tag{3.64a}$$

$$\text{For } j=n+1,n+2,\ldots,2n \Rightarrow F_j(s+w)F_j^{\star}(s+v)=F_j^{\star}(s+w)F_j(s+v) \tag{3.64b}$$

Thus the integral part of (3.63) becomes

$$\sum_{j=1}^{n}\int_{\bar{x}}^{\infty}dvK_p^{(2n+1)}(\bar{x},v)\int_{\bar{x}}^{\infty}ds\Big[F_j(s+w)F_j^{\star}(s+v)+F_j^{\star}(s+w)F_j(s+v)\Big] \tag{3.65}$$

Considering a trial solution of the form

$$K_i^{(n+1)}(\bar{x},s)=\sum_{k=1}^{N}\Big(\mathcal{L}_{i,k}(\bar{x},\bar{t})\mathsf{e}^{-\mathtt{i}\lambda_k^{\star}s}+\mathcal{M}_{i,k}(\bar{x},\bar{t})\mathsf{e}^{\mathtt{i}\lambda_k s}\Big) \tag{3.66}$$

the NSS for the CCmKdV found out to be

$$q_i(\bar{x},\bar{t})=2\sum_{j=1}^{N}\Big[\big(\mathbf{B}\mathfrak{D}(\mathbf{C}\mathfrak{D}+\mathfrak{C}\mathbf{D})^{-1}\big)_{ij}\mathsf{e}^{-\mathtt{i}\lambda_j^{\star}x} + \big(\mathbf{B}\mathfrak{C}(\mathfrak{C}\mathbf{D}+\mathbf{C}\mathfrak{D})^{-1}\big)_{ij}\mathsf{e}^{\mathtt{i}\lambda_j^{\star}x}\Big] \tag{3.67}$$

The elements of the matrices $\mathbf{B}$, $\mathbf{C}$, $\mathbf{D}$, $\mathfrak{C}$, $\mathfrak{D}$ are given below.

$$(\mathbf{B})_{i,j} = \mathtt{i}\mathcal{C}^{(j)}_{2n+1,i}(0)\mathtt{e}^{-\mathtt{i}\lambda^\star_k x+8\mathtt{i}\varepsilon\lambda^{\star 3}_k t} \tag{3.68}$$

$$(\mathbf{C})_{l,k} = \sum_{j=1}^{N} \frac{\kappa_{j,k}}{\Lambda_{j,k}\Lambda_{j,l}}\mathtt{e}^{\mathtt{i}(2\lambda_j-\lambda^\star_k-\lambda^\star_l)x+8\mathtt{i}\varepsilon(\lambda^3_j-\lambda^{\star 3}_k)t} + \delta_{l,k} \tag{3.69}$$

$$(\mathbf{D})_{l,k} = \sum_{j=1}^{N} \frac{\kappa_{j,k}}{\Lambda_{j,k}(\lambda_j+\lambda_l)}\mathtt{e}^{\mathtt{i}(2\lambda_j-\lambda^\star_k+\lambda_l)x+8\mathtt{i}\varepsilon(\lambda^3_j-\lambda^{\star 3}_k)t} + \delta_{l,k} \tag{3.70}$$

$$(\mathfrak{C})_{l,k} = \text{Complex Conjugate}\{(\mathbf{D})_{l,k}\} \tag{3.71}$$

$$(\mathfrak{D})_{l,k} = \text{Complex Conjugate}\{(\mathbf{C})_{l,k}\} \tag{3.72}$$

$\mathbf{B}$ is a $n \times N$ matrix while the matrices $\mathbf{C}$, $\mathbf{D}$, $\mathfrak{C}$, $\mathfrak{D}$ are $N \times N$.

On using the transformation (3.13), one may get the explicit NSS for the CSS equation (3.5c).

3.7 Summary

In this chapter, the N soliton solutions for the coupled nonlinear Schrödinger equation, the coupled higher order nonlinear Schrödinger equation of the Hirota type and the coupled higher order nonlinear Schrödinger equation of the Sasa-Satsuma type for an arbitrary n-couplings has been derived. At present, the couplings with $n = 2$ describe the propagation of two mutually perpendicular polarised fields. For the CNLS this is called as the Manakov system, while the 2-coupled Hirota and the 2-coupled Sasa-Satsuma equations are extensions of the Manakov system to include the higher order effects asociated with higher bitrate propagation by ultrashort optical pulses. Besides, being important from the theory of integrable models, the n-coupled NSS may find its application in some form of "multimode" propagation of optical solitons.

The NSS developed in this chapter is examined in detail in the next chapter.

Chapter 4

Soliton Solutions

4.1 Introduction

The N soliton solutions (3.54, 3.67) of the three dynamical systems that were derived in the previous chapter is compact and contains all the information about the propagating solitons of these dynamical systems. In order to bring out all the information given by these equations, they are being studied in detail in this chapter. The basic one soliton solution (1SS) is taken up first so that the fundamental features of solitons are projected. The two soliton solution (2SS) is the next level of sophistication and represents the simplest form of compound solitons. It is studied next. The next level of complexity is the three soliton solutions (3SS). All these studies are an intermediate step to the asymptotic study of the compound solitons. The 3SS study carries on to the restructuring of the NSS (3.54) necessary for the asymptotic study of the same. The asymptotic study is the path to bring out the nature of soliton collisions.

4.2 One Soliton Solution

4.2.1 CNLS Case:

For ease of algebraic manipulation the following parameter is introduced.

$$\eta_i(x,t) = 2\mathtt{i}\lambda_i x - 4\mathtt{i}\lambda_i^2 t - \mathtt{i}\frac{\pi}{2} \tag{4.1}$$

Then the elements of matrix $\mathbf{B}$ from (3.55) and the elements of matrix $\mathbf{C}$ from (3.56) are respectively

$$(\mathbf{B})_{ij} = \mathcal{C}^{(j)}_{n+1,i}(0)\mathtt{e}^{\eta^\star_j(x,t)+\mathtt{i}\lambda^\star_j x} \tag{4.2}$$

$$(\mathbf{C})_{ij} = \sum_{k=1}^{N} \frac{\kappa_{k,j}}{\Lambda_{k,i}\Lambda_{k,j}}\mathtt{e}^{\eta^\star_j+\eta_k-\mathtt{i}(\lambda^\star_i-\lambda^\star_j)x} + \delta_{ij} \tag{4.3}$$

The 1SS for CNLS (3.5a) can be obtained by assigning $N = 1$ in (3.54).

$$q_i(x,t) = 2(\mathbf{B}\ \mathbf{C}^{-1})_{i,1}\mathtt{e}^{-\mathtt{i}\lambda^\star_1 x} \qquad i = 1, 2, \ldots, n. \tag{4.4}$$

Here, $\mathbf{B}$ is a column matrix of dimension $n \times 1$ while matrix $\mathbf{C}$ has been reduced to a scalar. Thus,

$$q_i(x,t) = \mathcal{C}^{(1)}_{n+1,i}\mathtt{e}^{-\frac{\Delta^1_1}{2}}\mathrm{sech}\Big(\eta_{1_R} + \frac{\Delta^1_1}{2}\Big)\mathtt{e}^{-\mathtt{i}\eta_{1_I}} \tag{4.5}$$

where,

$$\eta_{1_R} = -2\lambda_{1_I}x + 8\lambda_{1_R}\lambda_{1_I}t \tag{4.6a}$$

$$\eta_{1_I} = 2\lambda_{1_R}x + 4(\lambda^2_{1_I} - \lambda^2_{1_R})t - \frac{\pi}{2} \tag{4.6b}$$

are the real and imaginary parts of $\eta_1(x,t)$ respectively, λ_i is expressed in its real and imaginary parts as

$$\lambda_i = \lambda_{i_R} + \mathtt{i}\lambda_{i_I} \tag{4.7}$$

and

$$\mathtt{e}^{\Delta^1_1} = \frac{\kappa_{1,1}}{\Lambda^2_{1,1}} \tag{4.8}$$

with

$$\kappa_{1,1} = \sum_{i=1}^{n} |\mathcal{C}^{(1)}_{n+1,i}|^2 \tag{4.9}$$

The $\Lambda_{1,1}$ parameter in (4.8) is given in (3.58). Equation (4.5) describes the complex wave envelope function for the one soliton of the CNLS system described by(3.5a). The actual wave envelope is the absolute of(4.5).

$$|q_i(x,t)| = |\mathcal{C}^{(1)}_{n+1,i}|\mathtt{e}^{-\frac{\Delta^1_1}{2}}\mathrm{sech}\Big(\eta_{1_R} + \frac{\Delta^1_1}{2}\Big) \tag{4.10}$$

Considering x and t to represent the position and time coordinates, from the above expression, it is seen that the 1SS has the following characteristics.

$$\text{Amplitude} \rightarrow \mathcal{A}_i^{(1)} = |\mathcal{C}_{n+1,i}^{(1)}| \mathrm{e}^{-\frac{\Delta_1^1}{2}} \tag{4.11a}$$

$$\text{Width} \rightarrow \Gamma^{(1)} = 2\lambda_{1_I} \tag{4.11b}$$

$$\text{Group Velocity} \rightarrow v_g^{(1)} = 4\lambda_{1_R} \tag{4.11c}$$

$$\text{Inital Phase} \rightarrow \Phi^{(1)} = \frac{\Delta_1^1}{4\lambda_{1_I}} \tag{4.11d}$$

The set of expressions (4.11) gives the dependance of the various features of the 1SS on the input variables $(\mathcal{C}_{n+1,i}^{(1)}, \lambda_1)$. As these variables are complex, $2n+2$ independent variables describe the behavior on a n-component 1SS completely. From (4.11a) it is evident that $\mathcal{C}_{n+1,i}^{(1)} = 0$ reduces that particular component of the solitons nonexistent. On the other hand, (4.11c) and (4.11b) respectively requires λ_{1_R} and λ_{1_I} to be nonzero. Thus, the $2n+2$ independent variables are necessary and sufficient for describing the n-component 1SS. Equations (4.11b) or (4.11d) restrict λ_{1_I} to have positive values only. Form (4.11d), the condition for the 1SS to have zero initial phase is

$$\sum_{i=1}^{n} \mathcal{C}_{n+1,i}^{(1)\star} \mathcal{C}_{n+1,i}^{(1)} = 4\lambda_{1_I}^2. \tag{4.12}$$

It can also been from equations (4.11) that the different components of the 1SS may differ form each other in terms of their amplitude only, all the other features — group velocity, pulse width and inital phase remain the same for all the components of the soliton.

Finally, the trajectory of the central maxima of the 1SS pulse is given by

$$t = \frac{1}{4\lambda_{1_R}} x - \frac{\Delta_1^1}{16\lambda_{1_R}\lambda_{1_I}}. \tag{4.13}$$

Form this equation (4.13), it is evident that, a positive group velocity, $v_g^{(1)} > 0$, requires the 1SS maxima to be located at $-\infty$ when $t \rightarrow -\infty$ and move to $+\infty$ when $t \rightarrow +\infty$. On the other hand, a soliton with a negative $v_g^{(1)}$ moves from $+\infty$ at $t \rightarrow -\infty$, to $-\infty$ when $t \rightarrow +\infty$.

4.2.2 Coupled Hirota Case:

The NSS for the CHNLS of the Hirota type (3.5b) is described by (3.54) with the matrices **B** and **C** defined by equations (3.60) and (3.61) respectively, and by defining

$$\eta_i(x,t) = 2\mathtt{i}\lambda_i x - 4\mathtt{i}(\lambda_i^2 + 2\varepsilon\lambda_i^3)t - \mathtt{i}\frac{\pi}{2}, \tag{4.14}$$

such that its real and imaginary parts are respectively

$$\eta_{1_R} = -2\lambda_{1_I}x + 8(\lambda_{1_R}\lambda_{1_I} + 3\varepsilon\lambda_{1_R}^2\lambda_{1_I} - \varepsilon\lambda_{1_I}^3)t \tag{4.15a}$$

$$\eta_{1_I} = 2\lambda_{1_R}x + 4(\lambda_{1_I}^2 - \lambda_{1_R}^2 + 6\varepsilon\lambda_{1_R}\lambda_{1_I}^2 - 2\varepsilon\lambda_{1_R}^3)t - \frac{\pi}{2} \tag{4.15b}$$

the 1SS for the coupled Hirota equation (3.5b) is given by the structure of (4.5). Similarly, with the redefined parameters (4.15a) and (4.15b), the actual wave envelope is given by (4.10). Thus, the characteristics of the 1SS for the coupled Hirota system are

$$\text{Amplitude} \quad \rightarrow \quad \mathcal{A}_i^{(1)} = |\mathcal{C}_{n+1,i}^{(1)}|\mathtt{e}^{-\frac{\Delta_1^1}{2}} \tag{4.16a}$$

$$\text{Width} \quad \rightarrow \quad \Gamma^{(1)} = 2\lambda_{1_I} \tag{4.16b}$$

$$\text{Group Velocity} \quad \rightarrow \quad v_g^{(1)} = 4[\lambda_{1_R} + 3\varepsilon(\lambda_{1_R}^2 - \lambda_{1_I}^2)] \tag{4.16c}$$

$$\text{Inital Phase} \quad \rightarrow \quad \Phi^{(1)} = \frac{\Delta_1^1}{4\lambda_{1_I}} \tag{4.16d}$$

From (4.16) and (4.11) it is seen that for the same input variables, the CNLS and the coupled Hirota system would exhibit one solitons of the same amplitude, width and initial phase. They would be differing only in their group velocities. Consequently, the trajectory of the central maxima of the coupled Hirota one solitons is given by

$$t = \frac{1}{4[\lambda_{1_R} + 3\varepsilon(\lambda_{1_R}^2 - \lambda_{1_I}^2)]}x - \frac{\Delta_1^1}{16\lambda_{1_I}[\lambda_{1_R} + 3\varepsilon(\lambda_{1_R}^2 - \lambda_{1_I}^2)]}. \tag{4.17}$$

Unlike the CNLS one solitons, from (4.16) it can be seen that λ_{1_R} may be zero for the coupled Hirota solitons. Thus $2n+2$ independent variables are sufficient to describe the motion of these one solitons, however the solitons can exist even with $2n+1$ variables. The condition for zero initial phase

(4.12) remain the same as that for the CNLS one solitons. The asymptotic aspects of the one soliton belonging to the coupled Hirota system remain the same with the CNLS system.

For both the cases of the CNLS and the coupled Hirota system (4.5) or (4.10) describe the behavior of each component of the 1SS. The sum of these components describe the 1SS as a whole and is given by

$$\begin{aligned} |q(x,t)| &= (q_i(x,t)q_i^{\star}(x,t))^{\frac{1}{2}} \\ &= \kappa_{1,1}\mathsf{e}^{-\frac{\Delta_1^1}{2}}\mathrm{sech}\Big(\eta_{1_R}+\frac{\Delta_1^1}{2}\Big) \end{aligned} \tag{4.18}$$

and its amplitude is,

$$\mathcal{A}(x,t) = 2\lambda_{1_I}\sqrt{\kappa_{1,1}}. \tag{4.19}$$

The other features of the 1SS remains the same as its components

4.3 Two Soliton Solution

The two soliton solution (2SS) for the CNLS system (3.5a) and the CHNLS system of the Hirota type (3.5b) are derived from (3.54) by putting $N = 2$ in this equation. Under such circumstances $\mathbf{B}$ and $\mathbf{C}$ are $2 \times N$ and 2×2 matrices respectively. The explicit form of the 2SS for these two dynamical systems is,

$$q_i(x,t) = \frac{2\sum_{j=1}^{2}\Big(\mathcal{C}_{n+1,i}^{(j)}\mathsf{e}^{\eta_j^{\star}} + \mathsf{e}^{\eta_1^{\star}+\eta_2^{\star}+\eta_j+\tilde{\Delta}_{i,j}^{1,2}}\Big)}{1+\sum_{j,k=1}^{2}\mathsf{e}^{\eta_j^{\star}+\eta_k+\Delta_k^j}+\mathsf{e}^{\eta_1+\eta_1^{\star}+\eta_2+\eta_2^{\star}+\Delta_{1,2}^{1,2}}} \tag{4.20}$$

Here,

$$\mathsf{e}^{\tilde{\Delta}_{i,j}^{1,2}} = \begin{vmatrix} \mathcal{C}_{n+1,i}^{(1)} & \mathcal{C}_{n+1,i}^{(2)} \\ \frac{\kappa_{j,1}}{\Lambda_{j,1}} & \frac{\kappa_{j,2}}{\Lambda_{j,2}} \end{vmatrix} \cdot \begin{vmatrix} 1 & 1 \\ \frac{1}{\Lambda_{j,1}} & \frac{1}{\Lambda_{j,2}} \end{vmatrix} \tag{4.21}$$

$$\mathsf{e}^{\Delta_k^j} = \frac{\kappa_{k,j}}{\Lambda_{k,j}^2} \tag{4.22}$$

$$\mathsf{e}^{\Delta_{1,2}^{1,2}} = \begin{vmatrix} \frac{\kappa_{1,1}}{\Lambda_{1,1}} & \frac{\kappa_{1,2}}{\Lambda_{1,2}} \\ \frac{\kappa_{2,1}}{\Lambda_{2,1}} & \frac{\kappa_{2,2}}{\Lambda_{2,2}} \end{vmatrix} \cdot \begin{vmatrix} \frac{1}{\Lambda_{1,1}} & \frac{1}{\Lambda_{1,1}} \\ \frac{1}{\Lambda_{2,1}} & \frac{1}{\Lambda_{2,2}} \end{vmatrix} \tag{4.23}$$

The parameters $\kappa_{i,j}$ and $\Lambda_{i,j}$ appearing in the above expressions are defined in equations (3.57) and (3.58) respectively. In order to describe the n-component two solitons solutions of the CNLS system by (4.20),

$$\eta_i(x,t) = 2\mathtt{i}\lambda_i x - 4\mathtt{i}\lambda_i^2 t - \mathtt{i}\frac{\pi}{2} \tag{4.24a}$$

$$\eta_{i_R}(x,t) = -2\lambda_{i_I} x + 8\lambda_{1_R}\lambda_{i_I} t \tag{4.24b}$$

$$\eta_{i_I}(x,t) = 2\lambda_{i_R} x + 4(\lambda_{i_I}^2 - \lambda_{i_R}^2)t - \frac{\pi}{2} \tag{4.24c}$$

where $i = 1, 2$. On the other hand, if

$$\eta_i(x,t) = 2\mathtt{i}\lambda_i x - 4\mathtt{i}(\lambda_i^2 + 2\varepsilon\lambda_i^3)t - \mathtt{i}\frac{\pi}{2}, \tag{4.25a}$$

$$\eta_{i_R}(x,t) = -2\lambda_{i_I} x + 8(\lambda_{i_R}\lambda_{i_I} + 3\varepsilon\lambda_{i_R}^2\lambda_{i_I} - \varepsilon\lambda_{i_I}^3)t \tag{4.25b}$$

$$\eta_{i_I}(x,t) = 2\lambda_{i_R} x + 4(\lambda_{i_I}^2 - \lambda_{i_R}^2 + 6\varepsilon\lambda_{i_R}\lambda_{i_I}^2 - 2\varepsilon\lambda_{i_R}^3)t - \frac{\pi}{2} \tag{4.25c}$$

with $i = 1, 2$, then (4.20) describes the 2SS of the coupled Hirota system.

The 2SS of the system are completely defined by $4(n+1)$ independent variables. The 2SS denotes two peaked pulses, with the two peaks moving independently in a nature similar to figure (2.3) but with n-components. Another way to percive the 2SS is as an interaction of two one-solitons. Thus 2SS denotes the next level of complexity after 1SS and further investigation of all these characteristics of the 2SS will be done in the next chapter.

4.4 Three Soliton Solution

By putting $N = 3$ in (3.54), one arrives at the three soliton solutions for the CNLS system (3.5a) and the CHNLS system of the Hirota type (3.5b).

$$q_i(x,t) = \frac{2\sum_{j=1}^{3}\mathcal{C}_{n+1,i}^{(j)}\mathsf{e}^{\eta_j^\star} + \sum_{j,k,l=1}^{3}\mathsf{e}^{\eta_j^\star+\eta_k^\star+\eta_l+\tilde{\Delta}_{i,l}^{j,k}} + \sum_{j,k=1}^{3}\mathsf{e}^{\eta_1^\star+\eta_2^\star+\eta_3^\star+\eta_j+\eta_k+\tilde{\Delta}_{i,j,k}^{1,2,3}}}{1 + \sum_{j,k=1}^{3}\mathsf{e}^{\eta_j^\star+\eta_k+\Delta_k^j} + \frac{1}{4}\sum_{j,k,l,m=1}^{3}\mathsf{e}^{\eta_j^\star+\eta_k^\star+\eta_l+\eta_m+\Delta_{l,m}^{j,k}} + \mathsf{e}^{\eta_1+\eta_1^\star+\eta_2+\eta_2^\star+\eta_3+\eta_3^\star+\Delta_{1,2,3}^{1,2,3}}} \tag{4.26}$$

The new parameters appearing in this expressions for the three soliton solution are defined as

$$\mathsf{e}^{\tilde{\Delta}_{i,l}^{j,k}} = \begin{vmatrix} \mathcal{C}_{n+1,i}^{(j)} & \mathcal{C}_{n+1,i}^{(k)} \\ \frac{\kappa_{l,j}}{\Lambda_{l,j}} & \frac{\kappa_{l,k}}{\Lambda_{l,k}} \end{vmatrix} \cdot \begin{vmatrix} 1 & 1 \\ \frac{1}{\Lambda_{l,j}} & \frac{1}{\Lambda_{l,k}} \end{vmatrix} \tag{4.27}$$

$$\mathsf{e}^{\tilde{\Delta}_{i,j,k}^{1,2,3}} = \begin{vmatrix} \mathcal{C}_{n+1,i}^{(1)} & \mathcal{C}_{n+1,i}^{(2)} & \mathcal{C}_{n+1,i}^{(3)} \\ \frac{\kappa_{j,1}}{\Lambda_{j,1}} & \frac{\kappa_{j,2}}{\Lambda_{j,2}} & \frac{\kappa_{j,3}}{\Lambda_{j,3}} \\ \frac{\kappa_{k,1}}{\Lambda_{k,1}} & \frac{\kappa_{k,2}}{\Lambda_{k,2}} & \frac{\kappa_{k,3}}{\Lambda_{k,3}} \end{vmatrix} \cdot \begin{vmatrix} 1 & 1 & 1 \\ \frac{1}{\Lambda_{j,1}} & \frac{1}{\Lambda_{j,2}} & \frac{1}{\Lambda_{j,3}} \\ \frac{1}{\Lambda_{k,1}} & \frac{1}{\Lambda_{k,2}} & \frac{1}{\Lambda_{k,3}} \end{vmatrix} \tag{4.28}$$

$$\mathsf{e}^{\Delta_{l,m}^{j,k}} = \begin{vmatrix} \frac{\kappa_{j,l}}{\Lambda_{j,l}} & \frac{\kappa_{k,l}}{\Lambda_{k,l}} \\ \frac{\kappa_{j,m}}{\Lambda_{j,m}} & \frac{\kappa_{k,m}}{\Lambda_{k,m}} \end{vmatrix} \cdot \begin{vmatrix} \frac{1}{\Lambda_{j,l}} & \frac{1}{\Lambda_{k,l}} \\ \frac{1}{\Lambda_{j,m}} & \frac{1}{\Lambda_{k,m}} \end{vmatrix} \tag{4.29}$$

$$\mathsf{e}^{\Delta_{1,2,3}^{1,2,3}} = \begin{vmatrix} \frac{\kappa_{1,1}}{\Lambda_{1,1}} & \frac{\kappa_{1,2}}{\Lambda_{1,2}} & \frac{\kappa_{1,3}}{\Lambda_{1,3}} \\ \frac{\kappa_{2,1}}{\Lambda_{2,1}} & \frac{\kappa_{2,2}}{\Lambda_{2,2}} & \frac{\kappa_{2,3}}{\Lambda_{2,3}} \\ \frac{\kappa_{3,1}}{\Lambda_{3,1}} & \frac{\kappa_{3,2}}{\Lambda_{3,2}} & \frac{\kappa_{3,3}}{\Lambda_{3,3}} \end{vmatrix} \cdot \begin{vmatrix} \frac{1}{\Lambda_{1,1}} & \frac{1}{\Lambda_{1,2}} & \frac{1}{\Lambda_{1,3}} \\ \frac{1}{\Lambda_{2,1}} & \frac{1}{\Lambda_{2,2}} & \frac{1}{\Lambda_{2,3}} \\ \frac{1}{\Lambda_{3,1}} & \frac{1}{\Lambda_{3,2}} & \frac{1}{\Lambda_{3,3}} \end{vmatrix} \tag{4.30}$$

For the equation (4.26) to represent the 3SS for the CNLS system (3.5a), $\eta_i(x,t)$, $\eta_{i_R}(x,t)$ and $\eta_{i_I}(x,t)$ are defined by the equation set (4.24). On the other hand, $\eta_i(x,t)$, $\eta_{i_R}(x,t)$ and $\eta_{i_I}(x,t)$ defined by the equation set (4.25) cause (4.26) to define the 3SS belonging to the CHNLS system of the Hirota type (3.5b). A total of $6(n+1)$ independent parameters define the 3SS completely. The 3SS can represent three moving solitonic pulses and can also be interpreted as the interaction of three one-solitons.

4.5 N Soliton Solution

Proceeding in a manner similar to the development of the explicit expressions for the 1SS, 2SS and 3SS, the NSS given by (3.54) can be rewritten as

$$q_i(x,t) = 2\,\frac{\mathbb{N}}{\mathbb{D}} \tag{4.31}$$

where,

$$\begin{aligned}\mathbb{N} = &\sum_{a_1=1}^{N} \mathsf{e}^{\eta^\star_{a_1}+\tilde{\Delta}_i^{a_1}} + \frac{1}{2!1!}\sum_{\substack{a_1,a_2,\\ b_2=1}}^{N} \mathsf{e}^{\eta^\star_{a_1}+\eta^\star_{a_2}+\eta_{b_2}+\tilde{\Delta}_{i,b_2}^{a_1,a_2}} \\ &+ \frac{1}{3!2!}\sum_{\substack{a_1,a_2,a_3,\\ b_2,b_3=1}}^{N} \mathsf{e}^{\eta^\star_{a_1}+\eta^\star_{a_2}+\eta^\star_{a_3}+\eta_{b_2}+\eta_{b_3}+\tilde{\Delta}_{i,b_2,b_3}^{a_1,a_2,a_3}} \\ &+ \dots \\ &+ \frac{1}{(N-1)!(N-2)!}\sum_{\substack{a_1,a_2,\dots a_{N-1},\\ b_2,b_3,\dots b_{N-1}=1}}^{N} \mathsf{e}^{\eta^\star_{a_1}+\eta^\star_{a_2}+\dots+\eta^\star_{a_{N-1}}+\eta_{b_2}+\eta_{b_3}+\dots+\eta_{b_{N-1}}} \\ &\qquad\qquad \times e^{\tilde{\Delta}_{i,b_2,b_3,\dots b_{N-1}}^{a_1,a_2,\dots a_{N-1}}} \\ &+ \frac{1}{(N-1)!}\sum_{b_2,b_3,\dots b_N=1}^{N} \mathsf{e}^{\eta^\star_1+\eta^\star_2+\dots+\eta^\star_N+\eta_{b_2}+\eta_{b_3}+\dots+\eta_{b_N}+\tilde{\Delta}_{i,b_2,b_3,\dots b_N}^{1,2,3,\dots,N}}\end{aligned} \tag{4.32a}$$

and,

$$\begin{aligned}\mathbb{D} = 1 &+ \sum_{a_1,b_1=1}^{N} \mathsf{e}^{\eta^\star_{a_1}+\eta_{b_1}+\Delta_{b_1}^{a_1}} \\ &+ \frac{1}{2!^2}\sum_{\substack{a_1,a_2,\\ b_1,b_2=1}}^{N} \mathsf{e}^{\eta^\star_{a_1}+\eta^\star_{a_2}+\eta_{b_1}+\eta_{b_2}+\Delta_{b_1,b_2}^{a_1,a_2}} \\ &+ \dots \\ &+ \frac{1}{(N-1)!^2}\sum_{\substack{a_1,\dots a_{N-1},\\ b_1,\dots b_{N-1}=1}}^{N} \mathsf{e}^{\eta^\star_{a_1}+\dots\eta^\star_{a_{N-1}}+\eta_{b_1}+\dots+\eta_{b_{N-1}}+\Delta_{b_1,b2,\dots b_{N-1}}^{a_1,a2,\dots a_{N-1}}} \\ &+ e^{\eta_1+\eta^\star_1+\eta_2+\eta^\star_2+\dots\eta_N+\eta^\star_N+\Delta_{1,2,\dots,N}^{1,2,\dots,N}}\end{aligned} \tag{4.32b}$$

with,

$$e^{\tilde{\Delta}_{i,b_2,b_3,\dots,b_N}^{a_1,a_2,\dots,a_N}} = \begin{vmatrix} \mathcal{C}_{n+1,i}^{(a_1)} & \mathcal{C}_{n+1,i}^{(a_2)} & \dots & \mathcal{C}_{n+1,i}^{(a_N)} \\ \frac{\kappa_{b_2,a_1}}{\lambda_{b_2,a_1}} & \frac{\kappa_{b_2,a_2}}{\lambda_{b_2,a_2}} & \dots & \frac{\kappa_{b_2,a_N}}{\lambda_{b_2,a_N}} \\ \vdots & \vdots & \vdots & \vdots \\ \frac{\kappa_{b_N,a_1}}{\lambda_{b_N,a_1}} & \frac{\kappa_{b_N,a_2}}{\lambda_{b_N,a_2}} & \dots & \frac{\kappa_{b_N,a_N}}{\lambda_{b_N,a_N}} \end{vmatrix} \cdot \begin{vmatrix} 1 & 1 & \dots & 1 \\ \frac{1}{\lambda_{b_2,a_1}} & \frac{1}{\lambda_{b_2,a_2}} & \dots & \frac{1}{\lambda_{b_2,a_N}} \\ \vdots & \vdots & \vdots & \vdots \\ \frac{1}{\lambda_{b_N,a_1}} & \frac{1}{\lambda_{b_N,a_2}} & \dots & \frac{1}{\lambda_{b_N,a_N}} \end{vmatrix} \tag{4.33a}$$

$$e^{\Delta^{a_1,a_2,\ldots,a_N}_{b_1,b_2,\ldots,b_N}} = \begin{vmatrix} \frac{\kappa_{b_1,a_1}}{\lambda_{b_1,a_1}} & \frac{\kappa_{b_1,a_2}}{\lambda_{b_1,a_2}} & \cdots & \frac{\kappa_{b_1,a_N}}{\lambda_{b_1,a_N}} \\ \frac{\kappa_{b_2,a_1}}{\lambda_{b_2,a_1}} & \frac{\kappa_{b_2,a_2}}{\lambda_{b_2,a_2}} & \cdots & \frac{\kappa_{b_2,a_N}}{\lambda_{b_2,a_N}} \\ \vdots & \vdots & \vdots & \vdots \\ \frac{\kappa_{b_N,a_1}}{\lambda_{b_N,a_1}} & \frac{\kappa_{b_N,a_2}}{\lambda_{b_N,a_2}} & \cdots & \frac{\kappa_{b_N,a_N}}{\lambda_{b_N,a_N}} \end{vmatrix} \cdot \begin{vmatrix} \frac{1}{\lambda_{b_1,a_1}} & \frac{1}{\lambda_{b_1,a_2}} & \cdots & \frac{1}{\lambda_{b_1,a_N}} \\ \frac{1}{\lambda_{b_2,a_1}} & \frac{1}{\lambda_{b_2,a_2}} & \cdots & \frac{1}{\lambda_{b_2,a_N}} \\ \vdots & \vdots & \vdots & \vdots \\ \frac{1}{\lambda_{b_N,a_1}} & \frac{1}{\lambda_{b_N,a_2}} & \cdots & \frac{1}{\lambda_{b_N,a_N}} \end{vmatrix} \tag{4.33b}$$

The factorials appearing before the summations in (4.32) denote the degeneracy factor. The n-component NSS is completely defined by $2N(n+1)$ independent variables $(\mathcal{C}^{(j)}_{n+1,i}; \lambda_i)$ and represents N n-component one-solitons interacting with each other. For the NSS to represent the CNLS solitons, (4.1) is used in (4.31), and on the other hand (4.14) is used in (4.31) to represent the CHNLS solitons of the Hirota type.

4.6 Summary

In this chapter the explicit forms of the 1SS, 2SS and 3SS for the CNLS and the coupled Hirota systems have been developed. From the expression for the 1SS, the characteristic features of these solitons have been highlighted. The expression for the NSS has also been restructured. All these expresions have been developed to assist in the study of soliton collisions through their asymptotic analysis. Such a study is carried out in the subsequent chapter.

It appears that, for the same input parameters, the 1SS for the CNLS and coupled Hirota systems exhibit many similar features. Only their group velocities differ. Thus for the same input conditions, the solitons of femtosecond width move with a diferent speed as compared to the solitons with picosecond width. This difference of group velocities inbetween these two coupled system has surfaced from the different time evolutions of the scattering data, which has its source in the Lax operators [Chapter 3] and hence to the inclusion of the higher order effects in the CHNLS system. This is so because the pattern of the Lax pair is dependent on the dynamical system it describes.

Chapter 5

Collisions of Solitons

5.1 Introduction

The one soliton solutions represent a single solitonic pulse. The two and higher soliton solutions represent two or more solitonic pulses. These higher solitonic solutions can also be interpreted as the interaction of one-solitons. Asymptotically, or whenever the seperation of the solitons in these higher soliton solutions are large enough, the individual traits of each soliton becomes apparent. By asymptotically studying the nature of the soliton solutions, one can observe the behavior of the soliton interactions. In this chapter, the study of soliton collisions are carried out using such asymptotic analysis of the soliton solutions.

The study of soliton collisions for the scalar systems was first carried by Zakharov *et.al* [75]. Later, interesting results regarding the collisions of two solitons for the 2-coupled or 2-component CNLS system were presented by Radhakrishnan *et.al* [85].

In Zakharov's work it was established that scalar solitons interact with each other elastically. The only signature that an interaction has occured was a phase jump undergone by a soliton during the interaction with the other soliton. Such a phase jump occurs to each soliton partaking in the interaction.

In the work of Radhakrishnan *et.al.*, it was found that, for coupled systems each component of the soliton may interact in an inelastic manner. The

missing energy is transferred to the other components of the soliton and the net energy of the total soliton *i.e.*, sum of the energies of the components remains conserved. Therefore, these interesting results of coupled systems is also in agreement with the result for scalar systems. The energy exchange inbetween the components of a multicomponent soliton during its collision with another soliton was experimentally studied in [92].

This chapter commences with the development of a scaling that results in a change of the initial phase of the 1SS without affecting any of the other features of the soliton. After that, the simplest form of soliton collisions — the interaction of two solitons is presented. This is followed by the development of three soliton collisions, which can also be considered as the simplest form of collisions of any N solitons. This is due to the fact that the sequence of the collisions of N soliton collisions, cannot be studied from two soliton collisions. This is followed by the extension to the development of N soliton collisions. The studies presented in this chapter has been developed for the CNLS system and the CHNLS system of the Hirota type for fields with n-components. Reduction of the expressions for $n = 2$ describes the Manakov system and its extension to include higher order effects respectively. It should also be noted that an interchange of the time and position coordinates is present between the Manakov system and the dynamical systems presented here.

5.2 Exclusive Phase Change in 1SS

The nature of 1SS defined in (4.5) is controlled by $2(n+1)$ input parameters comprising of $(\mathcal{C}^{(1)}_{n+1,i}, \lambda_1)$ where $i = 1, 2, \ldots, n$. Any change in any of the n $\mathcal{C}^{(1)}_{n+1,i}$'s would cause a change in the amplitude and initial phase of the one-soliton, but the width and group velocity would remain unaffected. This is evident for the set of equations (4.11) and (4.16) for the CNLS (3.5a) and the coupled Hirota systems (3.5b) respectively. But if all the components the complex parameter $\mathcal{C}^{(1)}_{n+1,i}$ are scaled by any real parameter $\gamma > 0$, *i.e.*

$$\mathcal{C}^{(1)}_{n+1,i} \longrightarrow \mathcal{C}^{(1)'}_{n+1,i} = \gamma\, \mathcal{C}^{(1)}_{n+1,i}, \tag{5.1}$$

then

$$\kappa_{1,1} \longrightarrow \kappa_{1',1'} = \gamma^2\ \kappa_{1,1}; \qquad \mathsf{e}^{\frac{\Delta_1^1}{2}} \longrightarrow \mathsf{e}^{\frac{\Delta_{1'}^{1'}}{2}} = \gamma\ \mathsf{e}^{\frac{\Delta_1^1}{2}} \tag{5.2}$$

and

$$\mathcal{C}^{(1)}_{n+1,i}\mathsf{e}^{-\frac{\Delta_1^1}{2}} \longrightarrow \mathcal{C}^{(1)'}_{n+1,i}\mathsf{e}^{-\frac{\Delta_{1'}^{1'}}{2}} = \mathcal{C}^{(1)}_{n+1,i}\mathsf{e}^{-\frac{\Delta_1^1}{2}} \tag{5.3}$$

Thus the amplitude of the 1SS (4.11a) or (4.16a) remain invarient under such a γ-scaling. The initial phase $\Phi^{(1)}$ is the only characteristic of the soliton that undergoes change. Thus (5.1) causes a soliton to undergo a phase change only. From (4.11d) or (4.16d), the phase change undergone by the soliton is

$$\Phi^{(1)} \longrightarrow \Phi^{(1)'} = \Phi^{(1)} + \frac{\ln\gamma}{2\lambda_{1_I}} \tag{5.4}$$

This feature is graphically depicted in figures (`Fig:`5.1 and `Fig:`5.2) as a shift of the 'transformed' soliton S1′ in the (x,t) diagram relative to the original soliton, $\mathrm{S}^{(1)}$. The two one-solitons are identical except for a relative phase difference $\delta\Phi^{(1)} = \frac{\ln\gamma}{2\lambda_{1_I}}$. Figure (`Fig:`5.1) depicts a 2-component CNLS system and figure (`Fig:`5.2) depicts a 2-component coupled Hirota system.

This observation is useful for showing the elastic and inelastic nature of soliton collisions.

5.3 Asymptotic Nature of the Two Soliton Solution

The two pulses in the 2SS can be interpreted as the interaction of two one-solitons $\mathrm{S}^{(1)}$ and $\mathrm{S}^{(2)}$, characterised by the parameters, $(\mathcal{C}^{(1)}_{n+1,i}, \lambda_1)$ and $(\mathcal{C}^{(2)}_{n+1,i}, \lambda_2)$. Their n-component fields are respectively

$$q_i^{(1)}(x,t) = \mathcal{C}^{(1)}_{n+1,i}\mathsf{e}^{-\frac{\Delta_1^1}{2}}\mathrm{sech}\Big(\eta_{1_R} + \frac{\Delta_1^1}{2}\Big)\mathsf{e}^{-\mathrm{i}\eta_{1_I}} \tag{5.5a}$$

and

$$q_i^{(2)}(x,t) = \mathcal{C}^{(2)}_{n+1,i}\mathsf{e}^{-\frac{\Delta_2^2}{2}}\mathrm{sech}\Big(\eta_{2_R} + \frac{\Delta_2^2}{2}\Big)\mathsf{e}^{-\mathrm{i}\eta_{2_I}} \tag{5.5b}$$

where, $i = 1, 2, \ldots, n$. From (4.5) or (4.10) it is seen that the $\mathrm{sech}\Big(\eta_{1_R} + \frac{\Delta_1^1}{2}\Big)$ term controls the envelope profile of the one-soliton represented by $(\mathcal{C}^{(1)}_{n+1,i}, \lambda_1)$

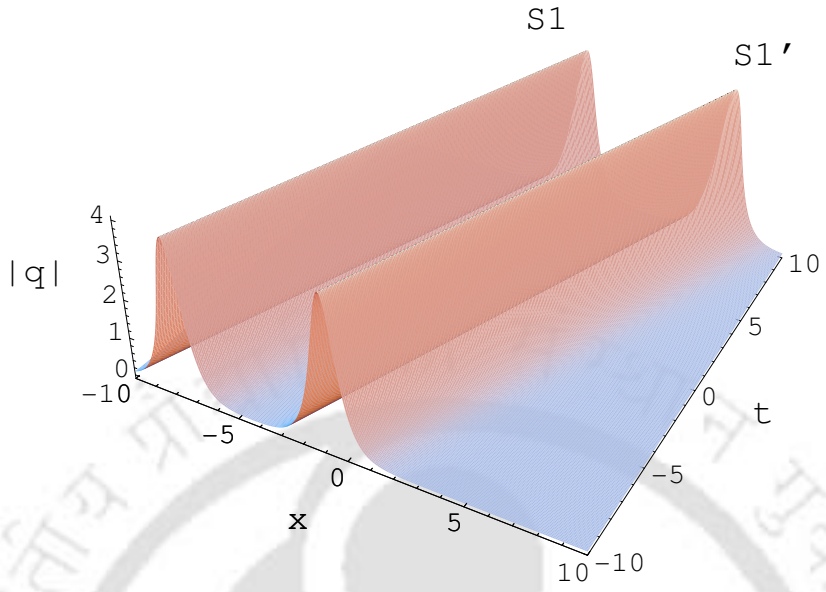

Figure 5.1: Effect of $\mathcal{C}^{(1)}_{3,i} \rightarrow \mathcal{C}^{(1)'}_{3,i} = \gamma\, \mathcal{C}^{(1)}_{3,i}$ in 1SS for $\mathcal{C}^{(1)}_{3,1} = \mathcal{C}^{(1)}_{3,2} = 10^{-3}, \gamma = 10^6, \lambda_1 = 0.1 + \mathtt{i}, \delta\Phi^{(1)} \approx 6.9$ in a 2-coupled CNLS.

i.e., $\eta_{1_R} + \frac{\Delta^1_1}{2} = 0$, locates the position of the central maxima for any (x,t). On the other hand if, $\eta_{1_R} + \frac{\Delta^1_1}{2} \rightarrow \pm\infty \Rightarrow \text{sech}\left(\eta_{1_R} + \frac{\Delta^1_1}{2}\right) \rightarrow 0$ and (x,t) represents a position away from the soliton's central maxima, or where the soliton is absent. Thus the points away from the soliton will be represented by

$$\eta_{1_R}(x,t) \rightarrow \pm\infty \tag{5.6}$$

and depending on the signs of λ_{1_R} and λ_{1_I} they represent points at the asymptototes $(x \rightarrow \pm\infty, t \rightarrow \pm\infty)$. A similar argument holds for $\mathrm{S}^{(2)}$ with

$$\eta_{2_R}(x,t) \rightarrow \pm\infty \tag{5.7}$$

representing the asymptotic regions where $\mathrm{S}^{(2)}$ is absent. Again, at a time t, the two one-solitons of the 2SS, represented by (5.5) for the CNLS system

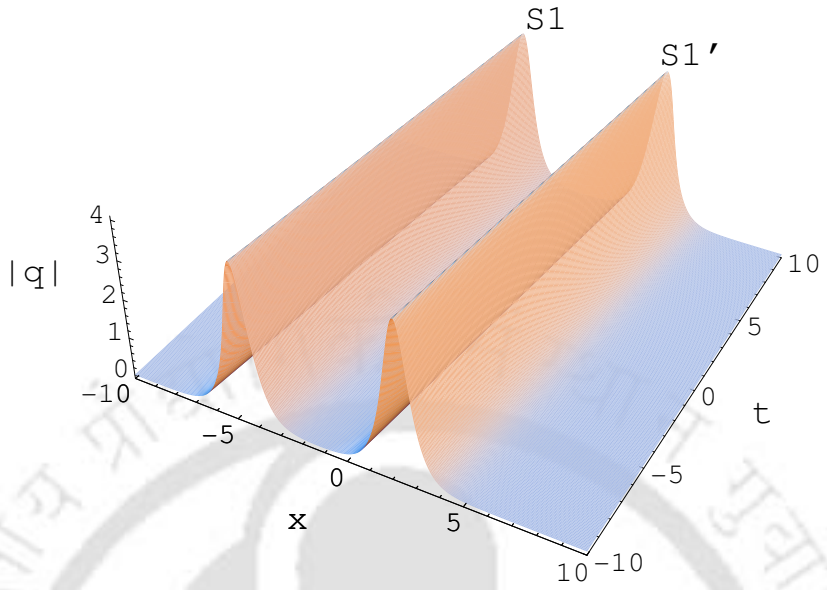

Figure 5.2: Effect of $\mathcal{C}_{3,i}^{(1)} \rightarrow \mathcal{C}_{3,i}^{(1)'} = \gamma\ \mathcal{C}_{3,i}^{(1)}$ in 1SS for $\mathcal{C}_{3,1}^{(1)} = \mathcal{C}_{3,2}^{(1)} = 10^{-3}$, $\gamma = 10^{6}$, $\lambda_1 = 0.1 + \mathtt{i}$, $\delta\Phi^{(1)} \approx 6.9$ in a 2-coupled CHNLS of the Hirota type. Note: `The solitons in this figure differ from those of fig:5.1 only in respect to their group velocities.`

(3.5a) have their central maxima located at x_1 and x_2 such that,

$$\eta_{1_R}(x_1,t) + \frac{\Delta_1^1}{2} = -2\lambda_{1_I}x_1 + 8\lambda_{1_R}\lambda_{1_I}t + \frac{\Delta_1^1}{2} = 0 \tag{5.8a}$$

$$\eta_{2_R}(x_2,t) + \frac{\Delta_2^2}{2} = -2\lambda_{2_I}x_2 + 8\lambda_{2_R}\lambda_{2_I}t + \frac{\Delta_2^2}{2} = 0 \tag{5.8b}$$

From the above equations, the seperation of the peaks at time t is

$$\delta x = x_1 - x_2 = 4(\lambda_{1_R} - \lambda_{2_R})t + \frac{1}{4}\left(\frac{\Delta_1^1}{\lambda_{1_I}} - \frac{\Delta_2^2}{\lambda_{2_I}}\right) \tag{5.9}$$

Thus initially or finally *i.e.*, at $t \rightarrow \pm\infty$ the seperation of the two peaks $|\delta x|$ is also infinite. Besides, the two solitons will meet, or the point of intersection of their paths based on their initial conditions at a time,

$$t = \frac{1}{16}\left(\frac{\Delta_2^2}{\lambda_{2_I}} - \frac{\Delta_1^1}{\lambda_{1_I}}\right)\frac{1}{\lambda_{1_R} - \lambda_{2_R}} \tag{5.10}$$

Similarly, the seperation of the two peaks of the one-solitons in 2SS for the CHNLS system of the Hirota type is given by

$$\delta x = 4[\lambda_{1_R} - \lambda_{2_R} + 3\varepsilon(\lambda_{1_R}^2 - \lambda_{2_R}^2 - \lambda_{1_I}^2 + \lambda_{2_I}^2)]t + \frac{1}{4}\left(\frac{\Delta_1^1}{\lambda_{1_I}} - \frac{\Delta_2^2}{\lambda_{2_I}}\right) \tag{5.11}$$

and the point of intersection is

$$t = \frac{1}{16}\left(\frac{\Delta_2^2}{\lambda_{2_I}} - \frac{\Delta_1^1}{\lambda_{1_I}}\right)\frac{1}{\lambda_{1_R} - \lambda_{2_R} + 3\varepsilon(\lambda_{1_R}^2 - \lambda_{2_R}^2 - \lambda_{1_I}^2 + \lambda_{2_I}^2)} \tag{5.12}$$

The asymptotic behavior of the 2SS is utilised in the study of the interaction of two one-soliton in the next section.

5.4 Collision of Two Solitons

The presence of the terms $\Delta_1^1,\ \Delta_2^2,\ \tilde{\Delta}_{i,1}^{1,2},\ \tilde{\Delta}_{i,2}^{1,2}$ and $\Delta_{1,2}^{1,2}$, in the expression for the 2SS (4.20) ensure nontrivial interaction between the two one-solitons in 2SS.

Considering $\eta_{2_R} \to -\infty$ in the 2SS (4.20) it reduces to (5.5a), the one-soliton $\mathrm{S}^{(1)}$ for $(\mathcal{C}_{n+1,i}^{(1)}, \lambda_1)$ which moves with $v_g^{(1)}$. As it contain none of the parameters fo the other soliton, it represents $\mathrm{S}^{(1)}$ before its collision with the other soliton. On the other hand, $\eta_{1_R} \to -\infty$ reduces the 2SS to (5.5b) representing the other one-soliton $\mathrm{S}^{(2)}$ described by the parameters $(\mathcal{C}_{n+1,i}^{(2)}, \lambda_2)$ moving with with $v_g^{(2)}$. Again, as it doesnot contain the any of the parameters of $\mathrm{S}^{(1)}$ it represents the soliton $\mathrm{S}^{(2)}$ before its collision with $\mathrm{S}^{(1)}$. The condition for a collision is represented by, $v_g^{(1)} \neq v_g^{(2)}$. For the CNLS system, this reduces to,

$$\lambda_{1_R} \neq \lambda_{2_R} \tag{5.13}$$

which is in agreement with equations (5.10) or (5.9). The condition for a collision to take place in the coupled Hirota solitons is

$$\lambda_{1_R} + 3\varepsilon(\lambda_{1_R}^2 - \lambda_{1_I}^2) \neq \lambda_{2_R} + 3\varepsilon(\lambda_{2_R}^2 - \lambda_{2_I}^2) \tag{5.14}$$

which is in agreement with equations (5.12) or (5.11).

On the other hand, the limit $\eta_{2_R} \to +\infty$ reduces the 2SS (4.20) to the 1SS for $S^{(1)}$ with a modified amplitude and phase.

$$q_i^{(1)'}(x,t) = \mathcal{C}_{n+1,i}^{(1)'} \mathrm{e}^{-\frac{\Delta_{1'}^{1'}}{2}} \mathrm{sech}\Big(\eta_{1_R} + \frac{\Delta_{1'}^{1'}}{2}\Big) \mathrm{e}^{-\mathrm{i}\eta_{1_I}} \tag{5.15}$$

The modified complex amplitude $\mathcal{C}_{n+1,i}^{(1)'} \mathrm{e}^{-\frac{\Delta_{1'}^{1'}}{2}}$ and phase $\frac{\Delta_{1'}^{1'}}{4\lambda_{1_I}}$ are described by a transformation of the $\mathcal{C}_{n+1,i}^{(1)}$ parameter.

$$\mathcal{C}_{n+1,i}^{(1)} \longrightarrow \mathcal{C}_{n+1,i}^{(1)'} = \mathrm{e}^{\tilde{\Delta}_{i,2}^{1,2} - \Delta_2^2} \tag{5.16}$$

with

$$\Delta_{1'}^{1'} = 2 \ln \Big[\frac{\kappa_{1',1'}}{\lambda_{1_I}^2}\Big] = \Delta_{1,2}^{1,2} - \Delta_2^2 \tag{5.17}$$

where,

$$\kappa_{1',1'} = \sum_{i=1}^{n} \mathcal{C}_{n+1,i}^{(1)'\star}\, \mathcal{C}_{n+1,i}^{(1)'}. \tag{5.18}$$

The changes undergone by the soliton $S^{(1)}$ contains parameters of the soliton $S^{(2)}$ and it can be considered to have interacted with $S^{(2)}$ nontrivially. However, the collision doesnot affect the group velocity and width of the soliton as can be seen from (5.5b). The modified amplitude and phase of the soliton are

$$\mathcal{A}_i^{(1)'} = |\mathcal{C}_{n+1,i}^{(1)'}| \mathrm{e}^{-\frac{\Delta_{1'}^{1'}}{2}} = \mathrm{e}^{\tilde{\Delta}_{i,2}^{1,2} - \frac{\Delta_{1,2}^{1,2} + \Delta_2^2}{2}} \tag{5.19}$$

and

$$\Phi^{(1)'} = \frac{\Delta_{1'}^{1'}}{4\lambda_{1_I}} = \frac{\Delta_{1,2}^{1,2} - \Delta_2^2}{4\lambda_{1_I}}. \tag{5.20}$$

In a similar manner, in the limit $\eta_{1_R} \to +\infty$ the 2SS represents soliton $S^{(2)}$ after it had interacted with $S^{(1)}$ and is given as

$$q_i^{(2)'}(x,t) = \mathcal{C}_{n+1,i}^{(2)'} \mathrm{e}^{-\frac{\Delta_{2'}^{2'}}{2}} \mathrm{sech}\Big(\eta_{2_R} + \frac{\Delta_{2'}^{2'}}{2}\Big) \mathrm{e}^{-\mathrm{i}\eta_{1_2}} \tag{5.21}$$

where,

$$\mathcal{C}_{n+1,i}^{(2)'} = \mathrm{e}^{\tilde{\Delta}_{i,1}^{2,1} - \Delta_1^1} \tag{5.22}$$

$$\Delta_{2'}^{2'} = 2 \ln \Big[\frac{\kappa_{2',2'}}{\lambda_{2_I}^2}\Big] = \Delta_{1,2}^{1,2} - \Delta_1^1 \tag{5.23}$$

$$\kappa_{2',2'} = \sum_{i=1}^{n} \mathcal{C}_{n+1,i}^{(2)'\star}\, \mathcal{C}_{n+1,i}^{(2)'}. \tag{5.24}$$

The modified amplitude and phase of $S^{(2)}$ after this interaction with $S^{(1)}$ are

$$\mathcal{A}_i^{(2)'} = |\mathcal{C}_{n+1,i}^{(2)'}|\mathsf{e}^{-\frac{\Delta_{2'}^{2'}}{2}} = \mathsf{e}^{\tilde{\Delta}_{i,1}^{1,2} - \frac{\Delta_{1,2}^{1,2}+\Delta_1^1}{2}} \tag{5.25}$$

$$\Phi^{(2)'} = \frac{\Delta_{2'}^{2'}}{4\lambda_{2_I}} = \frac{\Delta_{1,2}^{1,2} - \Delta_1^1}{4\lambda_{2_I}} \tag{5.26}$$

respectively.

As the velocities of $S^{(1)}$ and $S^{(2)}$ after their collisions with each other remains unchanged, they continue to move in the same direction as before. However, there is a shift in their trajectories due to their phase changes. This shift is same for both the solitons as it can be seen from (5.20) and (5.26) that

$$\delta\Phi^{(1)'} = \delta\Phi^{(2)'} = \mathsf{e}^{\Delta_{1,2}^{1,2}} \tag{5.27}$$

where we have defined, $\delta\Phi^{(j)'} = \Phi^{(j)'} - \Phi^{(j)}$ for $j = 1, 2$. The phase change is the same for all the components while the amplitude change may be different for different components. This is the inelastic collision of solitons at component level.

In order to understand the inelastic scattering for multicomponent systems, $\mathcal{C}_{n+1,i}^{(1)'}$ from (5.16) is written as

$$\mathcal{C}_{n+1,i}^{(1)'} = \mathsf{e}^{\tilde{\Delta}_{i,2}^{1,2} - \Delta_2^2 - \tilde{\Delta}_i^1}\mathcal{C}_{n+1,i}^{(1)} = \gamma_i^{(1)}\ \mathcal{C}_{n+1,i}^{(1)} \tag{5.28}$$

where,

$$\gamma_i^{(1)} = \mathsf{e}^{\tilde{\Delta}_{i,2}^{1,2} - \Delta_2^2 - \tilde{\Delta}_i^1}$$

and using $\mathcal{C}_{n+1,i}^{(1)} = \mathsf{e}^{\tilde{\Delta}_i^1}$ from (4.33a). In other words, after collision with soliton $S^{(2)}$, $\mathcal{C}_{n+1,i}^{(1)}$ of soliton $S^{(1)}$ undergoes a scale transformation by $\gamma_i^{(1)}$ for each of the $i = 1, 2, \ldots, n$ components, leaving λ_1 unchanged. If $\gamma_i^{(1)}$ for the different components $i = 1, 2, \ldots, n$ are unequal, the $\mathcal{C}_{n+1,i}^{(1)}$'s for the different components get scaled differently and consequently the amplitudes (4.11a) and (4.16a) of the different components get scaled by different amounts leading to inelastic collisions at component level. The scaling (5.28) for the soliton $S^{(2)}$ due to its interaction with $S^{(1)}$ is,

$$\mathcal{C}_{n+1,i}^{(2)'} = \mathsf{e}^{\tilde{\Delta}_{i,1}^{2,1} - \Delta_1^1 - \tilde{\Delta}_i^2}\mathcal{C}_{n+1,i}^{(2)} = \gamma_i^{(2)}\ \mathcal{C}_{n+1,i}^{(2)} \tag{5.29}$$

where,

$$\gamma_i^{(2)} = \mathsf{e}^{\tilde{\Delta}_{i,1}^{2,1} - \Delta_1^1 - \tilde{\Delta}_i^2}$$

The condition for inelastic collision at component level for a collision of two solitons is,

$$\gamma_i^{(k)} \neq \gamma_j^{(k)}, \quad \text{with } i \neq j \qquad i, j = 1, 2, \ldots, n; k = 1, 2. \tag{5.30}$$

On the other hand if

$$\gamma_i^{(k)} = \gamma_j^{(k)} = \gamma, \qquad i, j = 1, 2, \ldots, n; k = 1, 2. \tag{5.31}$$

where $\gamma > 0$ is a real quantity, then (5.1) ensures that the collision will be elastic for each of the components of the two solitons. In terms of the $\mathcal{C}_{n+1,i}^{(j)}$ parameters, the condition (5.31) reduces to

$$\frac{\mathcal{C}_{n+1,1}^{(2)}}{\mathcal{C}_{n+1,1}^{(1)}} = \frac{\mathcal{C}_{n+1,2}^{(2)}}{\mathcal{C}_{n+1,2}^{(1)}} = \cdots = \frac{\mathcal{C}_{n+1,n}^{(2)}}{\mathcal{C}_{n+1,n}^{(1)}} \tag{5.32}$$

It can also be seen from (4.19), (5.2) and (5.29), that the absolute value for the total soliton *i.e.*, $|q| = \sum_{i=1}^{n} q_i^\star q_i$ remains unchanged in inelastic collisions too. Thus, exchange of energy among the components during inelastic collision is only among the components of the same soliton and not from one soliton to the other colliding soliton. In figure (Fig:5.3) the elastic collision for the Manakov system (with x-t interchanged) is graphically depicted. Soliton $\mathrm{S}^{(1)}(\mathcal{C}_{3,1}^{(1)} = 1, \mathcal{C}_{3,2}^{(1)} = 1, \lambda_1 = 0.1 + \mathtt{i})$ is moving with group velocity $v_g^{(1)} = -0.4$ and the phase shift undergone due to the collision with $\mathrm{S}^{(2)}$ is $\delta\Phi^{(1)} = 0.39$. Soliton $\mathrm{S}^{(2)}$ $(\mathcal{C}_{3,1}^{(2)} = 1, \mathcal{C}_{3,2}^{(2)} = 1, \lambda_1 = -0.1 + \mathtt{i})$ moves with $v_g^{(2)} = 0.4$ and undergoes a phase shift $\delta\Phi^{(2)} = -0.39$ due to its collision with $\mathrm{S}^{(1)}$. These phase shifts undergone by the solitons $\mathrm{S}^{(1)}$ and $\mathrm{S}^{(2)}$ during their collision are shown in the contour plot of $|q_1|$, $|q_2|$ in figure (Fig:5.4).

The inelastic scattering of the soliton components in CNLS is shown in figure (Fig:5.5). Soliton $\mathrm{S}^{(1)}$ is represented by $\mathcal{C}_{3,1}^{(1)} = \mathcal{C}_{3,2}^{(1)} = 1$, $\lambda_1 = 0.1 + \mathtt{i}$ while soliton $\mathrm{S}^{(2)}$ is represented by $\mathcal{C}_{3,1}^{(2)} = 49(1 - \mathtt{i})$, $\mathcal{C}_{3,2}^{(1)} = 1$, $\lambda_2 = -0.1 + \mathtt{i}$. Thus, $\gamma_1^{(1)} = 1.034$, $\gamma_2^{(1)} = 0.976$, $\gamma_1^{(2)} = 0.0031$, $\gamma_2^{(2)} = 1.9979$, $\delta\Phi(1) = 0.39$, $\delta\Phi(2) = -0.39$. The corrosponding plot for the total magnitude of

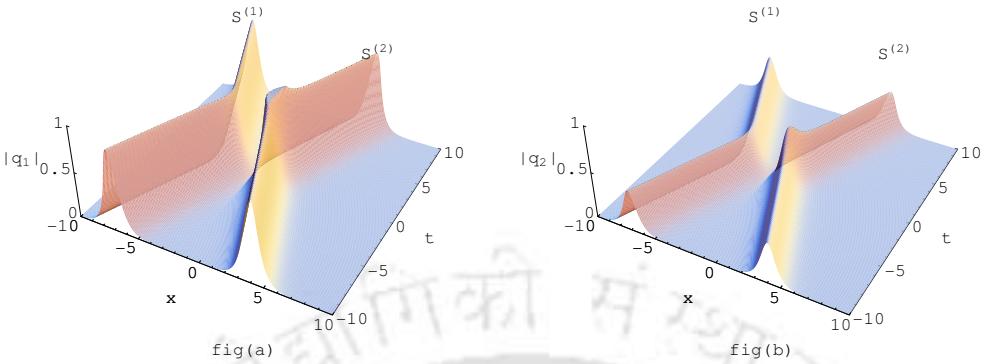

Figure 5.3: Elastic collisions of the soliton component for CNLS system with $n = 2$ where $\mathcal{C}_{3,1}^{(1)} = \mathcal{C}_{3,2}^{(1)} = \mathcal{C}_{3,1}^{(2)} = \mathcal{C}_{3,2}^{(2)} = 1$, $\lambda_1 = 0.1 + \mathtt{i}$, $\lambda_2 = -0.1 + \mathtt{i}$. `Fig:a` shows for the first components $|q_1|$ while `fig:b` are the fields for the second component $|q_2|$.

the soliton $|q|$ is shown in figure (`Fig:`5.6). Altough it components undergo inelastic collision, $|q|$ undergoes elastic collision only. The elastic and inelastic collision of the components of the 2-coupled Hirota system, together with their contour plots are depicted in figures (`Fig:`5.7, `Fig:`5.8, `Fig:`5.9, `Fig:`5.10).

5.5 Collision of Three Solitons

To study the collision of three solitons, the following asymptotic limits of (4.26) are considered.

$$\eta_{j_R}(x,t) \to \pm\infty, \qquad j = 1,2,3. \tag{5.33}$$

Before collision, asymptotically we have (*i.e.*, when $t \to -\infty$),

1. $\eta_{k_R}(x,t), \eta_{l_R}(x,t) \to -\infty$, $(j \neq k, j \neq l, k \neq l) \Rightarrow$ The three solution solution (4.26) reduces to the i-th component of one-soliton $\mathrm{S}^{(j)}$ defined

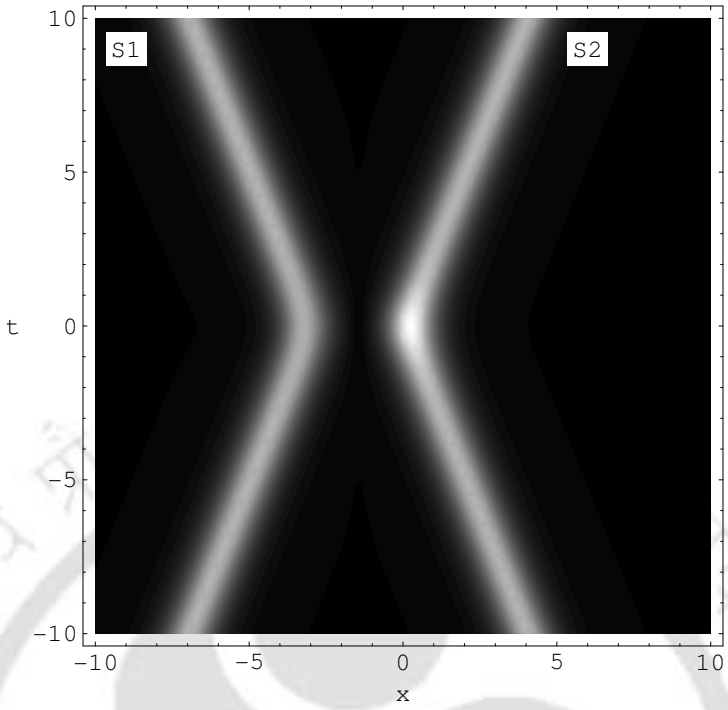

Figure 5.4: Contour plot of `Fig:5.3` for $|q|$ showing the phase shift of solitons undergoing elastic collisions for CNLS system with $n = 2$ where $\mathcal{C}^{(1)}_{3,1} = \mathcal{C}^{(1)}_{3,2} = \mathcal{C}^{(2)}_{3,1} = \mathcal{C}^{(2)}_{3,2} = 1,\ \lambda_1 = 0.1 + \mathtt{i},\ \lambda_2 = -0.1 + \mathtt{i}$. The phase shifts undergone by the solitons $\mathrm{S}^{(1)}$ and $\mathrm{S}^{(2)}$ due to their collision with each other are $\delta\Phi^{(1)} = 0.39$ and $\delta\Phi^{(2)} = -0.39$ respectively.

by $(\mathcal{C}^{(j)}_{n+1,i}, \lambda_j)$ *i.e.*,

$$q^{(j)}_i(x,t) = \mathcal{C}^{(j)}_{n+1,i} \mathtt{e}^{-\frac{\Delta^j_j}{2}} \mathrm{sech}\Big(\eta_{j_R} + \frac{\Delta^j_j}{2}\Big) \mathtt{e}^{-\mathtt{i}\eta_{j_I}},$$
$$i = 1, 2, \ldots, n, j = 1, 2, 3 \quad (5.34)$$

2. $\eta_{l_R}(x,t) \to -\infty$, $(j \neq k, j \neq l, k \neq l) \Rightarrow$ The 3SS (4.26) reduces to a two-soliton $\mathrm{S}^{(j)}$ defined by $(\mathcal{C}^{(j)}_{n+1,i}, \lambda_j)$ and $(\mathcal{C}^{(k)}_{n+1,i}, \lambda_k)$ *i.e.*, an expression similar to (4.20) except that the consituent one-solitons can have any two of the three sets of parameters $(\mathcal{C}^{(1)}_{n+1,i}, \lambda_1)$, $(\mathcal{C}^{(2)}_{n+1,i}, \lambda_2)$ or $(\mathcal{C}^{(3)}_{n+1,i}, \lambda_3)$.

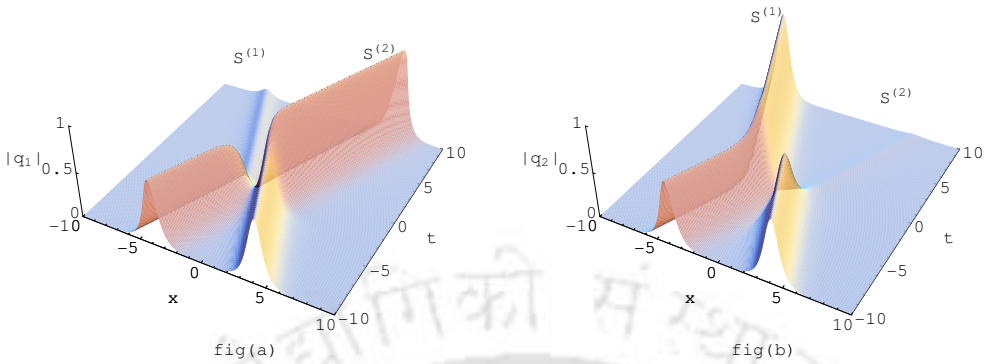

Figure 5.5: Inelastic collisions of the soliton component for CNLS system with $n = 2$ where $\mathcal{C}^{(1)}_{3,1} = \mathcal{C}^{(1)}_{3,2} = \mathcal{C}^{(2)}_{3,2} = 1,\ \mathcal{C}^{(2)}_{3,1} = 49(1-\mathtt{i}),\ \lambda_1 = 0.1+\mathtt{i},\ \lambda_2 = -0.1+\mathtt{i}$. `Fig:a` shows for the first components $|q_1|$ while `fig:b` are the fields for the second component $|q_2|$.

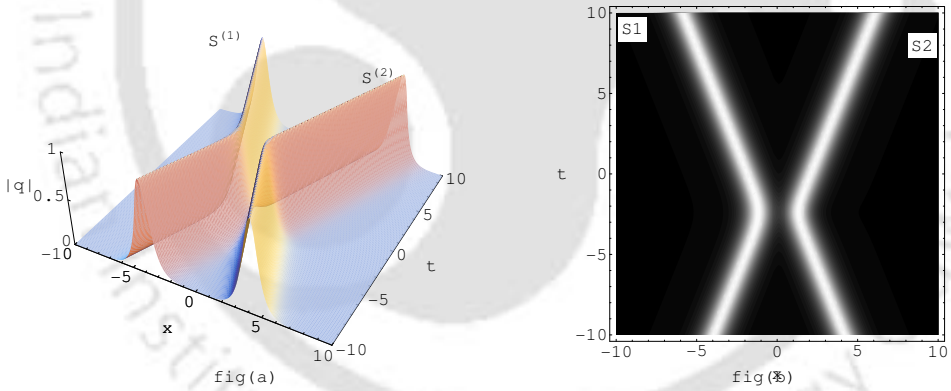

Figure 5.6: The colliding solitons of `Fig:`5.5. `Fig:a` shows $|q| = \sqrt{|q|_1 + |q|_2}$ which undergoes elastic collision only, even though its components q_1 and q_2 undergo inelastic collisions (`fig:` 5.5). `Fig:b` shows the trajectories of the solitons.

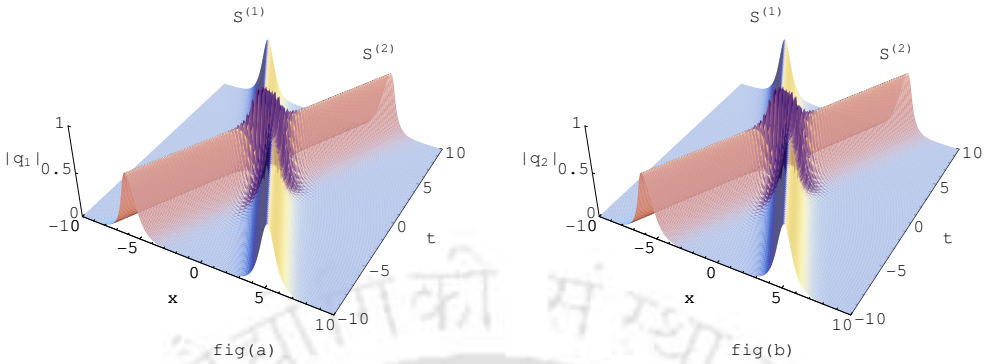

Figure 5.7: Elastic collisions of the soliton component for 2-coupled HNLS of the Hirota type where $\varepsilon = 0.1$, $\mathcal{C}^{(1)}_{3,1} = \mathcal{C}^{(1)}_{3,2} = \mathcal{C}^{(2)}_{3,1} = \mathcal{C}^{(2)}_{3,2} = 1$, $\lambda_1 \approx -0.0252 + \mathtt{i}$, $\lambda_2 \approx 0.2116 + \mathtt{i}$. Soliton $\mathrm{S}^{(1)}$ is travelling with a velocity -0.5, while soliton $\mathrm{S}^{(2)}$ is moving with a velocity +0.5. `Fig:a` shows for the first components $|q_1|$ while `fig:b` are the fields for the second component $|q_2|$.

From (5.9) and (5.11) the seperation of the central maxima at a time t for solitons S_j and S_k $(j, k = 1, 2, 3;\ j \neq k)$ taking part in an interaction of three solitons for the CNLS and coupled Hirota systems are

$$\delta x_{j,k} = 4(\lambda_{j_R} - \lambda_{k_R})t + \frac{1}{4}\left(\frac{\Delta^j_j}{\lambda_{j_I}} - \frac{\Delta^k_k}{\lambda_{k_I}}\right) \tag{5.35a}$$

and

$$\delta x_{j,k} = 4[\lambda_{j_R} - \lambda_{k_R} + 3\varepsilon(\lambda^2_{j_R} - \lambda^2_{k_R} - \lambda^2_{j_I} + \lambda^2_{k_I})]t + \frac{1}{4}\left(\frac{\Delta^j_j}{\lambda_{j_I}} - \frac{\Delta^k_k}{\lambda_{k_I}}\right) \tag{5.35b}$$

respectively. Therefore, at $t \to -\infty$ all the three one-solitons of 3SS are infinitely seperated, unless in the other case when the solitons are moving with the same velocity. Consequently, $t \to -\infty$ only one-solitons would be present and the limit $\eta_k \to -\infty$ which reduces the 3SS to a 2SS as mentioned previously, has to be abandoned.

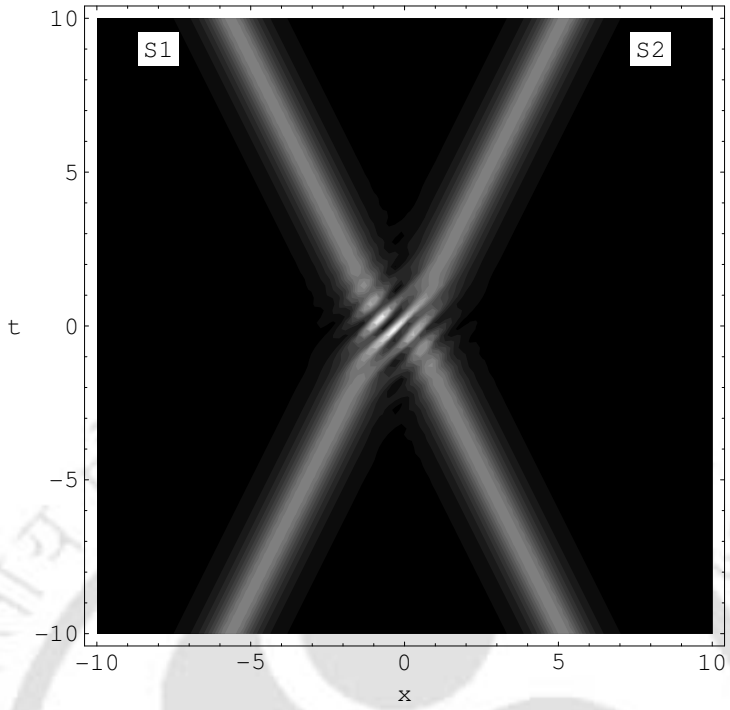

Figure 5.8: Contour plot of `Fig:5.7`

Thus, before collision, asymptotically the 3SS is represents three one-solitons $S^{(1)}$, $S^{(2)}$ and $S^{(3)}$ described by parameters $(\mathcal{C}^{(1)}_{n+1,i}, \lambda_1)$, $(\mathcal{C}^{(2)}_{n+1,i}, \lambda_2)$ and $(\mathcal{C}^{(3)}_{n+1,i}, \lambda_3)$ respectively.

To consider the situation after the collision among the three solitons have taken place, the asymptotic situation at $t \to +\infty$ is considered. Equations (5.35) suggest that, unless the solitons are moving with indentical velocities, they would again be infinitely seperated from each other.

To specifically look at soliton $S^{(1)}$ after its collision with $S^{(2)}$ and $S^{(3)}$ has occured, the limits $\eta_2 \to +\infty, \eta_3 \to +\infty$ are imposed on (4.26). This equation assumes the form

$$q_i^{(1)''}(x,t) = \mathcal{C}^{(1)''}_{n+1,i} \mathrm{e}^{-\frac{\Delta^{1''}_{1''}}{2}} \mathrm{sech}\left(\eta_{1_R} + \frac{\Delta^{1''}_{1''}}{2}\right) \mathrm{e}^{-\mathrm{i}\eta_{1_I}} \tag{5.36}$$

where,

$$\mathcal{C}^{(1)''}_{n+1,i} = \mathrm{e}^{\tilde{\Delta}^{1,2,3}_{i,2,3} - \Delta^{2,3}_{2,3}} \tag{5.37}$$

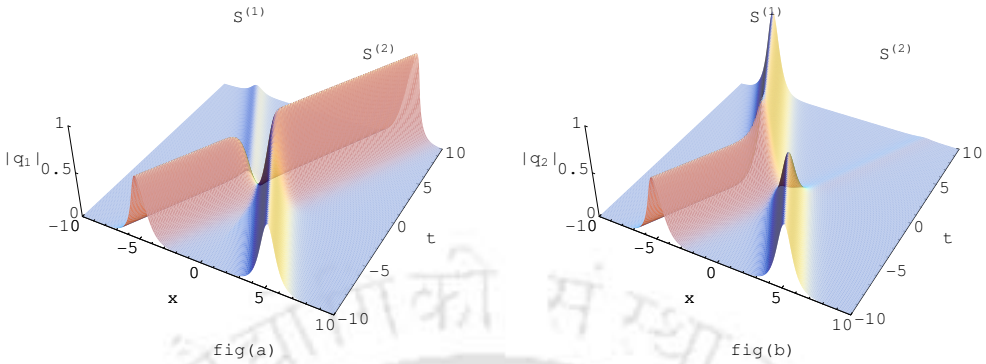

Figure 5.9: Inelastic collisions of the soliton component for 2-coupled HNLS of the Hirota type where $\varepsilon = 0.1$, $\mathcal{C}^{(1)}_{3,1} = \mathcal{C}^{(1)}_{3,2} = \mathcal{C}^{(2)}_{3,2} = 1$, $\mathcal{C}^{(2)}_{3,1} = 46(1 - \mathtt{i})$, $\lambda_1 \approx -0.0252 + \mathtt{i}$, $\lambda_2 \approx 0.2116 + \mathtt{i}$. The velocities of the solitons are identical with those solitons in `Fig:`5.7. `Fig:a` shows for the first components $|q_1|$ while `fig:b` are the fields for the second component $|q_2|$.

and,

$$\mathtt{e}^{\Delta^{1''}_{1''}} = \mathtt{e}^{\Delta^{1,2,3}_{1,2,3} - \Delta^{2,3}_{2,3}} \tag{5.38}$$

In the above equations, the matrices $\mathtt{e}^{\tilde{\Delta}^{1,2,3}_{i,2,3}}$, $\mathtt{e}^{\Delta^{1,2,3}_{1,2,3}}$ and $\mathtt{e}^{\Delta^{2,3}_{2,3}}$ are defined by (4.33). As,

$$\mathtt{e}^{\Delta^{1''}_{1''}} = \frac{\kappa_{1'',1''}}{\Lambda^2_{1,1}} = \frac{\sum_{p=1}^{n} \mathcal{C}^{(1)''\star}_{n+1,p} \mathcal{C}^{(1)''}_{n+1,p}}{\Lambda^2_{1,1}} \tag{5.39}$$

it is possible to consider equation (5.36) as a one-soliton moving with a velocity and width identical with the velocity and width of $\mathrm{S}^{(1)}$ before its interaction with $\mathrm{S}^{(2)}$ and $\mathrm{S}^{(3)}$, but with a modified amplitude,

$$\mathcal{A}^{(1)}_i = \mathcal{C}^{(1)''}_{n+1,i} \mathtt{e}^{-\frac{\Delta^{1''}_{1''}}{2}} = \mathtt{e}^{\tilde{\Delta}^{1,2,3}_{i,2,3} - \frac{\Delta^{1,2,3}_{1,2,3} + \Delta^{2,3}_{2,3}}{2}} \tag{5.40}$$

and a relative phase change

$$\frac{\Delta^{1''}_{1''} - \Delta^{1}_{1}}{4\lambda_{1_I}} = \frac{\Delta^{1,2,3}_{1,2,3} - \Delta^{2,3}_{2,3} - \Delta^{1}_{1}}{4\lambda_{1_I}} \tag{5.41}$$

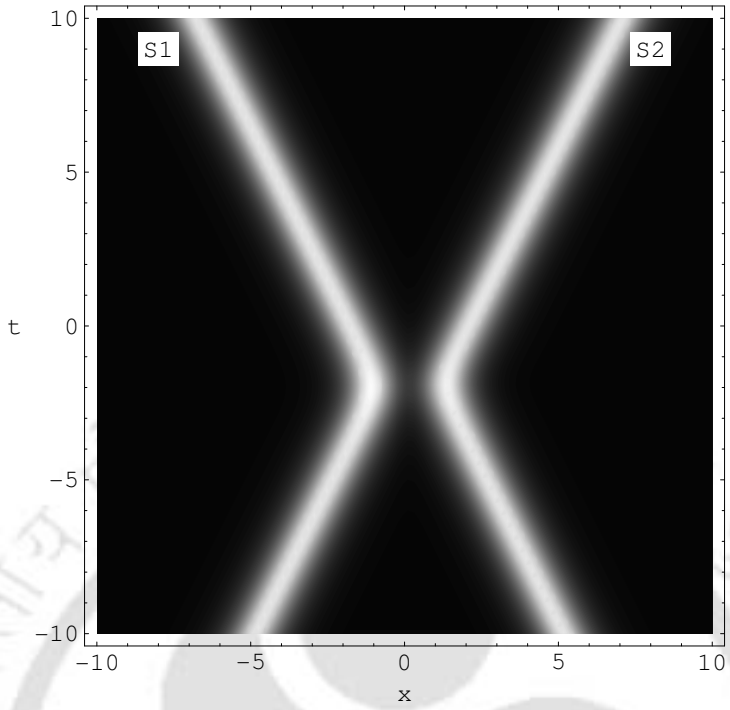

Figure 5.10: Contour plot for `Fig:5.9`.

Thus the entire change of soliton $\mathrm{S}^{(1)}$ in this three soliton interaction can be summed up as by the transformation

$$\mathcal{C}^{(1)}_{n+1,i} \longrightarrow \mathcal{C}^{(1)''}_{n+1,i}\{\mathcal{C}^{(j)}_{n+1,i}, \lambda_j\}, \qquad i = 1, 2, \ldots, n,\ j = 1, 2, 3 \tag{5.42}$$

as defined by (5.37). This asymptotic reduction of the 3SS at $t \to +\infty$ can be easily extended to the other solitons. In general, the asymptotic form of a soliton after it had interacted with two other solitons during a three soliton interaction is,

$$q_i^{(j)''}(x,t) = \mathcal{C}^{(j)''}_{n+1,i} \mathrm{e}^{-\frac{\Delta^{j''}_{j''}}{2}} \mathrm{sech}\Big(\eta_{j_R} + \frac{\Delta^{j''}_{j''}}{2}\Big) \mathrm{e}^{-\mathrm{i}\eta_{j_I}} \tag{5.43a}$$

where,

$$\mathcal{C}^{(j)''}_{n+1,i} = \mathrm{e}^{\tilde{\Delta}^{j,k,l}_{i,k,l} - \Delta^{k,l}_{k,l}} \tag{5.43b}$$

and

$$\mathrm{e}^{\Delta^{j''}_{j''}} = \sum_{i=1}^{n} \mathcal{C}^{(j)''\star}_{n+1,i}\ \mathcal{C}^{(j)''}_{n+1,i} \tag{5.43c}$$

In the above set of equation $i = 1, 2, \ldots, n;\ j, k, l = 1, 2, 3; j \neq k, j \neq l, k \neq l$.

The nature of the interactions, whether elastic or inelastic at the component level depends crucially the individual soliton parameters $(\mathcal{C}_{n+1,i}^{(j)''}, \lambda_j)$. This in turn, governs the exchange of energy inbetween the components of the soliton. Thus, three asymptotically $(t \to -\infty)$ seperated one-solitons interact in some finite region of (x, t) and in the subsequent asymtpotic limit $(t \to +\infty)$ reduced to three modified one-solitons. As in the case of two soliton interactions, the solitons energy is exchanged among the components of the same soliton, the sum total of the energies of each soliton remain unaffected.

As the three soliton interaction may not take place at a single point, they interact interact in sequences of two soliton interactions. By appropriate selection of velocities and phases of $S^{(1)}$, $S^{(2)}$ and $S^{(3)}$, we can control the sequence of interactions. For a two-component CNLS system this is depicted in figures (Fig:5.11) and (Fig:5.12). In figure (Fig:5.11), $S^{(1)}$-$S^{(2)}$ interact first and is followed by the $S^{(1)}$-$S^{(3)}$ interaction. Finally, $S^{(2)}$ and $S^{(3)}$ interact. In figure(Fig:5.12), $S^{(2)}$ and$S^{(3)}$ interact first followed by the $S^{(1)}$-$S^{(3)}$ interactions and finally $S^{(1)}$ and $S^{(2)}$ interact. The contour plots of these interactions (Fig:5.11, Fig:5.12) highlight these sequence of interactions.
As evident from the figures, this change in the sequence of interactions has been bought about by suitably altering the initial phase of $S^{(2)}$ vide (5.1) with $\gamma = 10^{14}$. However, the amplitude (5.40) and the relative phase change (5.41) of $S^{(2)}$ remain invarient under this γ-scaling. Infact, the amplitude and relative phase difference and so also the velocity and width maintain their invarience under any simple or combinations of γ-scaling of the three solitons. Therefore the amplitude change undergone by a soliton in this three soliton interaction is independent of the sequence of soliton collisions.

Finally, these elastic and inelastic collisions for three solitons of the coupled Hirota system and their sequence independence is graphically depicted in figures (Fig:5.15), (Fig:5.16), (Fig:5.17), (Fig:5.18), (Fig:5.19), (Fig:5.20), (Fig:5.21) and (Fig:5.22).

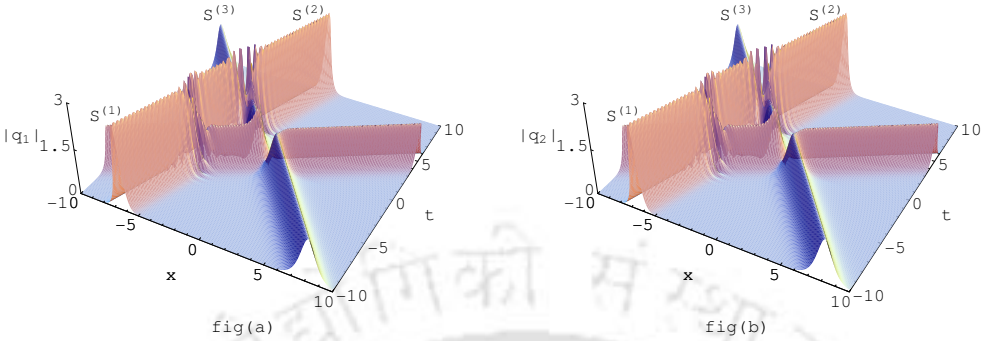

Figure 5.11: Elastic collisions of solitons for CNLS system with $N = 3,\ n = 2$ where $\mathcal{C}^{(1)}_{4,1} = \mathcal{C}^{(1)}_{4,2} = 1,\ \mathcal{C}^{(2)}_{4,1} = \mathcal{C}^{(2)}_{4,2} = 10^{-7},\ \mathcal{C}^{(3)}_{4,1} = \mathcal{C}^{(3)}_{4,2} = 10^{2},\ \lambda_1 = 0.4 + \mathtt{i},\ \lambda_2 = 0.08 + 2\mathtt{i},\ \lambda_3 = -0.2 + \mathtt{i}$. Here, the sequence of interaction is $S^{(1)}$-$S^{(2)}$, $S^{(1)}$-$S^{(3)}$ and finally $S^{(2)}$-$S^{(3)}$. `Fig:`(a) shows the first component while `fig:`(b) shows the second component.

5.6 Collision of N Solitons

The analysis in the previous sections can be extended to the NSS (4.31) for studying the collision of N solitions. In this case invoking the limit $\eta_{j_R} \to -\infty$ $(j = 1, 2, \ldots, N; j \neq p; 1 \leq p \leq N)$ on (4.31) gives the p-th soliton before interactions *i.e.*, a soliton characterised by $(\mathcal{C}^{(p)}_{n+1,i}, \lambda_p)$

$$q^{(p)}_i(x,t) = \mathcal{C}^{(p)}_{n+1,i} \mathsf{e}^{-\frac{\Delta^p_p}{2}} \operatorname{sech}\Big(\eta_{p_R} + \frac{\Delta^p_p}{2}\Big) \mathsf{e}^{-\mathtt{i}\eta_{p_I}} \tag{5.44a}$$

where,

$$\mathsf{e}^{\Delta^p_p} = \frac{\kappa_{p,p}}{\Lambda^2_{p,p}} \tag{5.44b}$$

and η_{p_R}, η_{p_I} are the real and imaginary parts of $\eta_p(x,t)$ respectively, which for the CNLS system (3.5a) is given (4.1) and for the coupled Hirota system (3.5b) is given by (4.14).

Again, in the asymptotic limit $\eta_{j_R} \to +\infty$, the equation (4.31) reduces to the one-soliton expression for the p-th soliton after it had interacted with

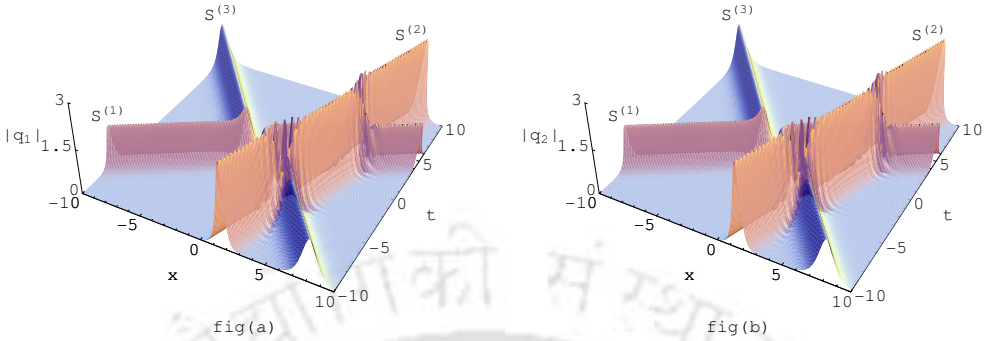

Figure 5.12: Elastic collisions of solitons for CNLS system with $N = 3,\ n = 2$ where $\mathcal{C}^{(1)}_{4,1} = \mathcal{C}^{(1)}_{4,2} = 1,\ \mathcal{C}^{(2)}_{4,1} = \mathcal{C}^{(2)}_{4,2} = 10^7,\ \mathcal{C}^{(3)}_{4,1} = \mathcal{C}^{(3)}_{4,2} = 10^2,\ \lambda_1 = 0.4 + \mathtt{i},\ \lambda_2 = 0.08 + 2\mathtt{i},\ \lambda_3 = -0.2 + \mathtt{i}$. Here, the sequence of interaction is $\mathrm{S}^{(2)}$-$\mathrm{S}^{(3)}$, $\mathrm{S}^{(1)}$-$\mathrm{S}^{(3)}$ and finally $\mathrm{S}^{(1)}$-$\mathrm{S}^{(2)}$. The change in the sequence of interaction is brought about by shifting $\mathrm{S}^{(2)}$ with the help of the γ-transformation, *i.e.*, $\mathcal{C}^{(2)'}_{4,i} = \gamma^{(2)}\mathcal{C}^{(2)}_{4,i},\ i = 1, 2\ \&\ \gamma^{(2)} = 10^{14}$. `Fig:`(a) shows the first component while `fig:`(b) shows the second component.

all the other $N-1$ solitons in this N soliton collision. This p-th soliton is given as,

$$q_i^{(p)\ddagger}(x,t) = \mathcal{C}^{(p)\ddagger}_{n+1,i}\mathtt{e}^{-\frac{\Delta^{p\ddagger}_{p\ddagger}}{2}}\mathrm{sech}\Big(\eta_{p_R} + \frac{\Delta^{p\ddagger}_{p\ddagger}}{2}\Big)\mathtt{e}^{-\mathtt{i}\eta_{p_I}} \tag{5.45}$$

where,

$$\mathtt{e}^{\Delta^{p\ddagger}_{p\ddagger}} = \frac{\kappa_{p,p}}{\Lambda^2_{p,p}}, \qquad \kappa_{p,p} = \sum_{i=1}^{n}\mathcal{C}^{(p)\ddagger\star}_{n+1,i}\mathcal{C}^{(p)\ddagger}_{n+1,i} \tag{5.46}$$

Thus the entire transformation of the p-th soliton before any collision took place, to the situation after all the collisions have taken place can be representation by a transformation of the $\mathcal{C}^{(p)}_{n+1,i}$ parameter.

$$\mathcal{C}^{(p)}_{n+1,i} \longrightarrow \mathcal{C}^{(p)\ddagger}_{n+1,i} = \mathtt{e}^{\tilde{\Delta}^{1,2,3,\ldots,(p-1),p,(p+1),\ldots,N}_{i,1,2,\ldots,(p-1),(p+1),\ldots,N}}\ \mathtt{e}^{-\Delta^{1,2,\ldots,(p-1),(p+1),\ldots,N}_{1,2,\ldots,(p-1),(p+1),\ldots,N}} \tag{5.47}$$

In the above expressions, $\mathtt{e}^{\tilde{\Delta}^{1,2,3,\ldots,(p-1),p,(p+1),\ldots,N}_{i,1,2,\ldots,(p-1),(p+1),\ldots,N}}$ and $\mathtt{e}^{\Delta^{1,2,\ldots,(p-1),(p+1),\ldots,N}_{1,2,\ldots,(p-1),(p+1),\ldots,N}}$ can be derived from the equations (4.33)

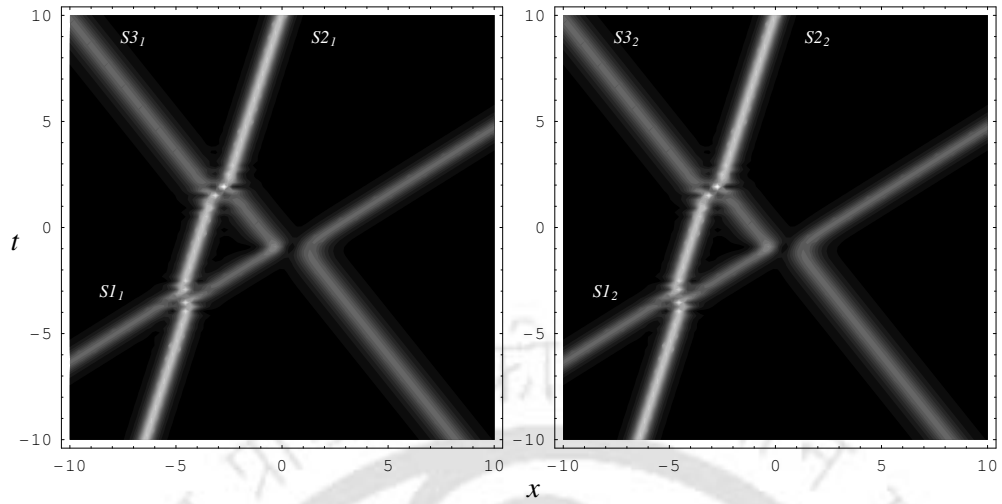

Figure 5.13: Contour plots of `Fig:`5.11 highlighting the $S^{(1)}$-$S^{(3)}$, $S^{(1)}$-$S^{(3)}$, $S^{(2)}$-$S^{(3)}$ collision sequence.

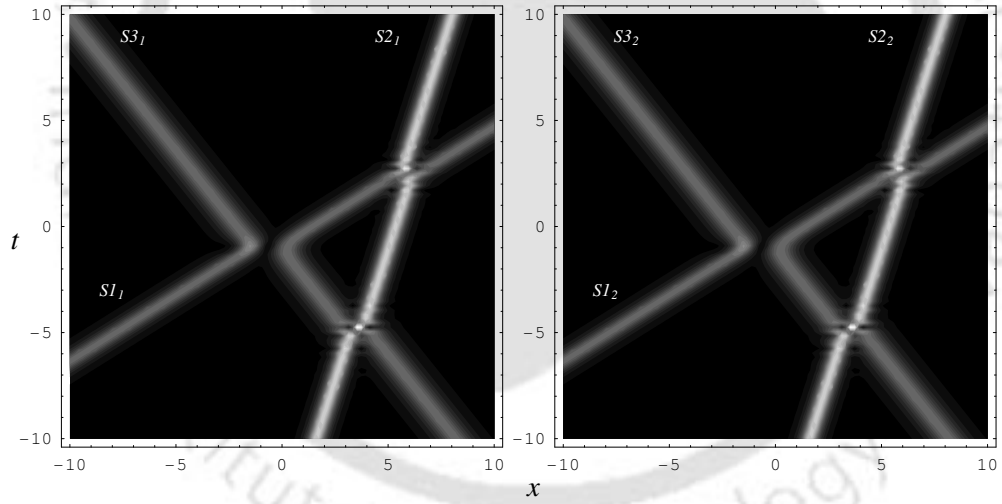

Figure 5.14: Contour plots of `Fig:`5.12 highlighting the changed $S^{(2)}$-$S^{(3)}$, $S^{(1)}$-$S^{(3)}$, $S^{(1)}$-$S^{(2)}$ collision sequence.

During the soliton $S^{(p)}$'s collision with the other $N-1$ solitons its group velocity and phase remain unchanged. Its changed amplitude and phase are

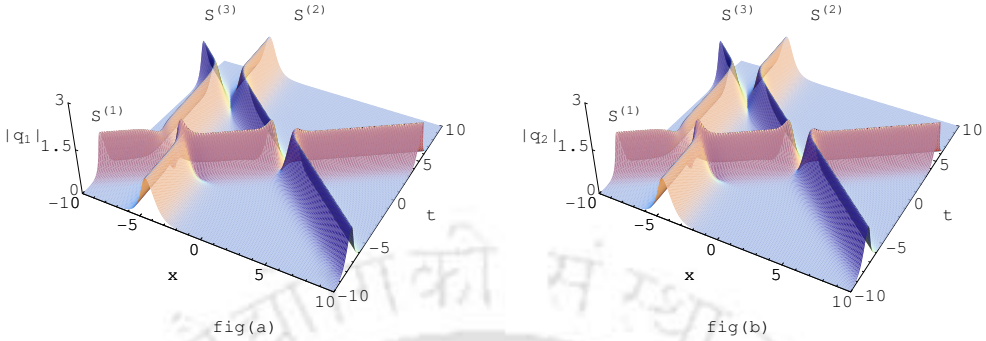

Figure 5.15: Elastic collisions of three solitons ($N = 3$) for a 2-coupled Hirota system ($n = 2$) where, $\varepsilon = 0.1$, $\mathcal{C}_{4,1}^{(1)} = \mathcal{C}_{4,2}^{(1)} = 1$, $\mathcal{C}_{4,1}^{(2)} = \mathcal{C}_{4,2}^{(2)} = 10^{-3}$, $\mathcal{C}_{4,1}^{(3)} = \mathcal{C}_{4,2}^{(3)} = 10^{2}$, $\lambda_1 = 0.4+\mathtt{i}$, $\lambda_2 = 0.08+\mathtt{i}$, $\lambda_3 = -0.2+\mathtt{i}$. The collision sequence $\mathrm{S}^{(1)}$-$\mathrm{S}^{(2)}$, $\mathrm{S}^{(1)}$-$\mathrm{S}^{(3)}$, $\mathrm{S}^{(2)}$-$\mathrm{S}^{(3)}$.

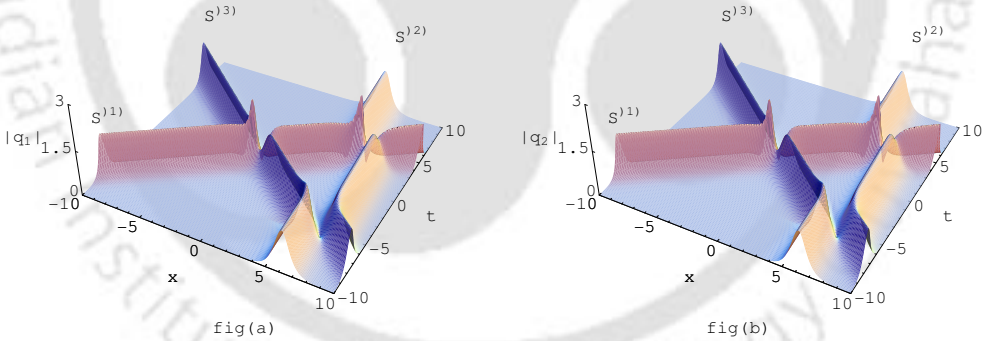

Figure 5.16: Elastic collisions of three solitons for the same system as in `Fig:`5.15 except for $\mathcal{C}_{4,1}^{(2)} = \mathcal{C}_{4,2}^{(2)} = 10^{7}$ leading to a collision sequence $\mathrm{S}^{(2)}$-$\mathrm{S}^{(3)}$, $\mathrm{S}^{(1)}$-$\mathrm{S}^{(3)}$, $\mathrm{S}^{(2)}$-$\mathrm{S}^{(2)}$.

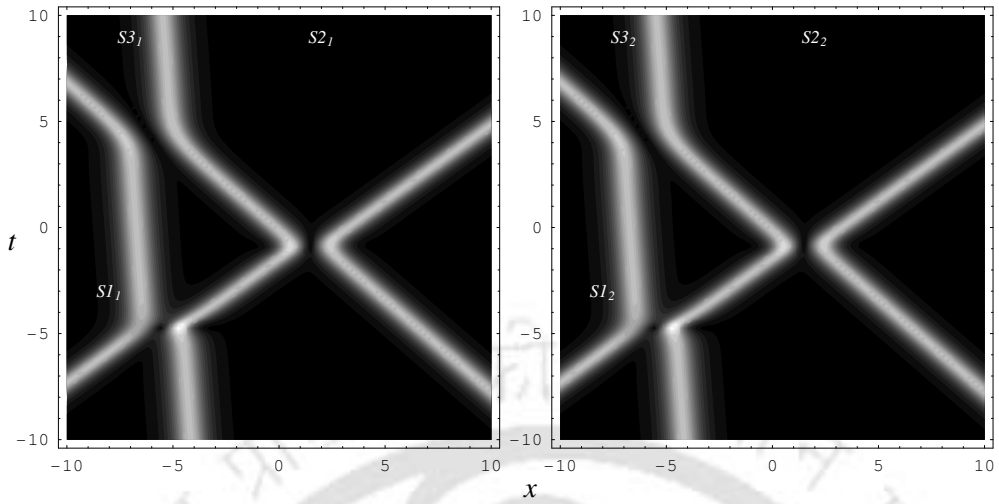

Figure 5.17: Contour plot for `Fig:5.15`.

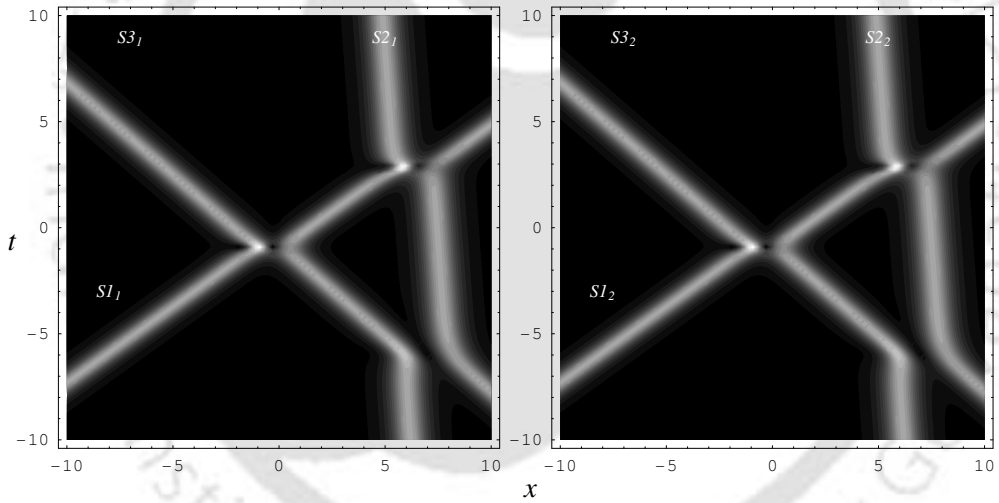

Figure 5.18: Contour plot for `Fig:5.16`.

given as

$$\mathcal{A}_i^{(p)\ddagger} = |\mathcal{C}_{n+1,i}^{(p)\ddagger}| \mathrm{e}^{-\frac{1}{2}\Delta_{p\ddagger}^{p\ddagger}} \tag{5.48a}$$

and

$$\frac{\Delta_{p\ddagger}^{p\ddagger}}{4\lambda_{p_I}} = \frac{\mathrm{e}^{\tilde{\Delta}_{i,1,2,\ldots,(p-1),(p+1),\ldots,N}^{1,2,3,\ldots,(p-1),p,(p+1),\ldots,N}} \mathrm{e}^{-\Delta_{1,2,\ldots,(p-1),(p+1),\ldots,N}^{1,2,\ldots,(p-1),(p+1),\ldots,N}}}{4\lambda_{p_I}} \tag{5.48b}$$

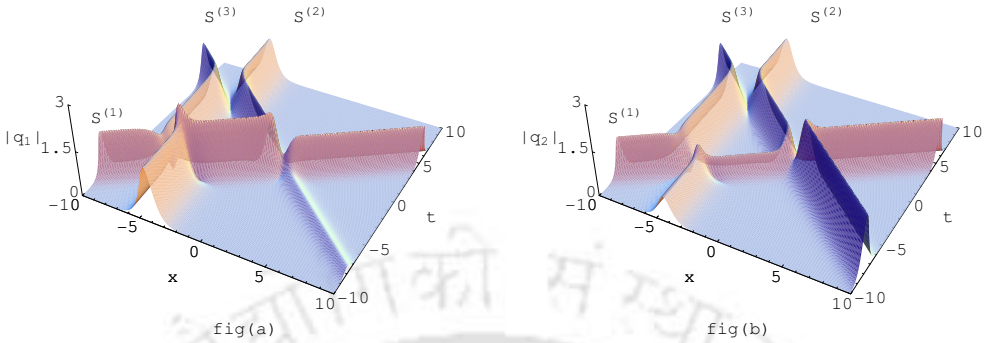

Figure 5.19: Inelastic collisions of three solitons ($N = 3$) for a 2-coupled Hirota system ($n = 2$) where, $\varepsilon = 0.1$, $\mathcal{C}_{4,1}^{(1)} = 1.12497 + 0.172731\mathtt{i}$, $\mathcal{C}_{4,2}^{(1)} = 1$, $\mathcal{C}_{4,1}^{(2)} = \mathcal{C}_{4,2}^{(2)} = 10^{-3}$, $\mathcal{C}_{4,1}^{(3)} = \mathcal{C}_{4,2}^{(3)} = 10^{2}$, $\lambda_1 = 0.4 + \mathtt{i}$, $\lambda_2 = 0.08 + \mathtt{i}$, $\lambda_3 = -0.2 + \mathtt{i}$. The collision sequence $\mathrm{S}^{(1)}$-$\mathrm{S}^{(2)}$, $\mathrm{S}^{(1)}$-$\mathrm{S}^{(3)}$, $\mathrm{S}^{(2)}$-$\mathrm{S}^{(3)}$.

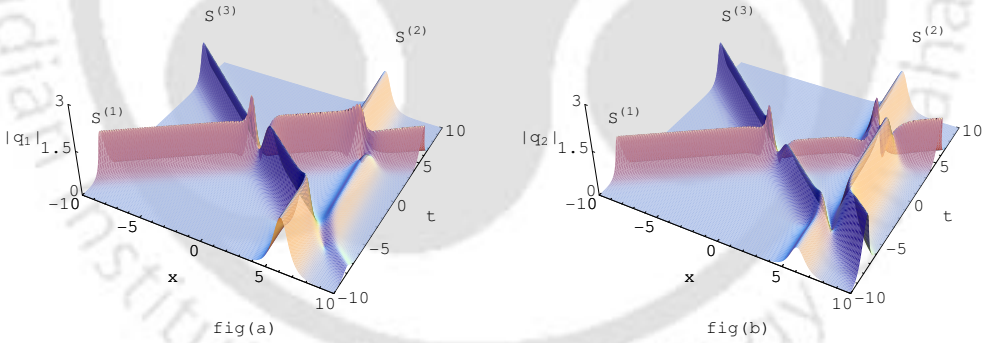

Figure 5.20: Inelastic collisions of three solitons for the same system as in `Fig:`5.19 except for $\mathcal{C}_{4,1}^{(2)} = \mathcal{C}_{4,2}^{(2)} = 10^{6}$ leading to a collision sequence $\mathrm{S}^{(2)}$-$\mathrm{S}^{(3)}$, $\mathrm{S}^{(1)}$-$\mathrm{S}^{(3)}$, $\mathrm{S}^{(2)}$-$\mathrm{S}^{(2)}$.

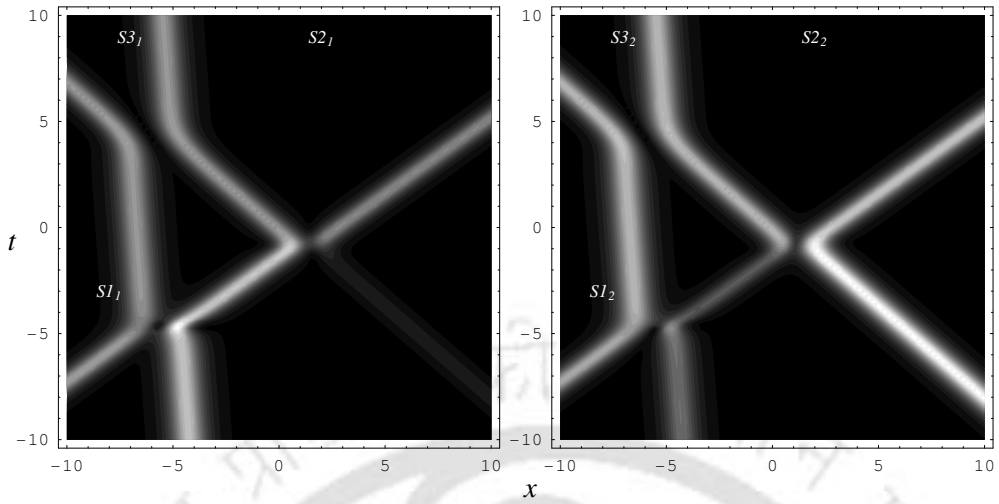

Figure 5.21: Contour plot for `Fig:5.19`.

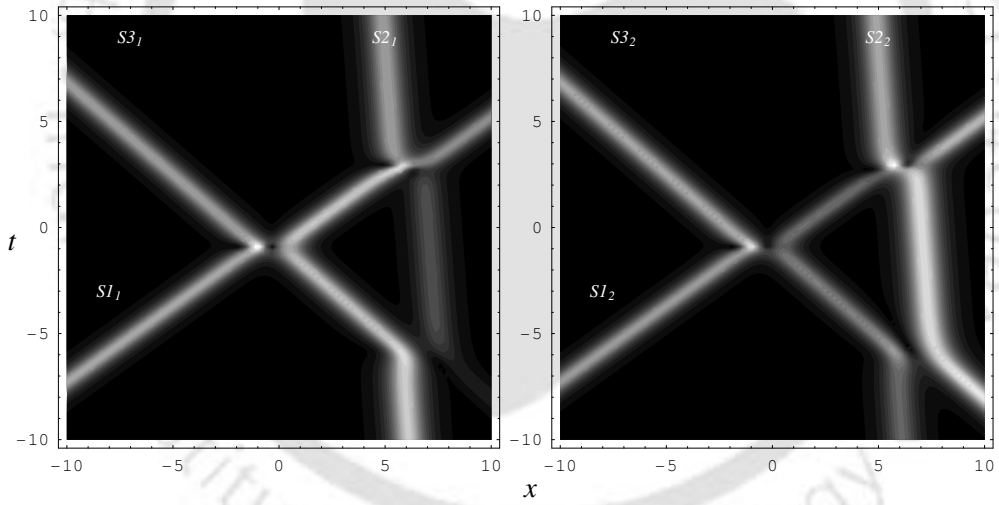

Figure 5.22: Contour plot for `Fig:5.20`.

As in the case of three soliton interactions, the sequence of interactions among the N one-solitons do not affect the soliton characteristics asymptotically.

5.7 Summary

In this chapter, the soliton collisions were studied and their characteristics highlighted. A scaling of a soliton parameter leading to only amplitude change was introduced. The two soliton collisions were studied and the conditions of elastic and inelastic collisions were analyzed. The collision of three solitons and the sequence independence of their collisions were highlighted. Finally the collision of N solitons was generalised.

These results will be used in the development of soliton based logic gates in the next chapter. Altough the results have been developed for n-component solitons for completeness, the 2-component soliton interaction refer to the collisions of the Manakov solitons (with x, t interchanged) and the collisions of 2-component CHNLS system of the Hirota type.

Chapter 6

Solitonic Logic Gates

6.1 Introduction

Due to their robustness, solitons are the natural replacements for the information carriers in particle-machine based computing. On the other hand, the transfer of energy inbetween the components of a multicomponent soliton can be used in the implimentation of binary logic operations. This is due to the fact that the output of colliding multicomponent solitons depend on the other soliton(s) taking part in the collision. This transactive nature of solitons was presented in the previous chapter, specially in the context of two and three soliton collisions. The transactive nature of n-component N soliton collisions had also been highlighted. In this chapter, we study the possibilities of implimenting binary logic operations using the solitons of the CNLS (3.5a) and the CHNLS of the Hirota type (3.5b) systems.

Ideas of solitonic presence in particle machines has been in discussion for quite some time [115, 116, 117, 118, 120]. After the discovery of energy switching among the components during multicomponent soliton collisions [85], the idea of using such multicomponent collisions in the construction of logic gates is well discussed in [86, 87, 92, 93, 94, 95, 96, 119, 121, 122]. In some these works, the NOT, COPY, FANOUT and NAND logic gates based on these solition collisions were presented. In [95] the possibility of stable collision cycles of soliton was also presented as a means of realising soliton based flip-flops for data storage.

In contrary to some of the techniques used in the above mentioned works, here the different data solitons move with different velocities. This has been motivated by the fact that this allows one to realise the logic gates with lesser number of soliton usage.

Again, the models presented in this chapter has been developed on the basis of temproral solitons and not spatial solitons. This is due to the fact that (2+1) systems for spatial solitions are not exactly integrable and the solitons are not truly robust [123]. Of course, the spatial solitions are interesting in their own respects.

6.2 Model for Soliton Based Logic Gates

In order to carry out computations using temporal solitons in birefringent optical fibers, the 2 coupled or the 2 component NLS dynamical system is considered. This is the well known integrable Manakov system [64]. This system describes the propagation of vector soliton in the weak nonlinear regime. The vector solitons have the two components electric fields perpendicular to each other and perpendicular to the direction of propagation. Mathematically this is represented by (3.5a) with $n = 2$ and with x and t interchanged. To achive faster information exchange and computation the information carrying Manakov solitons need to be of shorter widths. In the Manakov model the solions are of picoseconds width, but as their width shortens to the femtoseconds range, the higher order effects due to susceptibility of the nonlinear medium have to be included. Therefore, to consider solitons with femtoseconds widths, the Manakov model has to be extended to include the higher order effects and such an extension is described by the 2 coupled CHNLS system. In context to the dynamical systems discussed in this work, they are represented by the 2-coupled Hirota equations and 2-coupled Sasa-Satsuma equations, *i.e.*, with $n = 2$ imposed in equation (3.5b) and (3.5c) respectively. In order to maintain the flow, the x and t interchange relative to the dynamical representation of actual temporal solitons in optical fibers is retained.

For executing logic operations using temporal solitons in (2+1) dimen-

sional systems the following scheme is adapted (Fig:6.1). Each 2-component vector soliton is a carrier of one bit. In this manner different solitons with

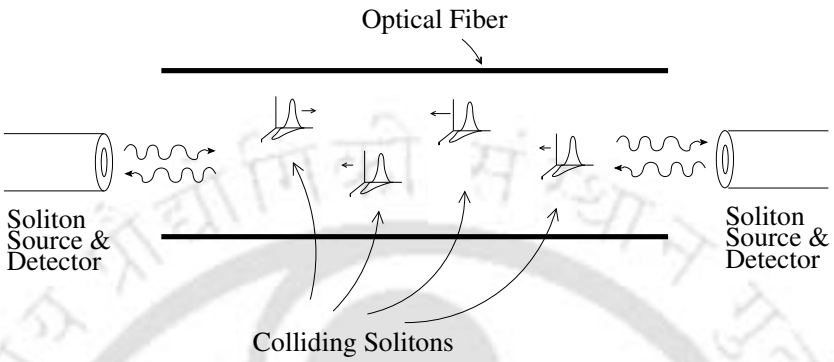

Figure 6.1: Soliton Gates

their own binary information rush along in the same one dimensional motion colliding against each other. Besides this, there may be other solitons, which can be called as actuators, moving along in the same x-direction and colliding with the data solitons in a nontrivial manner bringing about inelastic collisions among the components. Finally, depending on the logic scheme implemented and after all the collisions have taken place, one or more of these solitons will bear the output(s) of the logic gate implementation. In this implementation, the data solitons moves with different velocities and the actuator(s) may get converted as the data output soliton(s). The different solitons, with their appropriate characteristics – $(\mathcal{C}^{(j)}_{n+1,i}, \lambda_i)$, would be produced by lasers acting according to the requirements. The output solitons will be collected by appropriate detectors placed coaxially with the soliton sources. Altough cascaded soliton interaction has been used to impliment complex algorithms [94], in this case a different approach is taken, as will been seen at the time of implimentation.

In order to represent the binary levels of **0**'s and **1**'s in such two compo-

nent vector solitons, the following scheme is adapted from [91].

$$\varrho_{\text{IN}}^{(1)} = \left.\frac{q_1^{(j)}(x,t)}{q_2^{(j)}(x,t)}\right|_{before\ collision} = \left.\frac{\mathcal{C}_{3,1}^{(j)}(x,t)}{\mathcal{C}_{3,2}^{(j)}(x,t)}\right|_{before\ collision} \tag{6.1a}$$

$$\varrho_{\text{OUT}}^{(1)} = \left.\frac{q_1^{(j)'}(x,t)}{q_2^{(j)'}(x,t)}\right|_{after\ collision} = \left.\frac{\mathcal{C}_{3,1}^{(j)'}(x,t)}{\mathcal{C}_{3,2}^{(j)'}(x,t)}\right|_{after\ collision} \tag{6.1b}$$

In the set of equations (6.1) the functions are evaluated at the "*before collision*" are actually evaluated before collision at the $t \to -\infty$ asymptote. On the other hand, the functions evaluated at the "*after collision*" are actually evaluated at the $t \to +\infty$ asymptotes. Depending on the values of these complex functions the logic levels are defined as

$$\varrho^{(j)} = \mathbf{0} \quad \Rightarrow \quad \texttt{binary}\ \ 0$$
$$\varrho^{(j)} = \mathbf{1} \quad \Rightarrow \quad \texttt{binary}\ \ 1$$

Thus, in terms of the 2-CNLS and 2-CHNLS, the binary levels are represented by the 2-component solitons polarised in one particular direction only, for example, the soliton may have its field in the y-direction and its field in the z-direction is completely absent. A change of a soliton from one binary state to the other is a rotation of its state of polarization by $\frac{\pi}{2}$. This means the soliton with its field only in the y-direction initially will now have its field in the z-direction only and its field in the y-direction is now zero.

To identify a soliton collision with a particular logic gate, the following scheme is adapted.

> The input and the output solitons for a particular collision sequence are identified. If the input and the corrosponding output of the solitons have a one-to-one mapping with the truth table of a particular logic gate, then that particular logic gate is represented completely by that particular collision of solitons. (♣)

Input	Output
0	0
1	1

Table 6.1: COPY Gate

Input	Output
0	1
1	0

Table 6.2: NOT Gate

6.3 Logic Gates from Two Soliton Collisions

The simplest logic gates are those with one input and one output. The COPY and NOT gates fall in this category and their respective Truth Tables are given in (Tab:6.1) and (Tab:6.2)

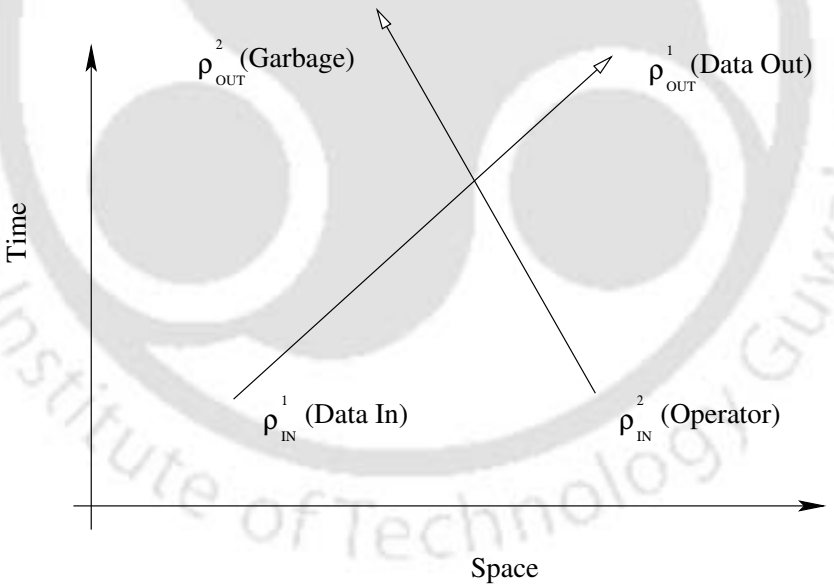

Figure 6.2: 1-Input/1-Output Soliton Gates using LFT

If these single input gates are to be implemented by the use of Linear

Fractional Transformation, as shown in the Fig:6.2, then the corrosponting transformation derived from (4.20) is,

$$\varrho^{(1)}_{\text{OUT}} = \frac{a\ \varrho^{(1)}_{\text{IN}} + b}{c\ \varrho^{(1)}_{\text{IN}} + d} \tag{6.2}$$

where,

$$a = \Lambda_{2,1}(1 + |\varrho^{(2)}_{\text{IN}}|^2) - \Lambda_{2,2}\ |\varrho^{(2)}_{\text{IN}}|^\star \tag{6.3a}$$

$$b = -\Lambda_{2,2}\ \varrho^{(2)}_{\text{IN}} \tag{6.3b}$$

$$c = -\Lambda_{2,2}\ \varrho^{(2)\star}_{\text{IN}} \tag{6.3c}$$

$$d = \Lambda_{2,1}(1 + |\varrho^{(2)}_{\text{IN}}|^2) - \Lambda_{2,2} \tag{6.3d}$$

In order for the above scheme to work for the COPY gate,

$$\varrho^{(1)}_{\text{IN}} = 0,\ \varrho^{(1)}_{\text{OUT}} = 0 \quad \Rightarrow b = 0 \quad \Rightarrow \varrho^{(2)}_{\text{IN}} = 0 \tag{6.4a}$$

and,

$$\varrho^{(1)}_{\text{IN}} = 1,\ \varrho^{(1)}_{\text{OUT}} = 1 \quad \Rightarrow a = c + d \quad \Rightarrow \varrho^{(2)}_{\text{IN}} = 1 \tag{6.4b}$$

It can be seen from the above equations that a contradiction surfaces (value of $\varrho^{(2)}_{\text{IN}}$) and so the COPY gate is impossible to realize with two soliton collisions using the linear fractional transformation (LFT) given in (6.2).

In a similar manner, for the NOT gate,

$$\varrho^{(1)}_{\text{IN}} = 0,\ \varrho^{(1)}_{\text{OUT}} = 1 \quad \Rightarrow b = d \tag{6.5a}$$

and,

$$\varrho^{(1)}_{\text{IN}} = 1,\ \varrho^{(1)}_{\text{OUT}} = 0 \quad \Rightarrow a = -b,\ b = d \tag{6.5b}$$

These relations between the coefficients can be simplified to yield,

$$\lambda_{1_I} = 0 \tag{6.6}$$

which is not allowed. Thus, NOT gate from the two soliton collisions using LFT (6.2) is also not possible.

On the other hand abandoning the LFT gives another possibility for realising logical operation. This scheme is graphically represented in figure Fig:(6.3) and is given as

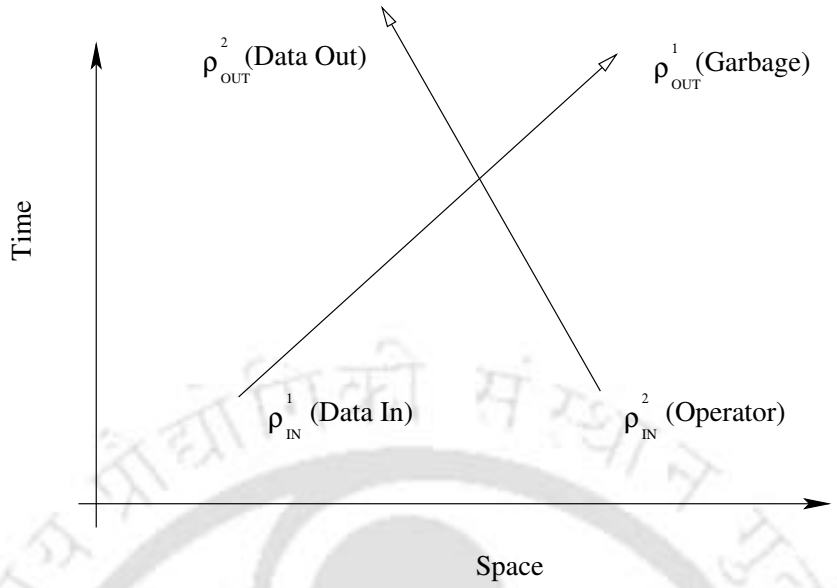

Figure 6.3: 1-Input/1-Output Soliton Gates without LFT

$$\varrho_{\text{OUT}}^{(2)} = \frac{\varrho_{\text{IN}}^{(2)}(1+|\varrho_{\text{IN}}^{(1)}|^{\star})\Lambda_{1,2} - \varrho_{\text{IN}}^{(1)}(1+\varrho_{\text{IN}}^{(1)\star}\varrho_{\text{IN}}^{(2)})\Lambda_{1,1}}{(1+|\varrho_{\text{IN}}^{(1)}|^{\star})\Lambda_{1,2} - (1+\varrho_{\text{IN}}^{(1)\star}\varrho_{\text{IN}}^{(2)})\Lambda_{1,1}} \tag{6.7}$$

But for the implimentation of COPY and NOT gate is still not possible as imposing the truth tables ((Tab:6.1),(Tab:6.2)) yield inconsistancies ($\varrho_{\text{IN}}^{(1)}$ has to be 0 and 1 at the same time) or trivial situations ($\lambda_{1_R} = \lambda_{2_R}$, both the solitons move with the same velocities).

Form all these observations it is concluded that the one-input and one-output logic gates are not feasible under the any two-soliton collision scheme.

6.4 Logic Gates from Three Soliton Collisions

The LFT based on three-soliton collisions can be derived from (4.26), and it takes the form,

$$\varrho_{\text{OUT}}^{(1)} = \frac{a\ \varrho_{\text{IN}}^{(1)} + b}{c\ \varrho_{\text{IN}}^{(1)} + d} \tag{6.8}$$

with

$$a = 1 - \frac{\Lambda_{2,2}\Lambda_{3,3}}{\Lambda_{2,3}\Lambda_{3,2}} + |\varrho_{\text{IN}}^{(2)}|^2\Big(1 - \frac{\Lambda_{2,2}}{\Lambda_{2,1}}\Big) + |\varrho_{\text{IN}}^{(3)}|^2\Big(1 - \frac{\Lambda_{3,3}}{\Lambda_{3,1}}\Big) + |\varrho_{\text{IN}}^{(2)}|^2|\varrho_{\text{IN}}^{(3)}|^2\Big(1 - \frac{\Lambda_{2,2}}{\Lambda_{2,1}} - \frac{\Lambda_{3,3}}{\Lambda_{3,1}} + \frac{\Lambda_{2,2}\Lambda_{3,3}}{\Lambda_{2,1}\Lambda_{3,2}} + \frac{\Lambda_{2,2}\Lambda_{3,3}}{\Lambda_{2,3}\Lambda_{3,1}} - \frac{\Lambda_{2,2}\Lambda_{3,3}}{\Lambda_{2,3}\Lambda_{3,2}}\Big) + \varrho_{\text{IN}}^{(2)}\varrho_{\text{IN}}^{(3)\star}\Big(\frac{\Lambda_{2,2}\Lambda_{3,3}}{\Lambda_{2,3}\Lambda_{3,1}} - \frac{\Lambda_{2,2}\Lambda_{3,3}}{\Lambda_{2,3}\Lambda_{3,2}}\Big) + \varrho_{\text{IN}}^{(2)\star}\varrho_{\text{IN}}^{(3)}\Big(\frac{\Lambda_{2,2}\Lambda_{3,3}}{\Lambda_{2,1}\Lambda_{3,2}} - \frac{\Lambda_{2,2}\Lambda_{3,3}}{\Lambda_{2,3}\Lambda_{3,2}}\Big) \tag{6.9a}$$

$$b = \varrho_{\text{IN}}^{(2)}\Big(\frac{\Lambda_{2,2}\Lambda_{3,3}}{\Lambda_{2,3}\Lambda_{3,1}} - \frac{\Lambda_{2,2}}{\Lambda_{2,1}}\Big) + \varrho_{\text{IN}}^{(3)}\Big(\frac{\Lambda_{2,2}\Lambda_{3,3}}{\Lambda_{2,1}\Lambda_{3,2}} - \frac{\Lambda_{3,3}}{\Lambda_{3,1}}\Big) + |\varrho_{\text{IN}}^{(2)}|^2\varrho_{\text{IN}}^{(3)}\Big(\frac{\Lambda_{2,2}\Lambda_{3,3}}{\Lambda_{2,3}\Lambda_{3,1}} - \frac{\Lambda_{3,3}}{\Lambda_{3,1}}\Big) + \varrho_{\text{IN}}^{(2)}|\varrho_{\text{IN}}^{(3)}|^2\Big(\frac{\Lambda_{2,2}\Lambda_{3,3}}{\Lambda_{2,1}\Lambda_{3,2}} - \frac{\Lambda_{2,2}}{\Lambda_{2,1}}\Big) \tag{6.9b}$$

$$c = \varrho_{\text{IN}}^{(2)\star}\Big(\frac{\Lambda_{2,2}\Lambda_{3,3}}{\Lambda_{2,1}\Lambda_{3,2}} - \frac{\Lambda_{2,2}}{\Lambda_{2,1}}\Big) + \varrho_{\text{IN}}^{(3)\star}\Big(\frac{\Lambda_{2,2}\Lambda_{3,3}}{\Lambda_{2,3}\Lambda_{3,1}} - \frac{\Lambda_{3,3}}{\Lambda_{3,1}}\Big) + |\varrho_{\text{IN}}^{(2)}|^2\varrho_{\text{IN}}^{(3)\star}\Big(\frac{\Lambda_{2,2}\Lambda_{3,3}}{\Lambda_{2,1}\Lambda_{3,2}} - \frac{\Lambda_{3,3}}{\Lambda_{3,1}}\Big) + \varrho_{\text{IN}}^{(2)\star}|\varrho_{\text{IN}}^{(3)}|^2\Big(\frac{\Lambda_{2,2}\Lambda_{3,3}}{\Lambda_{2,3}\Lambda_{3,1}} - \frac{\Lambda_{2,2}}{\Lambda_{2,1}}\Big) \tag{6.9c}$$

$$d = 1 - \frac{\Lambda_{2,2}}{\Lambda_{2,1}} - \frac{\Lambda_{3,3}}{\Lambda_{3,1}} + \frac{\Lambda_{2,2}\Lambda_{3,3}}{\Lambda_{2,1}\Lambda_{3,2}} + \frac{\Lambda_{2,2}\Lambda_{3,3}}{\Lambda_{2,3}\Lambda_{3,1}} - \frac{\Lambda_{2,2}\Lambda_{3,3}}{\Lambda_{2,3}\Lambda_{3,2}} + |\varrho_{\text{IN}}^{(2)}|^2\Big(1 - \frac{\Lambda_{3,3}}{\Lambda_{3,1}}\Big) + |\varrho_{\text{IN}}^{(3)}|^2\Big(1 - \frac{\Lambda_{2,2}}{\Lambda_{2,1}}\Big) + |\varrho_{\text{IN}}^{(2)}|^2|\varrho_{\text{IN}}^{(3)}|^2\Big(1 - \frac{\Lambda_{2,2}\Lambda_{3,3}}{\Lambda_{2,3}\Lambda_{3,2}}\Big) + \varrho_{\text{IN}}^{(2)}\varrho_{\text{IN}}^{(3)\star}\Big(\frac{\Lambda_{2,2}\Lambda_{3,3}}{\Lambda_{2,1}\Lambda_{3,2}} - \frac{\Lambda_{2,2}\Lambda_{3,3}}{\Lambda_{2,3}\Lambda_{3,2}}\Big) + \varrho_{\text{IN}}^{(2)\star}\varrho_{\text{IN}}^{(3)}\Big(\frac{\Lambda_{2,2}\Lambda_{3,3}}{\Lambda_{2,3}\Lambda_{3,1}} - \frac{\Lambda_{2,2}\Lambda_{3,3}}{\Lambda_{2,3}\Lambda_{3,2}}\Big) \tag{6.9d}$$

In the above equations all $\lambda_1,\ \lambda_2,\ \lambda_3$ are different from each other. This follows from the fact that the above expressions for the 3SS LFT was derived from the 3SS expressions (4.26) and if any of the λ_j's are equal indicating that two of the three colliding solitons are moving with the same velocity, a non-trivial three soliton collision does not take place. At the same time the determinants having only the $\Lambda_{i,j}$ terms vanish.

In this scheme, the schemetic representation of the soliton collisions are given by `Fig:`(6.4)

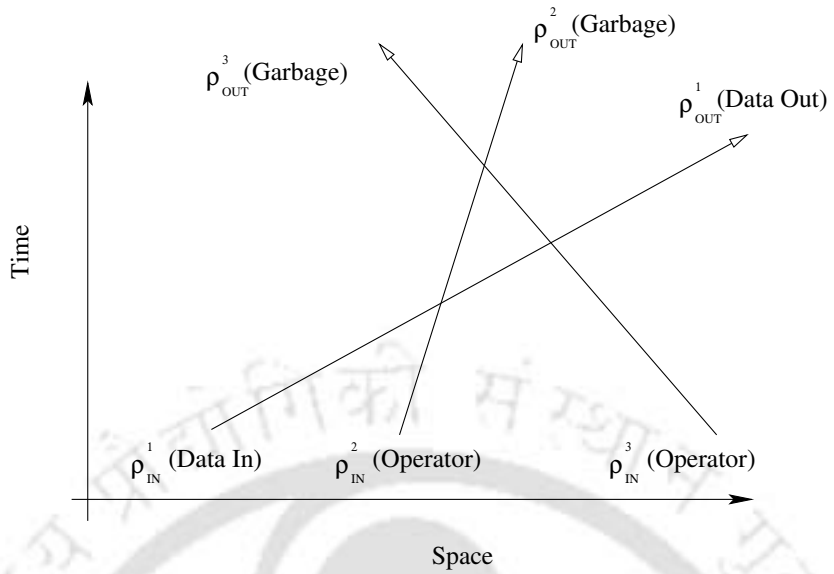

Figure 6.4: 1-Input,1-Output and 2-Operator Solitons for COPY and NOT gates.

The COPY gate is easily realizable. Imposing the truth table criteria in (6.8) yields many possible solutions with simple solutions like,

$$\varrho_{\text{IN}}^{(2)} = \varrho_{\text{IN}}^{(3)} = -\frac{1}{2} \pm \frac{\sqrt{5}}{2} \tag{6.10a}$$

$$\lambda_1 = \frac{\Lambda_{2,2}\Lambda_{3,2}\lambda_3^\star - \Lambda_{3,3}\Lambda_{2,3}\lambda_2^\star}{\Lambda_{2,2}\Lambda_{3,2} - \Lambda_{3,3}\Lambda_{2,3}} \tag{6.10b}$$

In this form of COPY gate, the input and output solitons are the same and so the output bit travels with the same velocity as the input bit. The only difference with the trivial case where an input soliton moves without any collisions is that in this COPY gate the input and output bits has aquired a phase jump given by (5.41).

In another scheme, $\varrho_{\text{IN}}^{(2)}$ (or $\varrho_{\text{IN}}^{(3)}$) may act as the input instead of $\varrho_{\text{IN}}^{(1)}$, while $\varrho_{\text{OUT}}^{(1)}$ still remains as the output. The corrosponding output represented by (6.8) is no longer a linear fractional transformation in terms of the input soliton *i.e.*, $\varrho_{\text{IN}}^{(2)}$ (or $\varrho_{\text{IN}}^{(3)}$), but the truth table for the copy gate may still be

satisfied. The two states of the input reduces to

$$\varrho_{\text{IN}}^{(2)} = 0 \quad \Rightarrow \quad \varrho_{\text{OUT}}^{(1)} = 0 \tag{6.11a}$$

$$\varrho_{\text{IN}}^{(2)} = 1 \quad \Rightarrow \quad \varrho_{\text{OUT}}^{(1)} = 1 \tag{6.11b}$$

Imposing these conditions in (6.8) yields one-possible solution in the form

$$\varrho_{\text{IN}}^{(1)} = \pm\sqrt{\frac{\Lambda_{3,3}\Lambda_{3,1} + \frac{\Lambda_{2,2}\Lambda_{3,3}}{\Lambda_{2,3}\Lambda_{3,2}} - \frac{\Lambda_{2,2}\Lambda_{3,3}}{\Lambda_{2,1}\Lambda_{3,2}} - 1}{1 - \frac{\Lambda_{3,3}}{\Lambda_{3,1}}}} \tag{6.12}$$

In this form of the COPY gate, the output databit undergo a change of velocity in relation to the input databit. This form may be useful for controlling the velocity of the information bits to arrive at a required location at a required moment.

In the case of the NOT gate, imposing conditions from the NOT gate truth table *i.e.*,

$$\varrho_{\text{IN}}^{(1)} = 0 \quad \Rightarrow \quad \varrho_{\text{OUT}}^{(1)} = 1 \tag{6.13a}$$

$$\varrho_{\text{IN}}^{(1)} = 1 \quad \Rightarrow \quad \varrho_{\text{OUT}}^{(0)} = 0 \tag{6.13b}$$

as suggested by `Fig:`(6.4) has one of its possible solution as

$$\varrho_{\text{IN}}^{(2)} = \varrho_{\text{IN}}^{(3)} = -1 \pm \sqrt{2} \tag{6.14a}$$

$$\lambda_{1_R} = \frac{1}{2}\big(\lambda_{2_R} + \lambda_{3_R}\big) \tag{6.14b}$$

$$\lambda_{1_I} - \frac{1}{2}\big(\sqrt{-(\lambda_{2_R} - \lambda_{3_R})^2 - 4\lambda_{2_I}\lambda_{3_I}}\big) \tag{6.14c}$$

Thus the one input one output logic gates can be realised with the collision of three solitons. Moving on to the next level of sophistication, one arrives at the logic gates with two inputs. One such gate is the NAND gate.

The simplest NAND gate is a 2-input/1-output logic gate with its truth-table as given below (`Tab:` 6.3)
If the NAND gate is to be represented by the collision of three solitons, then a possible implementation of the truth table requires $\varrho_{\text{IN}}^{(2)}$ and $\varrho_{\text{IN}}^{(3)}$ to be the

Input 1	Input 2	Output
0	0	1
0	1	1
1	0	1
1	1	0

Table 6.3: 2-input NAND Gate

inputs, and $\varrho^{(1)}_{\text{OUT}}$ as the output. In such a case,

$$\varrho^{(2)}_{\text{IN}} = 0,\ \varrho^{(3)}_{\text{IN}} = 0,\ \varrho^{(1)}_{\text{OUT}} = 1 \tag{6.15a}$$
$$\varrho^{(2)}_{\text{IN}} = 0,\ \varrho^{(3)}_{\text{IN}} = 1,\ \varrho^{(1)}_{\text{OUT}} = 1 \tag{6.15b}$$
$$\varrho^{(2)}_{\text{IN}} = 1,\ \varrho^{(3)}_{\text{IN}} = 0,\ \varrho^{(1)}_{\text{OUT}} = 1 \tag{6.15c}$$
$$\varrho^{(2)}_{\text{IN}} = 1,\ \varrho^{(3)}_{\text{IN}} = 1,\ \varrho^{(1)}_{\text{OUT}} = 0 \tag{6.15d}$$

which leads to an inconsistency $\lambda_2 = \lambda_3$ in the equation (6.8). Another posibility is that, $\varrho^{(1)}_{\text{IN}}$ and $\varrho^{(2)}_{\text{IN}}$ as the inputs, and $\varrho^{(1)}_{\text{OUT}}$ is the output. In this case, the truth table gives

$$\varrho^{(1)}_{\text{IN}} = 0,\ \varrho^{(3)}_{\text{IN}} = 0,\ \varrho^{(1)}_{\text{OUT}} = 1 \tag{6.16a}$$
$$\varrho^{(1)}_{\text{IN}} = 0,\ \varrho^{(3)}_{\text{IN}} = 1,\ \varrho^{(1)}_{\text{OUT}} = 1 \tag{6.16b}$$
$$\varrho^{(1)}_{\text{IN}} = 1,\ \varrho^{(3)}_{\text{IN}} = 0,\ \varrho^{(1)}_{\text{OUT}} = 1 \tag{6.16c}$$
$$\varrho^{(1)}_{\text{IN}} = 1,\ \varrho^{(3)}_{\text{IN}} = 1,\ \varrho^{(1)}_{\text{OUT}} = 0 \tag{6.16d}$$

Using the above equations (6.16) in (6.8) leads to inconsistencies like $\lambda_1 = \lambda_2$. Therefore, the NAND gate cannot be realised with only three soliton collisions. More than three solitons will be required.

6.5 NAND Gate with four soliton collisions

In order to investigate the possibility of building the NAND logic gate from the collision of four one-solitons, an expression relating the inputs $\varrho^{(1)}_{\text{IN}}$, $\varrho^{(2)}_{\text{IN}}$, $\varrho^{(3)}_{\text{IN}}$, $\varrho^{(4)}_{\text{IN}}$ with the output (maybe $\varrho^{(1)}_{\text{OUT}}$ or any of the others) is to be developed. This scheme is represented in the `Fig:`(6.5) and is given as

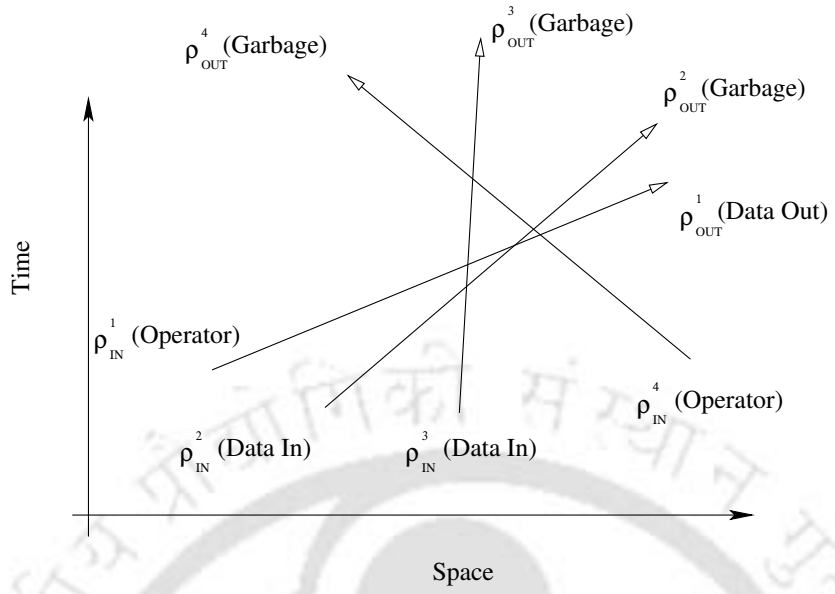

Figure 6.5: 2-Input,1-Output and 2-Operator Solitons for NAND gate.

$$\varrho^{(1)}_{\text{OUT}} = \frac{q_1^{(1)''''}}{q_1^{(2)''''}} = \frac{e^{\tilde{\Delta}^1_{1;2,3,4}}}{e^{\tilde{\Delta}^1_{2;2,3,4}}} \tag{6.17}$$

where, the terms $e^{\tilde{\Delta}^1_{i;2,3,4}}$ appearing above are defined by (4.33a). In context to the inputs which are now two in number, (6.17) can no longer be considered to be a linear fractional transformation of both the inputs at the same time. The imposition fo the NAND gate truth table yields, the set of constraints given by (6.15). On the other hand if the scheme is different, and is accordingly represented by a figure different from (`Fig:`6.5) and the set of constraints may be (6.16) or any other depending on the situation.

6.6 Logic Gates with Higher Soliton Collisions

It is seen that if a gate cannot be realised under a particular number of colliding solitons, one has to increase the number of colliding solitons to achieve the implimentation of the same logic gate. For example, the simplest COPY and NOT gate were not possible under two soliton collisions, however the

same gates were possible with three soliton collisions. In a similar manner altough the NAND gate was not realised with three soliton collisions, with four soliton collision it would be easily possible. In this way, more complicated gates can always be realised with the enough number of colliding solitons. The transformation that the solitons undergo after collisions can always be found out by using the corrosponding expression for the N-colliding solitons (4.31). This together with the constraints imposed by the truth table for that complicated gate will provide all the necessary information for realising that particular logic gate. In this manner complicated gates like HALF-ADDER, FULL-ADDER or even complete Arithmetic Logic Units can be developed using optical solitons. Theoretically, any calculating machine can be fabricated using colliding optical solitons.

6.7 Summary

In this chapter the simplest logic gates were developed using the collisions of Manakov optical solitons moving in a birefringent optical fiber. It was also shown that a logic gate not achievable with lesser solitons can be achieved by considering enough solitons in collision.

Chapter 7

Conclusion

This thesis is mainly concerned with a study of the nature of soliton collisions of the n-CNLS and n-CHNLS of the Hirota type. For this the N soliton solutions of these systems belonging to the AKNS heirarchy was obtained by the Inverse Scattering Method. The N soliton solutions of another dynamical system belonging to the same heirarchy, the n-CHNLS of the Sasa Satsuma type was also obtained. In the study of soliton collisions it was observed that all solitons, scalar or coupled, collide with each other elastically. But for the coupled systems, altough each component describes a soliton, these solitons at the component level may interact inelastically. During such a soliton collision, the component of a soliton undergo changes in their amplitude, and these changes are due to the transfer of energy of the soliton from one component to another component of the same soliton. Thus, what may be seen as a decrease of amplitude of one of the soliton, surfaces as an increase of amplitude among the other components. Besides this, it is also observed that the outcome of these inelastic collision of solitons at component level is independent of the sequence of interactions. Such observations were derived from the study of two and three soliton collisions and was generalised for the collision of any N solitons.

The other important area studied in this thesis is the construction of all optical logic gates using temporal solitons. The most economical scheme (using the least number of solitons) for the simplest one-input/one-output logic gates were studied. For this study it became evident that using the

expressions for the N soliton solutions, a gate that is not possible to fabricate with a definite number of solitons can be fabricated with a greater number of solitons. This was also seen in the case of the NAND gate. It was found that constructing a NAND gate with three solitons is not possible, but with four colliding solitons, the NAND gate may be easily constructed. This is because, each additional soliton taking part in the collision increases the options for fulfilling the criteria required by a particular truth-table of a logic gate. Such an approach allows one to design any complex logic gate using the proper number of solitons.

It is felt that such a study would generate further interest in this direction which would pave the way for the utilization of optical solitons for constructing all optical logic gates and all optical logical processing units.

Appendix A

Mathematical Derivations

A.1 Operator equation for the KdV Lax-operators

Lax operators are,

$$L = -\frac{\partial^2}{\partial x^2} + \phi \tag{A.1}$$

$$B = -4\mathtt{i}\frac{\partial^3}{\partial x^3} + 3\mathtt{i}\left(\phi\frac{\partial}{\partial x} + \frac{\partial}{\partial x}\phi\right) \tag{A.2}$$

For any arbitrary function $f(x,t)$, the operator equation for KdV (2.3) is

$$\begin{aligned} \mathtt{i}L_t f(x,t) &= [B,L]f(x,t) \\ \Rightarrow \qquad \mathtt{i}f(x,t)\frac{\partial\phi}{\partial t} &= \mathtt{i}f(x,t)\left(6\phi\frac{\partial\phi}{\partial x} - \frac{\partial^3\phi}{\partial x^3}\right) \end{aligned}$$

On dividing both sides of the above equation by $\mathtt{i}f(x,t)$, we get back the KdV equation

$$\phi_t = 6\phi\phi_x - \phi_{xxx} \tag{A.3}$$

A.2 Lax operators

If $U(t)$ is a time evolution operator for the wave function $\psi(x,t)$ from $t=0$ to $t=t$, *i.e.*,

$$\psi(x,t) = U(t)\psi(x,0) \tag{A.4}$$

This time evolution operator shifting its wave function to the 'same' time would also require $U(0)$ to be an identity matrix. Defining a relation between the time evolution operator and B

$$\mathtt{i}U_t(t) = BU(t) \tag{A.5}$$

$$\begin{aligned}
& & \Rightarrow \quad \mathtt{i}U^\dagger U_t &= U^\dagger BU \\
\text{and} \quad -\mathtt{i}U_t^\dagger = U^\dagger B & \Rightarrow & -\mathtt{i}U_t^\dagger U &= U^\dagger BU \\
& & \Rightarrow \quad \mathtt{i}U^\dagger U_t &= -\mathtt{i}U_t^\dagger U \\
& & \Rightarrow \quad (U^\dagger U)_t &= 0 \\
\Rightarrow \quad U(t)^\dagger U(t) = \text{const} = U(0)^\dagger U(0) &= I \text{ (Identitymatrix)}
\end{aligned}$$

Thus (A.4) & (A.5) requires $U(t)$ to be an unitary operator. Using this time evolution operator it can be shown that the time evolution of L is

$$L(t) = U(t)L(0)U(t)^\dagger \qquad \text{with } t > 0 \tag{A.6}$$

Therefore,

$$\begin{aligned}
\mathtt{i}L_t(t) &= \mathtt{i}U_t(t)L(0)U(t)^\dagger + \mathtt{i}U(t)L(0)U_t(t)^\dagger \\
&= BU(t)L(0)U(t)^\dagger + U(t)L(0)(-U_t(t)^\dagger B) \\
&= [B, U(t)L(0)U(t)^\dagger] \\
&= [B, L(t)]
\end{aligned}$$

Thus the operator equation (A.3) *i.e.*, $\mathtt{i}L_t = [B, L]$ validitates (A.6).

Altough the operator L evolves in time through its dependance in ϕ, its eigen values in the direct problem remain constant. If

$$\text{at } t = 0, \qquad L(0)\psi(0) = \lambda(0)\psi(0) \tag{A.7}$$

$$\text{and at } t > 0, \qquad L(t)\psi(t) = \lambda(t)\psi(t) \tag{A.8}$$

$$\begin{aligned}
(A.7) \quad \Rightarrow \quad & U(t)L(0)\psi(0) &= \lambda(0)U(t)\psi(0) \\
\Rightarrow \quad & U(t)L(0)U(t)^\dagger U(t)\psi(0) &= \lambda(0)U(t)\psi(0) \\
\Rightarrow \quad & L(t)U(t)\psi(0) &= \lambda(0)U(t)\psi(0) \\
(A.4) \quad \Rightarrow \quad & L(t)\psi(t) &= \lambda(0)\psi(t)
\end{aligned}$$

Comparing the above equation with (A.8) gives

$$\lambda(t) = \lambda(0) \tag{A.9}$$

In order to show the time evolution of $\psi(x,t)$ in terms of the B operator (2.9), from equation (A.4)

$$\begin{aligned} & & \mathtt{i}\psi_t(x,t) &= \mathtt{i}(U(t)\psi(x,0))_t \\ & & &= \mathtt{i}U_t(t)\psi(x,0) \\ (A.5) \quad \Rightarrow \quad & & \mathtt{i}\psi_t(x,t) &= BU(t)\psi(x,0) \\ (A.4) \quad \Rightarrow \quad & & \mathtt{i}\psi_t(x,t) &= B\psi(x,t) \end{aligned} \tag{A.10}$$

A.3 Proof of equations (3.10)

From the defination of the basis, $e_{i,j}$ it is seen that they obey the following product rule.

$$e_{i,j}\ e_{k,l} = e_{i,l}\ \delta_{j,k} \tag{A.11}$$

where, $\delta_{i,j}$ is the kroneker delta. For example

$$\begin{pmatrix} 0 & 1 & 0 & 0 \\ 0 & 0 & 0 & 0 \\ 0 & 0 & 0 & 0 \\ 0 & 0 & 0 & 0 \end{pmatrix} \begin{pmatrix} 0 & 0 & 0 & 0 \\ 0 & 0 & 0 & 1 \\ 0 & 0 & 0 & 0 \\ 0 & 0 & 0 & 0 \end{pmatrix} = \begin{pmatrix} 0 & 0 & 0 & 1 \\ 0 & 0 & 0 & 0 \\ 0 & 0 & 0 & 0 \\ 0 & 0 & 0 & 0 \end{pmatrix}$$

i.e.,

$$e_{1,2}\ e_{2,4} = e_{1,4}$$

Thus,

$$\begin{aligned} \mathbf{\Sigma}^2 &= \mathbf{\Sigma}\ \mathbf{\Sigma} \\ &= (\sum_{i=1}^{n} e_{i,i} - e_{n+1,n+1})(\sum_{j=1}^{n} e_{j,j} - e_{n+1,n+1}) \\ &= \sum_{i,j=1}^{n} e_{i,i}\ e_{j,j} - \sum_{i=1}^{n} e_{i,i}\ e_{n+1,n+1} - \sum_{j=1}^{n} e_{n+1,n+1}\ e_{j,j} + e_{n+1,n+1}\ e_{n+1,n+1} \\ &= \sum_{i=1}^{n} e_{i,i} + e_{n+1,n+1}\ e_{n+1,n+1} \\ &= \sum_{i=1}^{n+1} e_{i,i} = \mathbf{I} \end{aligned}$$

In a similar manner,

$$\begin{aligned}
\mathbf{\Sigma\ A + A\ \Sigma} &= (\sum_{i=1}^{n} e_{i,i} - e_{n+1,n+1})(\sum_{j=1}^{n} q_j(x,t)e_{j,n+1} - \sum_{j=1}^{n} q_j^{\star}(x,t)e_{n+1,j}) \\
&+ (\sum_{i=1}^{n} q_i(x,t)e_{i,n+1} - \sum_{i=1}^{n} q_i^{\star}(x,t)e_{n+1,i})(\sum_{j=1}^{n} e_{j,j} - e_{n+1,n+1}) \\
&= \sum_{i=1}^{n} q_i\ e_{i,n+1} + \sum_{i=1}^{n} q_i^{\star}\ e_{n+1,i} - \sum_{i=1}^{n} q_i\ e_{i,n+1} - \sum_{i=1}^{n} q_i^{\star}\ e_{n+1,i} \\
&= 0
\end{aligned}$$

Bibliography

[1] J.S.Russell, Report on Water Waves, Rep. 14th Meet. British. Assoc. Adv.Sci. (1844) 311.

[2] H.Brazin, Recherches Hydrauliques (1865).

[3] J.Bossinesq, C.R.Acad.Sci. Paris **72** (1871) 755.

[4] L.Rayleigh, Phil.Mag(5) **1** (1876) 257.

[5] D.J.Kortweg and G. de Vries, Philos. Mag. **39** (1895) 422.

[6] E.Fermi, J.R.Pasta and S.M.Ulam, Los Alamos Sci.Lab.Rep., LA-1940.

[7] N.Zabusky and M.Kruskal, Phys.Rev.Lett. **15** (1965) 240.

[8] C.S.Gardner, J.M.Green, M.D.Kruskal and R.M.Muira, Phys.Rev. Lett. **19**, (1967) 1095.

[9] C.S.Gardner, J.M.Green, M.D.Kruskal and R.M.Muira, Commun. Pure Appl. Math. **27**, (1974) 97.

[10] M.Wadati and M.Toda, J.Phys.Soc.Jpn. **32** (1972) 1403.

[11] P.D.Lax, Commun. Pure Appl. Math. **21**, (1968) 467.

[12] V.E.Zakharov, J.Appl.Mech.Tech.Phys.**9** (1968) 86.

[13] V.E.Zakharov and A.B.Shabat, Sov.Phys.JETP **34** (1972) 62.

[14] H.C.Yuen and B.M.Lake, Phys.Fluids **18**, (1975) 956-960.

[15] M.Wadati, J.Phys.Soc.Jpn. **32** (1972) 1681.

[16] M.Wadati, J.Phys.Soc.Jpn. **34** (1973) 1289.

[17] M.J.Ablowitz, D.J.Kaup, A.C.Newell and H.Segur, Phys.Rev.Lett. **31** (1973) 125.

[18] R.Hirota, Phys.Rev.Lett. **27** (1971) 1192.

[19] R.Hirota, J.Phys.Soc.Jpn. **33** (1972) 1456.

[20] R.Hirota, J.Phys.Soc.Jpn. **14** (1973) 805.

[21] R.Hirota, Prog.Theor.Phys. **52** (1974) 1498.

[22] R.Hirota, J.Phys.Soc.Jpn. **66** (1997) 2530.

[23] R.Hirota, RIMS kokyuroku **1020** (1997) 143.

[24] S.Kakei, N.Sasa and J.Satsuma, R.Hirota, J.Phys.Soc.Jpn. **64** (1995) 577.

[25] J.Hietarinta, J.Math.Phys. **28** (1987) 1732.

[26] J.Hietarinta, J.Math.Phys. **29** (1988) 628.

[27] J.Hietarinta, hep-th (1997) 9708006.

[28] C.Rogers & W.F.Shadwick, Mathematics in Science and Engineering, Academic Press, **161** (1982).

[29] Jr.G.L.Lamb, Elements of Soliton Theory, Wiley-Interscience (1980).

[30] J.B.Ablowitz, A.Ramani & H.Segur, Lett.Nuovo Cim. **23** (1978) 333.

[31] J.B.Ablowitz, A.Ramani & H.Segur, J.Maths.Phys. **21** (1980) 715 & 1006.

[32] J.B.Ablowitz & H.Segur, Phys.Rev.Lett. **38** (1977) 1103.

[33] J.B.McLeod & P.J.Olver, SIAM J.Math.Anal **14** (1983) 488.

[34] A.P.Frody, *Soliton theory: a Survey of Results*, Manchester University Press (1990).

[35] F.Margi, J.Math.Phys **19** (1978) 1156.

[36] L.D.Fadeev & L.A.Takhtajan, *Hamiltonian Methods in the Theory of Solitons*, Springer (1987).

[37] A.S.Fokas, Stud.Appl.Math. **77** (1987) 253.

[38] A.V.Mikhailov, A.B.Shabat & R.I.Yamilov, Russ.Math.Surv. **42:4** (1987) 1.

[39] J.B.Ablowitz & H.Segur, Solitons and Inverse Scattering Transform, SIAM Stud.Appl.Math., **4** (1981).

[40] A.C.Newell, Solitons in Mathematics and Physics, SIAM (1985)

[41] A.P.Frody & P.P.Kulish, Commun.Math.Phys. **89** (1983) 427.

[42] A.P.Frody, J.Phys. A **17** (1984) 1235

[43] I.T.Habibullin, V.V.Sokolov & R.I.Yamilov, Nonlinear Physics: Theory and Experiments, ed. E.alfinito *et.al.*, World Scientific (1996) 139.

[44] S.I.Svinolupov, Commum.Math.Phys. **143** (1992) 559.

[45] S.I.Svinolupov, Func.Anal.Appl. **27** (1993) 257.

[46] S.I.Svinolupov & V.V Sokolov, Theor.Math.Phys. **100** (1994) 959.

[47] R.K.Dodd, J.C.Eilbeck, J.D.Gibbon & H.C.Morris, Solitons and Nonlinear Wave Equations, Academic Press (1982).

[48] L.A.Ostrovskii, Zh.Tek.Fiz **33** (1963) 905.

[49] V.I.Bespalov and V.I.Talanov, Zh.Eksp.Teor.Fiz.Pis'ma, JETP Lett. **3** (1966) 307.

[50] V.I.Karpman, Zh.Eksp.Teor.Fiz.Pis'ma, JETP Lett. **6** (1967) 277.

[51] A.Hasegawa and F.Tappert, Appl.Phys.Lett. **23** (1973) 142.

[52] A.Hasegawa and F.Tappert, Appl.Phys.Lett. **23** (1973) 171.

[53] L.F.Mollenauer, R.H.Stolen and J.P.Gordon, Phys.Rev.Lett. **45** (1980) 1095.

[54] I.Morita, K.Tanaka, No.Edagawa ans M.Suzadi, 1998 European Conference on Optical Communication **3** (1998) 47.

[55] K.Fukuchi, M.Kakui, A.Sasaki, T.Ito, Y.Inada, T.Suzaki, T.Shitomi, K.Fujii, S.Shikii, Ho.Sugahara and A.Hasegawa, Technical Digest of ECOC 99. (1999) PD2-10.

[56] M.Segev and G.I.Stegeman, Physics Today **51**(8) 1998 42.

[57] G.I.Stegeman and M.Segev, Science **286** (1999) 1518.

[58] Y.Kodama and A.Hasegawa, IEEE J.QE. **QE-23** (1987) 510.

[59] N.Sasa and J.Satsuma, J.Phys.Soc.Jpn. **60** (1991) 409.

[60] D.Mihalache and L.Torner, Phys.Rev.E **48** (1993) 4699.

[61] S.Ghosh and S.Nandy, J.Math.Phys. **60** (1999) 1991.

[62] M.Gedalin, T.C.Scott and Y.B.Band, Phys.Rev.Lett. **78** (1997) 448.

[63] V.E.Zakharov and A.L.Berkhoer, Sov.Phys.JETP. **31** (1970) 486.

[64] S.V.Manakov, Sov.Phys.JETP. **38** (1974) 248.

[65] P.K.A.Wai, C.R.Menyuk and H.H.Chen, Opt.Lett. **16** (1991) 1935.

[66] C.R.Menyuk, Opt.Lett. **12** (1987) 614.

[67] N.J.Doran and D.Wood, Opt.Lett. **13** (1988) 56.

[68] K.B.Blow, N.J.Doran and D.Wood, Opt.Lett. **12** (1987) 202.

[69] D.N.Christodoulides and R.I.Joseph, Opt.Lett. **9** (1988) 408.

[70] D.N.Christodoulides and R.I.Joseph, Opt.Lett. **62** (1989) 1746.

[71] K.Nakkeeran, K.Porsezian, P.S.Sundaram and A.Mahalingam, Phys.Rev.Lett. **80** (1998) 1425.

[72] R.S.Tasgal and M.J.Potasec, J.Math.Phys. **33** (1992) 1208.

[73] R.Radhakrishnan and M.Lakshmanan, Phys.Rev.E **54** (1996) 2949.

[74] S.Ghosh and S.Nandy, Nucl.Phys.B **561** (1991) 451.

[75] V.E.Zakharov,S.V.Manakov,S.P.Novikov and L.P.Pitaevsky, *Theory of Solitons*, Consultants Bureau, New York.

[76] J.P.Gordon, Opt.Lett. **8** (1983) 596.

[77] K.G.Gorshkov and L.A.Ostrovsky, Physica **D3** (1981) 341.

[78] I.V.Karpman and V.V.Solov'ev, Physica **D3** (1981) 487.

[79] K.J.Blow and N.J.Doran, Electr.Lett. **19** (1983) 429.

[80] B.Hermansson and D.Yervick, Electr.Lett. **19** (1983) 570.

[81] F.M.Mitschke and L.F.Mollenauer, Opt.Lett. **11** (1986) 659.

[82] F.Abdullaev, S.Darmanyan and P.Khabibullaev, *Optical Solitons* Springer-Verlag (1993).

[83] E.M.Dianov, A.V.Luchinkov, A.N.Pilipetskii, A.N.Starodumov, Opt.Lett. **15** (1990) 314.

[84] L.F.Mollenauer, F.M.Mitschke and L.F.Smith, Opt.Lett. **14** (1989) 1284.

[85] R.Radhakrishnan, M.Lakshmanan and J.Hietarinta, Phys Rev.E. **56** (1997) 2213.

[86] T.Kanna and Lakshmanan, Phys.Rev.Lett. **86** (2001) 5043.

[87] M.Lakshmanan, T.Kanna and R.Radhakrishnan, Rep.Math.Phys. **46** (2000) 143.

[88] A.Borah, S.Ghosh and S.Nandy, Eur.Phys.J.B **29** (2002) 221.

[89] T.Tsuchida, arXiv:nlin.SI/0302059 v1 (2003).

[90] M.H. Jakubowski, K.Steiglitz and R.Squirer, Phys.Rev.E **56** (1997) 7267.

[91] M.H. Jakubowski, K.Steiglitz and R.Squirer, Phys.Rev.E **58** (1998) 6752.

[92] C.Anastassiou, M.Segev, K.Steiglitz, J.A.Giordmaine, M.Mitchell, M.Shih, S.Lan and J.Martin, Phys.Rev.E **83** (1999) 2332.

[93] C.Anastassiou, J.W.Fleischer, T.Carmon, M.Segev, K.Steiglitz, Opt.Lett. **26** (2001) 1498.

[94] K.Steiglitz, Phys.Rev.E **63** (2000) 016608.

[95] K.Steiglitz, Phys.Rev.E **63** (2000) 046607.

[96] K.Steiglitz, Multiple-Valued Logic, **6** (2001) 439.

[97] D.M.Bloom, L.F.Mollenauer, Ch Lin, N.Taylor and A.M.Del Gaudio, Opt.Lett. **4** (1979) 297.

[98] L.F.Mollenauer, R.H.Stolen and M.N.Islam, Opt.Lett. **10** (1985) 229.

[99] M.Jain and Z.Tzoar, J.Appl.Phys. **49** (1978) 4649.

[100] B.Bendow, P.D.Gianino, N.Tzoar and M.Jain, J.Opt.Soc.Am. **70** (1980) 539.

[101] V.E.Zakharov and S.V.Manakov, Theor.Mat.Fiz. **19** (1974) 332.

[102] J.Satsuma and N.Yajima, Prog.Teor.Phys.Suppl. **N55** (1974) 284.

[103] E.Olmedilla, Physica **D25** (1987) 330.

[104] A.Hasegawa, *Optical Solitons in Fibers*, Sringer-Verlag (1990).

[105] G.P.Agarwal, *Nonlinear Fiber Optics*, Academic Press (1995).

[106] D.J.Kaup and A.C.Newell, J.Math.Phys. **19** (1978) 798.

[107] K.Porsezian and K.Nakkeeran, Phys.Rev.Lett. **78** (1997) 448.

[108] V.E.Zakharov and I.E.Schulman, Physica **D4** (1982) 270.

[109] R.Sahadevan, K.N.Tamizhmani and M.Lakshmanan, J.Phys. **A19** (1986) 1783.

[110] A.Uthayakumar,K.Porsezian and K.Nakkeeran, Pure Appl.Opt. **7** (1998) 1459.

[111] C.R.Menyuk, IEEE J.Quant.Electron **23** (1987) 174.

[112] K.Porsezian, Int.J.Nonlinear Phys. **5** (1998) L126.

[113] K.Porsezian, P.S.Sundaram and A.Mahalingam, Phys.Rev. E **50** (1994) 1543.

[114] K.Porsezian, P.S.Sundaram and A.Mahalingam, J.Phys. A **32** (1999) 8731.

[115] J.K.Park, K.Steiglitz and W.T Thruston, Physica D, **19:D** (1986) 423.

[116] K.Steiglitz, I.Kamal and A Watson, IEEE Transactions on Computers, **37(20)**, (1988) 138.

[117] W. Hordijk and J. P. Crutchfield and M. Mitchell, *Embedded-particle computation in evolved cellular automata*, Proc. Fourth Workshop on Physics and Computation (PhysComp96)", (1996).

[118] M. H. Jakubowski, K. Steiglitz, and R. K. Squier, Complex Systems, **10** (1996) 1.

[119] M. H. Jakubowski, K. Steiglitz, and R. K. Squier,*Relative computational power of integrable and nonintegrable soliton systems*, Proc. Fourth Workshop on Physics and Computation (PhysComp96), Nov. 22-24, 1996, T. Toffoli, M. Biafore and J. Le (eds.), New England Complex Systems Institute, Boston, Mass.

[120] A. Adamatzky (ed.), Collision-Based Computing, Springer, (2002).

[121] M. Soljacic, K. Steiglitz, S. Sears, M. Segev, M. Jakubowski, R. Squier, Phys. Rev. Lett., **90,25**, (2003) 254102.

[122] T. Kanna and M. Lakshmanan, *Exact soliton solutions of coupled nonlinear Schrödinger equations: Shape changing collisions, logic gates and partially coherent solitons*, To appear in Phys.Lett.E., (2003).

[123] A.A.Sukhorukov and Y.S.Kivshar, Pramana, **57** (2001) 1097.

Papers presented in International Workshops/ Conferences/Symposiums.

1. A.Borah, S.Ghosh and S.Nandy, *Solitons in nonlinear fibers.* International Conference on "Geometry, Integrability and Nonlinearity in Condensed Matter and Soft Condensed Matter Physics", July 15-20, 2001, Banko, Bulgaria.
   `published as` *Interaction of coupled higher order nonlinear Schrödinger equation solitons*, Eur. Phys. J. B, **29** (2002) 221-225.

2. A.Borah, S.Ghosh and S.Nandy, *Three Soliton Interactions in the Manakov System*, International Workshop on Optical Solitons: Theory and Experiments" January 24-29, 2002, Kochi, India.

3. A.Borah and S.Nandy, *N-Interacting Solitons in Coupled Sasa-Satsuma Equations*, International Workshop on Optical Solitons: Theory and Experiments" January 24-29, 2002, Kochi, India.